COOPERATIVE RESEARCH CENTRE FOR **CATCHMENT HYDROLOGY**

# MONTE CARLO SIMULATION OF FLOOD FREQUENCY CURVES FROM RAINFALL

**TECHNICAL REPORT**
**Report 01/4**
March 2001

**Ataur Rahman / Erwin Weinmann / Tam Hoang / Eric Laurenson / Rory Nathan**

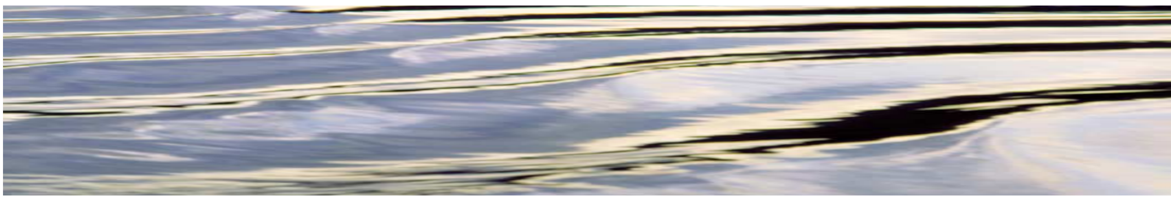

COOPERATIVE RESEARCH CENTRE FOR
CATCHMENT HYDROLOGY

# Monte Carlo Simulation of Flood Frequency Curves from Rainfall

**Ataur Rahman[1], Erwin Weinmann[2,3], Tam Hoang[2,4], Eric Laurenson[3] and Rory Nathan[5]**

1 Physical Infrastructure Centre, School of Civil Engineering, Queensland University of Technology (formerly with Cooperative Research Centre for Catchment Hydrology, Monash University)

2 Cooperative Research Centre for Catchment Hydrology

3 Department of Civil Engineering, Monash University

4 Bureau of Meteorology, Melbourne

5 Sinclair Knight Merz, Melbourne

**March 2001**

## Preface

CRC Project FL1 (Holistic approach to rainfall-based design flood estimation) took a different look at ways to estimate design floods. Currently, the recommended procedure in Australia is to use a design rainfall event (with appropriate intensity, temporal and spatial pattern, and areal reduction factor), subtract median losses, then route the rainfall-excess (using a runoff-routing model, with 'average' parameters) and add baseflow. This approach ignores the interactions between the many named components, and can produce significant bias and uncertainty.

Project FL1 aimed to reduce the bias and uncertainties in Australian design flood estimates by developing rainfall-based design flood estimation procedures which better take account of the interaction and joint probability of the different flood producing components, i.e. a holistic approach.

The work described in this report examines a range of joint probability approaches to allow for the interaction of different components. The results certainly seem very promising, and suggest that a shift in thinking on design floods is not far away.

Russell Mein
Leader
Flood Program

## Acknowledgements

The authors would like to thank Professor Russell Mein, Dr Sri Srikanthan, Professor Tom McMahon, Dr Q J Wang and Dr Bryson Bates for their inputs to the project as members of the Project Reference Panel, and the Bureau of Meteorology and Thiess Environmental Services for providing rainfall and streamflow data respectively.

## Summary


This report describes a Monte Carlo simulation technique for deriving flood frequency curves. It is based on the Joint Probability Approach, a holistic approach to design flood estimation that considers probability-distributed inputs and model parameters, and their correlations, to determine probability-distributed flood outputs. The technique can be used for both complete storms and parts of complete storms (defined here as storm-cores); this report focuses on storm-cores. At present, the technique has been applied to a small number of Victorian catchments.

The adopted new modelling framework uses existing loss models and runoff routing models as the deterministic elements in the simulation of a derived flood frequency curve. However, it differs from currently applied approaches in that it makes explicit allowance for the probability-distributed nature of the key variables and the dependencies between them.

Four input variables/parameters are treated as random variables: rainfall duration, rainfall intensity, rainfall temporal pattern and initial loss. The distributions of these component variables have been identified. The storm-core duration was found to be exponentially distributed. The storm-core intensity-frequency-duration (IFD) curves have been developed based on the partial series of storm-core rainfall events. The fitted IFD curves show a fairly consistent relationship with 'Australian Rainfall and Runoff' IFD curves (I. E. Aust., 1987). The observed set of rainfall temporal patterns has been used directly in the Monte Carlo simulation to randomly select a historic temporal pattern. Initial loss was found to have a beta distribution.

A simple runoff routing model (with a single non-linear storage concentrated at the catchment outlet) has been used here. The adopted Monte Carlo simulation technique involves generation of a large set (in the order of thousands) of data from the four component distributions. Each set of rainfall duration, rainfall intensity, rainfall temporal pattern and initial loss data is run through the calibrated runoff routing model to simulate a streamflow hydrograph. The peaks (or other selected characteristics) of all the simulated hydrographs are then used to determine a derived flood frequency curve, using an appropriate probability plotting position formula.

The technique has been applied to three catchments in Victoria: Tarwin River, Boggy Creek and Avoca River. The derived flood frequency curves for these catchments have been compared with the flood frequency curves defined by the observed floods, and it was found that the new method provides a relatively precise reproduction of observed frequency curves over a wide range of flood frequencies and this can cope well with non-linearity of the rainfall and runoff process.

A sensitivity analysis has been conducted to examine the effect of changes in the component distributions on the derived flood frequency curve. The results show that the derived flood frequency curve is very sensitive to a change in the distribution of rainfall intensity, as expected, and moderately sensitive to changes in the representation of temporal patterns and initial loss distributions.

Different sets of Monte Carlo simulation runs with the same distributional parameters indicated that the lower part of the frequency curve, to an ARI of the order of 100 years, could be confidently estimated from the results of several thousand runs, while the upper tail showed noticeable differences between sets of runs.

Much of the existing design data (rainfall intensity, losses and temporal patterns) can be used with the proposed new technique. The method is easy to apply.

The results of the initial application of the Monte Carlo Simulation technique described in this report show that the method has great potential for development into a practical design tool. However, further work is needed before it can be handed over to industry for practical use in typical design situations.

# List of Tables

# List of Figures

# 1. Introduction

## 1.1 Purpose of the Report

The purpose of this report is to present the results of research undertaken in the Cooperative Research Centre for Catchment Hydrology (CRCCH) to determine derived flood frequency curves using the Joint Probability Approach. This research was part of CRCCH Project FL1: Holistic Approaches to Design Flood Estimation.

This report focuses on the determination of derived frequency curves of flood peaks, although other flood hydrograph characteristic could be used, e.g. flood volume or time to peak. Both complete storms and parts of complete storms (defined here as *storm-cores*) can be used to obtain derived flood frequency curves. This report deals more specifically with the techniques developed in relation to storm-cores.

## 1.2 Background and Project Objectives

Rainfall-based flood estimation techniques are commonly adopted in hydrologic practice. The currently used methods are based on the *Design Event Approach*; they use a probabilistic rainfall depth, in combination with representative values of other inputs, and then assume that the resulting flood has the same frequency as that of the rainfall depth input. In many cases, this assumption is unreasonable, and the arbitrary and independent treatment of various inputs is likely to introduce significant bias in flood estimates for a given frequency.

The Joint Probability Approach has the potential to overcome the limitations of the *Design Event Approach* by considering the probability-distributed inputs and model parameters and their correlations to determine probability-distributed outputs. The method of combining probability distributed inputs to form a probability-distributed output is known as the *derived distribution approach*, and was pioneered by Eagleson (1972). A number of researchers contributed to the further development of the approach e.g. Beran (1973), Laurenson (1974), Russell et al. (1979), Sivapalan et al. (1990). Rahman et al. (1998) summarised the previous work on the Joint Probability Approaches and found that most of the previous applications were limited to theoretical studies; mathematical complexity, difficulties in parameter estimation and limited flexibility generally preclude the application of these techniques to practical situations. More recently, Sivapalan et al. (1996) and Blöschl and Sivapalan (1997) adopted intensity-frequency-duration (IFD) curves in the derived flood frequency approach, making an important step towards applying the approach under practical situations.

While 'Australian Rainfall and Runoff' (I. E. Aust., 1987), referred to as ARR henceforth, adopted the Design Event Approach to rainfall-based design flood estimation, it recognised the importance of considering the probabilistic nature of the flood producing inputs and their interactions. It thus recommended further investigation into Joint Probability Approaches. More recently, Hill and Mein (1996), in a study of incompatibilities between storm temporal patterns and losses for design flood estimation, mentioned that "a holistic approach will perhaps produce the next significant improvement in design flood estimation procedures".

One component of CRCCH Project FL1.1 was devoted to developing a *practical* modelling technique for design flood estimation based on the Joint Probability Approach. The proposed technique offers further development beyond recent work on the Joint Probability Approach (e.g. Muzik, 1993; Sivapalan et al., 1996; Blöschl and Sivapalan, 1997). The technique uses a commonly applied loss model (as a runoff production function) and a runoff routing model (as a transfer function) as its deterministic modelling elements . In this initial application, a simple conceptual runoff routing model (with a single non-linear storage concentrated at the catchment outlet) has been adopted. However, the ultimate goal is to adopt a semi-distributed runoff routing model, e.g. RORB (Laurenson and Mein, 1997) or URBS (Carroll, 1994). Thus the new technique aims to use models applied in current Australian design practice. The approach also aims to establish links with currently available design data (e.g. rainfall intensity, rainfall temporal pattern, losses), and to make explicit allowance for dependencies between different design inputs. The salient features of the proposed modelling framework are described in Rahman et al., 1998 and Weinmann et al., 1998.

### 1.3 Outline of the Report

This report consists of ten chapters. Chapter 2 describes the adopted modelling framework. Data assembly is covered in Chapter 3, while rainfall event definitions are presented in Chapter 4. Identification of the probability distributions of the component variables - rainfall duration, rainfall intensity, rainfall temporal pattern and initial loss - is described in Chapter 5. The calibration of the runoff routing model is detailed in Chapter 6. Data generation from component distributions and the derivation of streamflow hydrographs by Monte Carlo simulation are described in Chapter 7. The construction of flood frequency curves from frequency analysis of the simulated floods is presented in Chapter 8, while the validation of results and sensitivity analyses are documented in Chapter 9. The last chapter contains a summary and conclusions.

## 2. Modelling Approach

The modelling framework used to determine derived flood frequency curves is based on three principal elements (Rahman et al., 1998; Weinmann et al., 1998):

(i) a (deterministic) hydrologic modelling framework to simulate the flood formation process;
(ii) the key model variables (inputs and parameters), referred to as component variables henceforth, with their probability distributions; and
(iii) a stochastic modelling framework to synthesise the derived flood distribution from the distributions of component variables.

These elements are described below.

### 2.1 Hydrologic Modelling Framework

The proposed hydrologic model of the flood formation process involves the same components as the models most commonly used with the current Design Event Approach to flood hydrograph estimation: a runoff production function (or loss model), and a runoff transfer function (or runoff routing model). The design rainfall inputs are converted to a design flood output in two steps: runoff production and streamflow hydrograph formation.

***Runoff Production Function - Loss Model***

A runoff production model (or loss model) is needed to partition the gross rainfall input into effective runoff (or rainfall excess) and loss. Various loss models used with the Joint Probability Approach have been discussed in Rahman et al. (1998). In this study, the *initial loss-continuing loss model* has been adopted, it is widely used in Australian flood estimation practice for rural catchments.

***Transfer Function - Runoff Routing Model***

A catchment routing model is needed to convert the rainfall excess hyetograph produced by the loss model into a surface runoff hydrograph. The models commonly used in previous joint probability studies are reviewed by Rahman et al. (1998). In Australian flood design practice, it is common to use a semi-distributed and non-linear type of catchment routing model, referred to as *runoff routing model.* This type of model, being distributed in nature, can account for the areal variation of rainfall and losses, and consider the non-linearity of the catchment routing response. Examples of models in this group include RORB (Laurenson and Mein, 1988) and URBS (Carroll, 1994), a further development of the concepts embodied in RORB. There is a considerable body of experience available for RORB and similar models on appropriate parameter values for different types of catchments in Australia.

Based on its ready adaptability for the purposes of this project, the URBS model had been proposed for use. However, the proposed modifications of the URBS code to streamline its application within the proposed joint probability modelling framework could not be implemented in the project time frame. As an interim measure, a simple conceptual runoff routing model with a single concentrated storage at the catchment outlet has thus been implemented. This model will be referred to as *single non-linear storage model* henceforth. For catchments in the order of 500 sq km, use of this model with the proposed joint probability framework provides an indication of what could be achieved with URBS. For the single non-linear storage model, the storage-discharge relationship is expressed by:

$$S = kQ^m \tag{2.1}$$

where $S$ is catchment storage in $\boldsymbol{m^3}$, k is a storage delay parameter, $Q$ is the rate of outflow in $m^3/s$ and $m$ is a non-linearity parameter (taken as 0.8 here).

A number of input variables/parameters are involved in the above two steps: (i) design rainfall data: rainfall duration, average rainfall intensity, rainfall temporal pattern; (ii) loss parameters: initial and continuing losses; (iii) runoff routing model parameters; and (iv) baseflow. Design rainfall data are generally available for both gauged and ungauged catchments; the losses, runoff routing model parameters, and baseflow are obtained from observed rainfall and streamflow data (for gauged catchments) or regional equations (for ungauged catchments). The input variables/parameters that need to be considered in a probabilistic fashion are further discussed below.

## 2.2 Input Variables/Parameters Specified in Probabilistic Fashion

The major factors affecting storm runoff production are: rainfall duration, rainfall intensity, temporal and areal patterns of rainfall, and storm losses. Factors affecting hydrograph formation are the catchment response characteristics embodied in the runoff routing model (model type, structure, and parameters) and design baseflow. Ideally, all the variables should be treated as random variables but, for practical reasons, consideration of a smaller number of variables would be preferable, if it did not result in a significant loss of accuracy. Given the dominant role of rainfall and loss in the flood formation process under typical Australian conditions, it might be expected that the incorporation of the probabilistic nature of these variables would result in significant reduction of bias and uncertainties in design flood estimates. Thus, in this initial investigation, four variables have been selected for probabilistic representation: rainfall duration, rainfall intensity, rainfall temporal pattern and initial loss (Rahman et al., 1998; Weinmann et al., 1998). In contrast to this, the traditional design flood simulation methods treat only the rainfall depth as a probabilistic variable.

The areal distribution of rainfall over the catchment is assumed to be uniform, and the average catchment rainfall is obtained from point design rainfall using an areal reduction factor (Siriwardena and Weinmann, 1996). The continuing loss is assumed to be a constant (e.g. the median value from Hill et al., 1996); likewise, a constant baseflow is assumed, determined as the average baseflow at the start of surface runoff generation. A single set of parameter values for the runoff routing model is used here; the calibration procedure allows the determination of a set of model parameters for a given catchment which can be applied with reasonable confidence. It has been left to future studies to determine if the probabilistic treatment of any of these variables might further improve the flood estimates.

## 2.3 Stochastic Modelling Framework

The basic idea underlying the proposed new modelling framework is that the distribution of the flood outputs can be directly determined by simulating the possible combinations of hydrologic model inputs and parameter values. Two stochastic modelling frameworks may be used: the deterministic simulation approach and the stochastic or Monte Carlo simulation approach (Rahman et al, 1998; Weinmann et al., 1998). The first approach uses a discrete representation of continuous probability distributions, and complete enumeration of all possible event combinations. Here, we adopted a Monte Carlo simulation approach for its relative simplicity and flexibility.

For each run of the combined loss and runoff routing model, a specific set of input and model parameter values is selected by randomly drawing values from their respective distributions. Any significant correlation between the variables can be allowed for by using conditional probability distributions. For example, the strong correlation between rainfall duration and intensity can be allowed for by first drawing a value of duration and then a value of intensity from the conditional distribution of rainfall intensity for that duration interval. The results of the run (e.g. the flood peak) are then stored and the Monte Carlo simulation process is repeated a sufficiently large number of times to fully reflect the range of variation of input and parameter values in the generated output. The output values of a selected flood characteristic (e.g. flood peak) can then be subjected to a frequency analysis to determine the derived flood frequency curve.

The adopted Monte Carlo simulation approach is illustrated in Figure 2.1, and the steps involved in the modelling process are detailed below:

- draw a random value of duration $D_i$ from the identified marginal distribution of rainfall duration;
- given the duration $D_i$, draw a random value of rainfall intensity $I_i(D_i)$ from the conditional distribution of rainfall intensity;
- given the duration $D_i$, draw a random temporal pattern $TP_i(D_i)$ from the conditional distribution of temporal pattern (or the set of observed temporal patterns for duration $D_i$);
- given the duration $D_i$, draw a random value of initial loss $IL_i(D_i)$ from the conditional distribution of initial loss;
- run the randomly selected variables $D_i$, $I_i$, $TP_i$, and $IL_i$ (with a constant continuing loss) through the runoff generation and runoff routing models to simulate a flood hydrograph;

- add the baseflow to the simulated flood hydrograph and note the flood peak $Q_i$;
- repeat the above steps $N$ times ($N$ in the order of thousands); and
- use the $N$ simulated flood peaks to determine the derived flood frequency curve in a distribution-free manner using rank-order statistics.

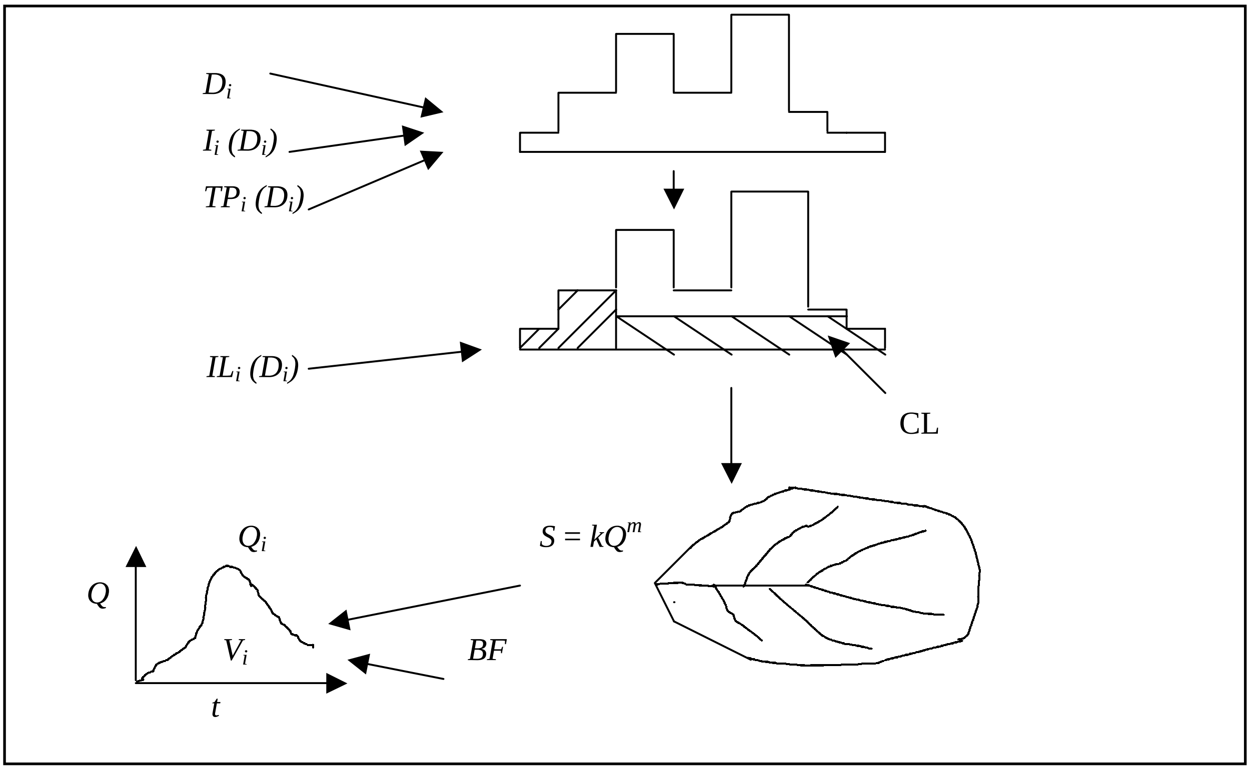


Figure 2.1 Monte Carlo simulation to determine the derived flood frequency curve

## 3. Data Assembly

Two types of data are required for the development of the proposed joint probability approach: (a) pluviograph data to identify probability distributions of rainfall variables (e.g., duration, intensity and temporal pattern); and (b) streamflow data (combined with pluviograph data) to identify the probability distribution of initial loss; streamflow data is also used to assess the adequacy of the proposed joint probability method (e.g., the derived flood frequency curves are compared with the observed flood frequency curves). Furthermore, rainfall and streamflow data for selected flood events are required to calibrate the parameters of the runoff routing model.

The catchments and pluviograph stations selected for this study were restricted to Victoria. This part of south-eastern Australia is dominated by winter rainfall. The selection of study catchments had regard to the following factors:

(i) the catchment should be rural and unregulated;
(ii) the catchment should be small to medium sized (e.g. up to 500 km$^2$ in mountainous regions and 1000 km$^2$ in flat regions);
(iii) the selected set of catchments should cover a wide range of relevant characteristics, e.g. rainfall regime, evaporation, topography and drainage characteristics;
(iv) the catchments should have reasonably long and readily available pluviograph and streamflow data, preferably, a minimum of 25 years of streamflow data, and at least 10 years of concurrent pluviograph and streamflow data;
(v) the streamflow record should contain at least one large flood (e.g. 50-year or 100-year flood); and
(vi) where there is a significant spatial variation of rainfall, the catchment should have well-distributed rain gauges and pluviometers

Considering the above factors, eleven catchments plus three alternatives, i.e. a total of 14 catchments, were selected initially. Most of these catchments were included in the studies by Hill et al., 1996, and Rahman, 1996. The locations of the selected catchments are shown in Figure 3.1. Streamflow record lengths at the selected stations range from 24 to 64 years. The periods of record capture at least one large flood event for most catchments. Catchment sizes are in the range 88-956 km$^2$. The relevant characteristics of the selected catchments are listed in Appendix 1.

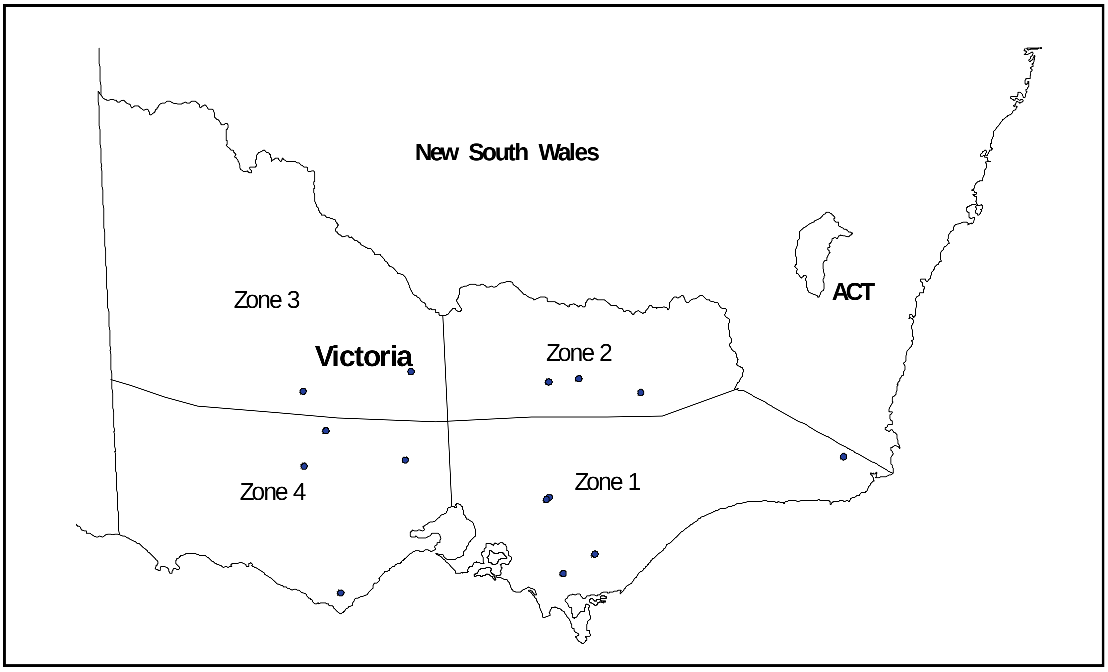


Figure 3.1 Location of the selected catchments and the four study zones for rainfall analysis

The analysis of rainfall characteristics was not limited to the immediate vicinity of the selected catchments, but rather the variation of probability distribution characteristics over the whole of Victoria was examined. A total of 101 pluviograph stations were initially selected; these are distributed all over the state, and have reasonably long records (at least about 20 years). Many of these stations are from Hill (1994). Of these, only 47 stations have been used directly in the analyses described in this report. The 29 pluviograph stations used in the analysis of the distribution of rainfall duration are listed in Table 5.1. For each of the catchment analysed, a selected pluviograph station was used for the analysis of rainfall intensities and temporal patterns. Several stations were used to determine the catchment rainfalls required in the loss computations. The original pluviograph data was processed for this project into hourly accumulations; a 1-hour minimum time step was considered sufficient for the size of catchments selected.

For the purpose of analysing the probability distributions of rainfall characteristics, Victoria was provisionally divided into four hydrometeorological zones, roughly cutting the state into quadrants along the Great Dividing Range and north from Melbourne, as shown in Figure 3.1. This division is made to examine the regional behaviour of the distribution characteristics of the component variables (rainfall duration, rainfall intensity, rainfall temporal pattern, and initial loss). The four quadrants are designated as follows:

- Zone 1 South-eastern Victoria
- Zone 2 North-eastern Victoria
- Zone 3 North-western Victoria
- Zone 4 South-western Victoria.

# 4. Rainfall Event Definitions

The Design Event Approach treats rainfall intensity as a random variable, and uses a number of trial rainfall burst durations with fixed temporal patterns to obtain design flood estimates. In the analysis used to derive the design rainfall data in ARR87, the burst durations were predetermined rather than random (I. E. Aust., 1987). In contrast, the proposed Joint Probability Approach treats all the three rainfall characteristics (i.e. rainfall duration, intensity and temporal pattern) as random variables. Thus, the new event definition has to incorporate the random nature of these three rainfall characteristics. It has to capture all those events that have the potential to produce a flood but, for the sake of simplicity of representation, include only those parts of an event that will have a significant influence on the flood response. A 'complete storm' and a 'storm-core' (the most intense part of the storm) are defined as described below.

***Complete Storm:***

A complete storm is defined in three steps, illustrated in Figure 4.1 (Hoang et al., 1999):

- Step 1: A 'gross' storm is a period of rain starting and ending by a non-dry hour (i.e. hourly rainfall > $C_1$ mm/h), preceded and followed by at least six dry hours.
- Step 2: 'Insignificant rainfall' periods at the beginning or at the end of a gross storm, if any, are then cut off from the storm, the remaining part of the gross storm being called the 'net' storm. [A period is defined as 'having insignificant rainfall' if all individual hourly rainfalls ≤ $C_2$ (mm/h), and average rainfall intensity during the dry period ≤ $C_1$ (mm/h)].
- Step 3: The net storms, from now on simply referred to as complete storms, are then evaluated in terms of their potential to produce significant storm runoff. This is performed by assessing their rainfall magnitudes, i.e. by comparing their average intensities with threshold intensities. A net storm is only selected for further analysis if the average rainfall intensity during the entire storm duration ($RFI_D$) or during a sub-storm duration ($RFI_d$), satisfies one of the following two conditions:

$$RFI_D \leq F1 \times {}^2I_D$$
$$RFI_d^{\max} \geq F2 \times {}^2I_d$$

where ${}^2I_D$ is the 2 year ARI intensity for the selected storm duration $D$, and ${}^2I_d$ the corresponding intensity for the sub-storm duration $d$. The values of ${}^2I_D$ and ${}^2I_d$ are estimated from the design rainfall data in Australian Rainfall and Runoff (ARR87).

In the above event definition, the use of appropriate reduction factors $F1$ and $F2$ allows the selection of only those events that have the potential to produce significant storm runoff. The use of smaller values of $F1$ and $F2$ captures a relatively larger number of events; appropriate values need to be selected such that events of very small average intensity are not included. In this study, the following parameter values have been found to be appropriate: $F1$ = 0.4, $F2$ = 0.5, $C_1$ = 0.25 (mm/h), and $C_2$ = 1.2 (mm/h). This typically resulted in 3 to 6 rainfall events, on average, being selected per year.

***Storm-Core:***

The available IFD information in ARR87 is not based on complete storms but on periods of *intense rainfall within complete storms*, called bursts. If this existing information is to be used with the proposed new approach, it is more useful to undertake the design rainfall analysis in terms of storm bursts. However, as the duration of the bursts in the ARR87 analysis was predetermined rather than random, it is necessary to consider a new storm burst definition that will produce randomly distributed storm burst durations. These newly defined storm bursts are referred to as *storm-cores* (Rahman et al, 1998).

For each *complete storm*, a single *storm-core* can be identified, defined as "the most intense rainfall burst within a complete storm". It is found by calculating the average intensities of all possible storm bursts, and the ratio with an index rainfall intensity ${}^2I_d$ for the relevant duration $d$, then selecting the burst of that duration which produces the highest ratio. In Figure 4.2, the storm-core has a duration of 3 hours. For that duration the ratio with ${}^2I_3$ is 3.0, compared to a value of 1.4 for a duration of 1 hour.

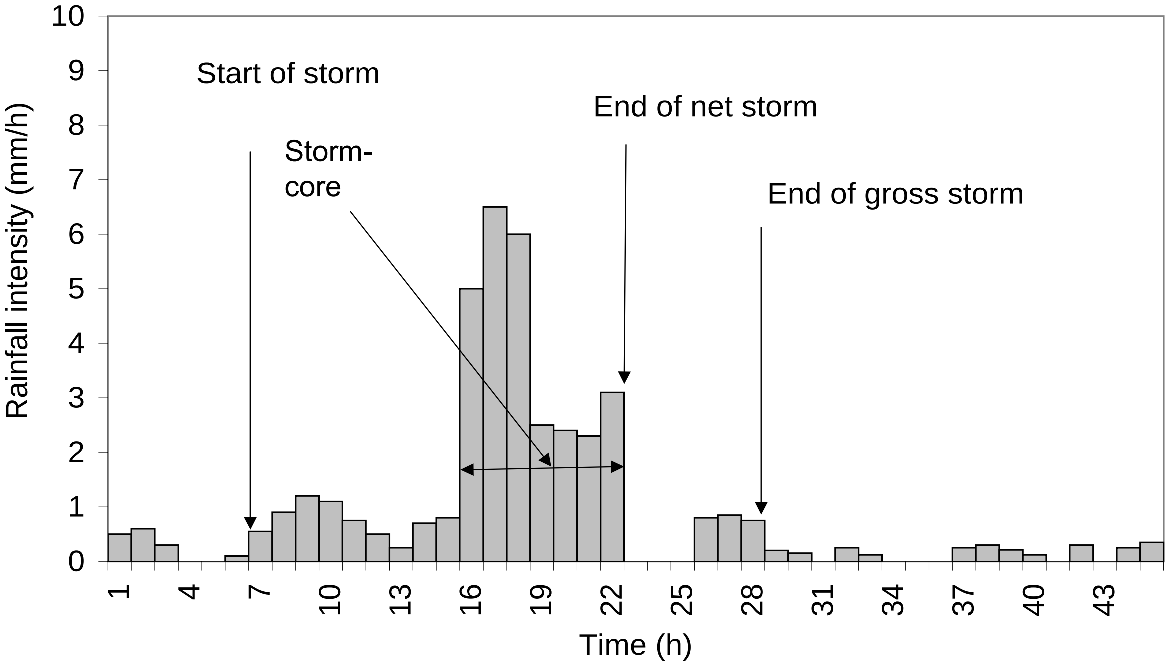


Figure 4.1 Rainfall events: complete storms and storm-cores

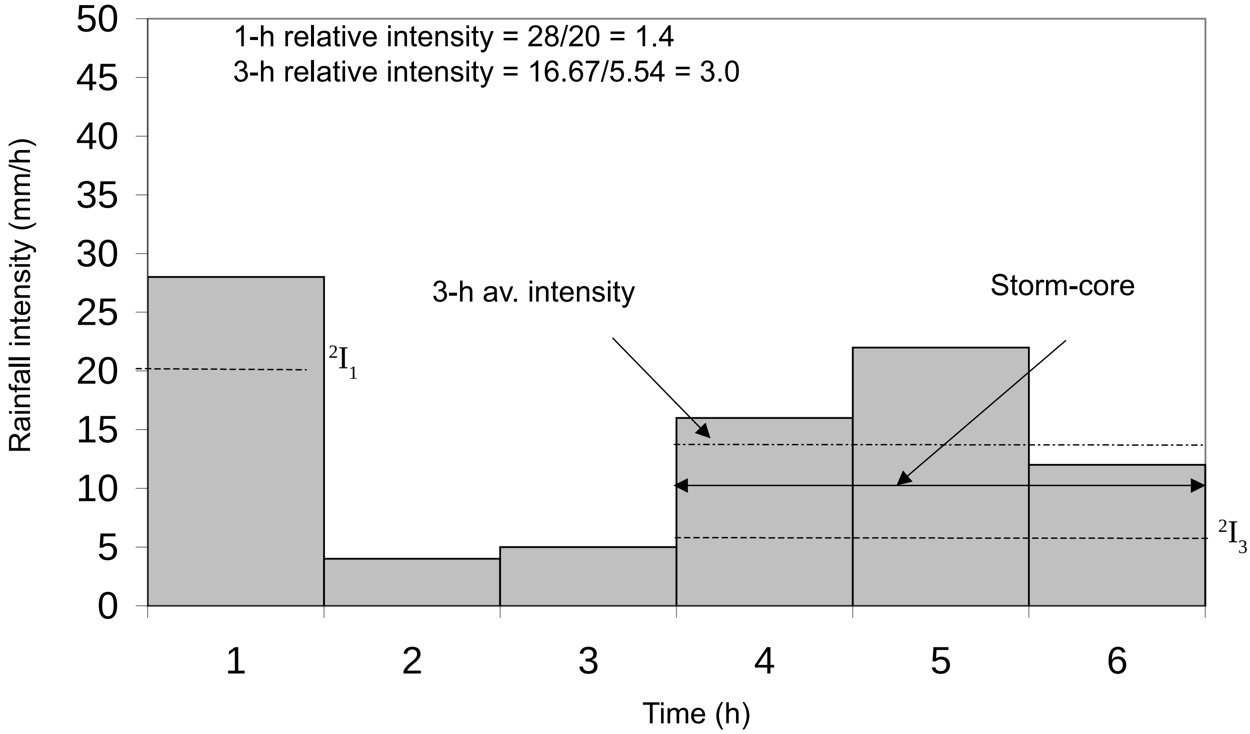


Figure 4.2 Identification of a storm-core

# 5 Identification of Component Distributions

Four input variables/parameters (component distributions) have been selected in Chapter 2 for stochastic description: rainfall duration, rainfall intensity, rainfall temporal pattern and initial loss. The identification of the marginal or conditional distributions of these components is described below.

## 5.1 Storm-Core Duration

The distributions of storm-core duration ($D_c$) have been obtained for 29 pluviograph stations spread over the whole of Victoria, but with the greatest concentration of stations in Zone 4 (South-western Victoria). The mean, standard deviation and skewness of the observed $D_c$ values for these stations are listed in Table 5.1. Figure 5.1 shows a typical histogram of the frequencies of different storm-core durations, indicating that $D_c$ values are exponentially distributed. This implies that, at a particular station, there are many more short duration storm-cores than longer duration ones, and that number of storms reduces exponentially with duration.

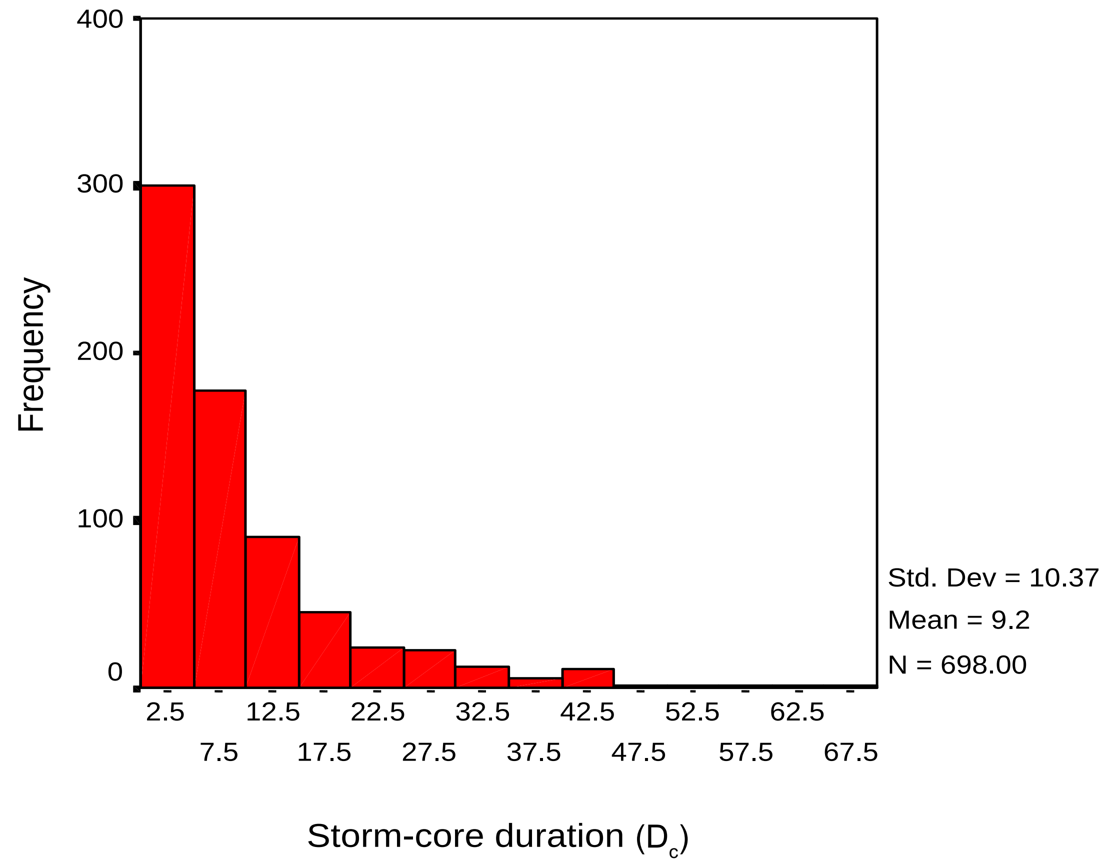


Figure 5.1 Histogram of storm-core durations ($D_c$) at Melbourne (86071)

Table 5.1 Some important statistics of the observed storm-core durations ($D_c$) at the 29 pluviograph stations

| Pluvio station | Name | Study zone | Record length (years) | No. of observed events | Av. no. of events per year | Statistics of storm-core durations ($D_c$) | | |
|---|---|---|---|---|---|---|---|---|
| | | | | | | Mean | S.D. | Skewness |
| 85034 | Glenmaggie Weir | 1 | 37 | 167 | 4.51 | 11.35 | 13.85 | 2.00 |
| 85072 | East Sale AMO | 1 | 39 | 196 | 5.02 | 12.51 | 12.70 | 1.53 |
| 85240 | Ellinbank | 1 | 33 | 290 | 8.78 | 13.28 | 16.09 | 1.88 |
| 86038 | Essendon Airport | 1 | 36 | 191 | 5.30 | 10.47 | 11.36 | 2.09 |
| 86071 | Melbourne | 1 | 125 | 698 | 5.58 | 9.21 | 10.36 | 2.31 |
| 86142 | Mt St Leonard | 1 | 30 | 198 | 6.6 | 12.94 | 16.41 | 2.36 |
| 86314 | Koo-Wee-Rup | 1 | 35 | 236 | 6.74 | 14.22 | 17.01 | 1.98 |
| 82121 | Wangaratta | 2 | 36 | 208 | 5.77 | 11.46 | 10.67 | 1.51 |
| 88023 | Lake Eildon | 2 | 36 | 241 | 6.69 | 9.41 | 11.36 | 2.20 |
| 76031 | Mildura MO | 3 | 40 | 151 | 3.77 | 10.24 | 8.52 | 1.77 |
| 80067 | Charlton | 3 | 42 | 167 | 3.97 | 10.62 | 10.25 | 2.43 |
| 79052 | Rocklands Res | 4 | 38 | 189 | 4.97 | 10.77 | 12.63 | 2.64 |
| 87029 | Lancefield | 4 | 46 | 249 | 5.41 | 14.59 | 16.13 | 1.87 |
| 87031 | Laverton AMO | 4 | 28 | 174 | 6.21 | 8.98 | 8.88 | 1.80 |
| 87033 | Little River | 4 | 17 | 79 | 4.64 | 7.91 | 6.62 | 1.31 |
| 87036 | Macedon - Forestry | 4 | 45 | 198 | 4.40 | 14.16 | 16.58 | 1.99 |
| 87061 | Sunbury | 4 | 38 | 231 | 6.07 | 10.55 | 11.80 | 1.88 |
| 87075 | Bullengarook East | 4 | 27 | 152 | 5.62 | 12.28 | 14.26 | 1.91 |
| 87097 | Parwan | 4 | 19 | 97 | 5.10 | 11.16 | 12.32 | 2.18 |
| 87104 | Werribee Cattle Yard | 4 | 18 | 108 | 6.00 | 10.26 | 10.06 | 1.41 |
| 87105 | Werribee | 4 | 15 | 79 | 5.27 | 9.08 | 8.47 | 1.89 |
| 87133 | Geelong North | 4 | 21 | 53 | 2.52 | 8.85 | 9.40 | 2.21 |
| 89002 | Ballarat Composite | 4 | 39 | 208 | 5.33 | 12.75 | 17.10 | 2.76 |
| 89016 | Lake Bolac PO | 4 | 25 | 115 | 4.60 | 10.15 | 11.05 | 2.47 |
| 89019 | Mirranatwa | 4 | 19 | 96 | 5.05 | 12.07 | 15.28 | 2.19 |
| 89025 | Skipton | 4 | 17 | 87 | 5.12 | 14.31 | 15.71 | 1.74 |
| 90087 | Wyelangata | 4 | 41 | 226 | 5.51 | 22.19 | 32.30 | 2.64 |
| 90135 | Casterton | 4 | 20 | 111 | 5.55 | 12.96 | 17.02 | 2.06 |
| 90153 | Camperdown RWC | 4 | 36 | 180 | 5.00 | 15.66 | 16.47 | 1.63 |

The exponential distribution has one parameter and its probability density function is given by:

$$p(D_c) = \frac{1}{\beta} e^{-D_c/\beta} \qquad (5.1)$$

where $p$ ( ) stands for probability density, $D_c$ is the storm-core duration and $\beta$ is the parameter of the exponential distribution.

The parameter $\beta$ can be taken as the mean of the observed $D_c$ values. The exponential distribution has a skewness of 2, and its mean and standard deviation are equal. The results in Table 5.1 show that the data at all stations satisfy these assumptions approximately. A Chi-squared test showed that the hypothesis of an exponential distribution cannot be rejected (at the 5% level of significance). The generated $D_c$ data from the fitted exponential distribution for Station 83031 (used in Chapter 9 to obtain the derived flood frequency curve for Boggy Creek) are compared in Figure 5.2 with the observed $D_c$ data.

Inspection of the data in Table 5.1 also indicates that the stations in each of the four study zones form a relatively homogeneous data set with respect to rainfall duration. For the seven pluviograph stations in Study Zone 1 (south-east quadrant of Victoria), the regional average $D_c$ is 12 hours, and the lower and upper 95% confidence limits (CLs) for the mean are 10.38 and 13.61 hours, respectively. The regional average skewness is 2.02 and the 95% CLs for the skewness are 1.76 and 2.27 respectively. A hypothesis test using the t-distribution shows that the regional average skewness is not significantly different from 2.0 at a significance level of 5%. The fitted regional distribution of $D_c$ with upper and lower 95% CL estimates for the mean for Study Zone 1 is shown in Figure 5.3, indicating that the confidence interval is remarkably narrow. This implies that the fitted distribution with mean $D_c$ equal to 12 hours can be safely taken as the regional distribution of $D_c$ for Study Zone 1.

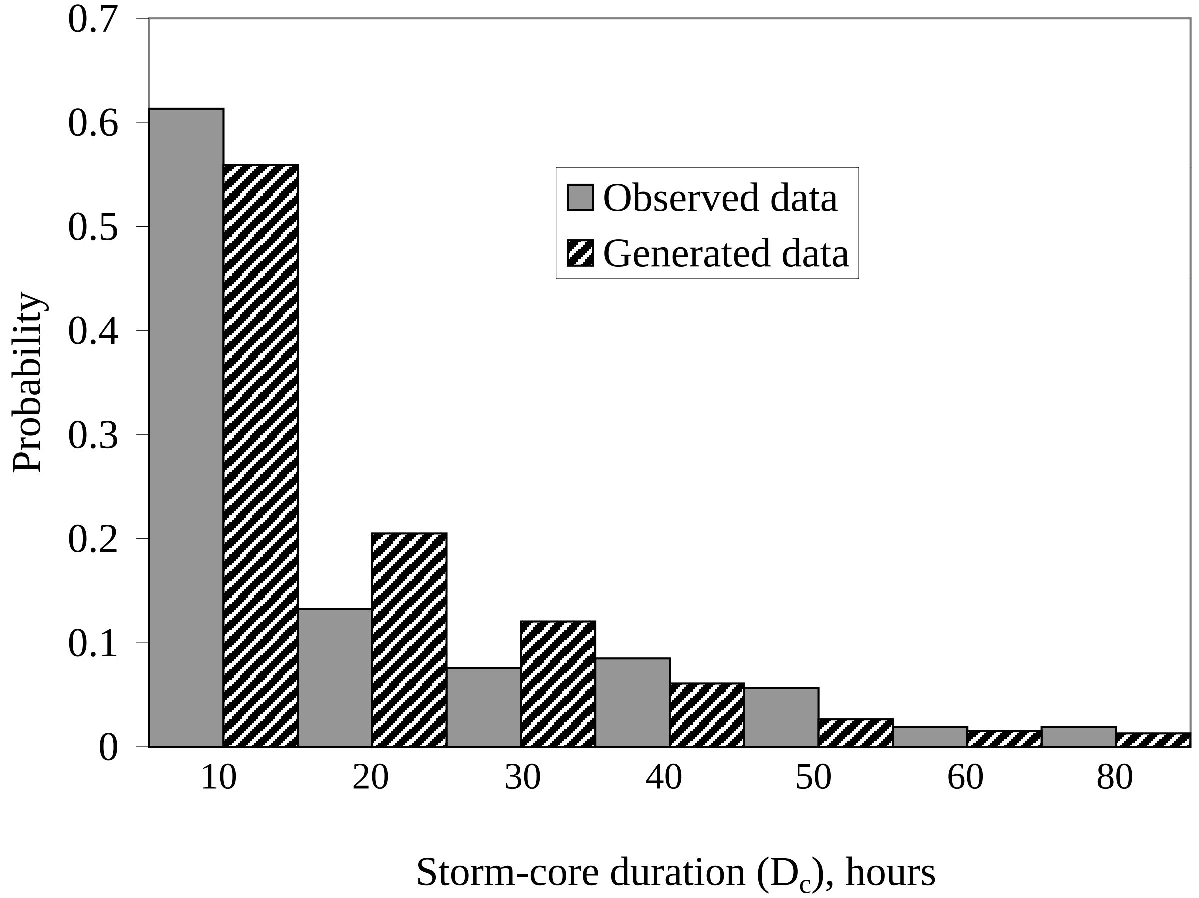


Figure 5.2 Generated and observed $D_c$ data at Station 83031

The regional distribution of $D_c$ for Study Zone 4 (south-west quadrant of Victoria), based on 18 pluviograph stations, is shown in Figure 5.4. For this study zone, the mean and 95% CLs for the mean are 12.15, 10.48 and 13.81 hours, respectively. The regional average skewness is 2.03 and the 95% CLs for skewness are 1.83 and 2.23, respectively.

The data sets in Study Zones 2 and 3 were too small for a regional analysis, but there is no indication from the data that the distribution parameters would be markedly different from the other zones.

It can thus be concluded from this analysis that the distribution of storm-core durations in Victoria can be described by an exponential distribution. There appear to be only small differences in distribution parameters for different parts of Victoria, and further analysis may confirm that a single distribution could adequately describe the variation of storm-core durations for Victoria. The sensitivity of the Monte Carlo simulation results to small changes in the distribution of $D_c$ is discussed in Section 9.3.1.

A separate analysis of pluviograph data for complete storms showed the 3-parameter generalised Pareto distribution to be the most appropriate distribution to describe the duration of complete storms in Victoria (Hoang et al., 1999).

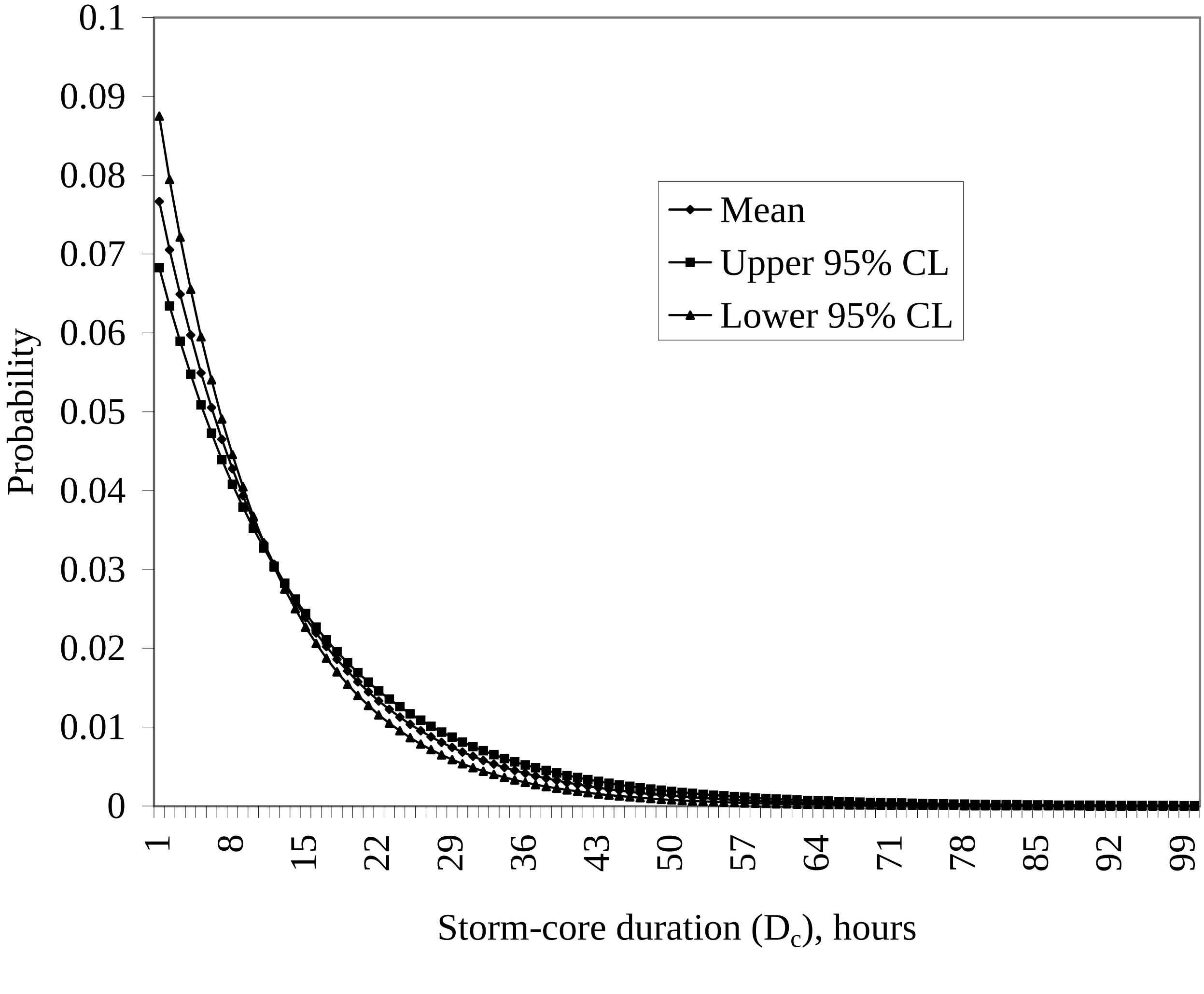


Figure 5.3 Regional distribution of storm-core duration ($D_c$) for Study Zone 1

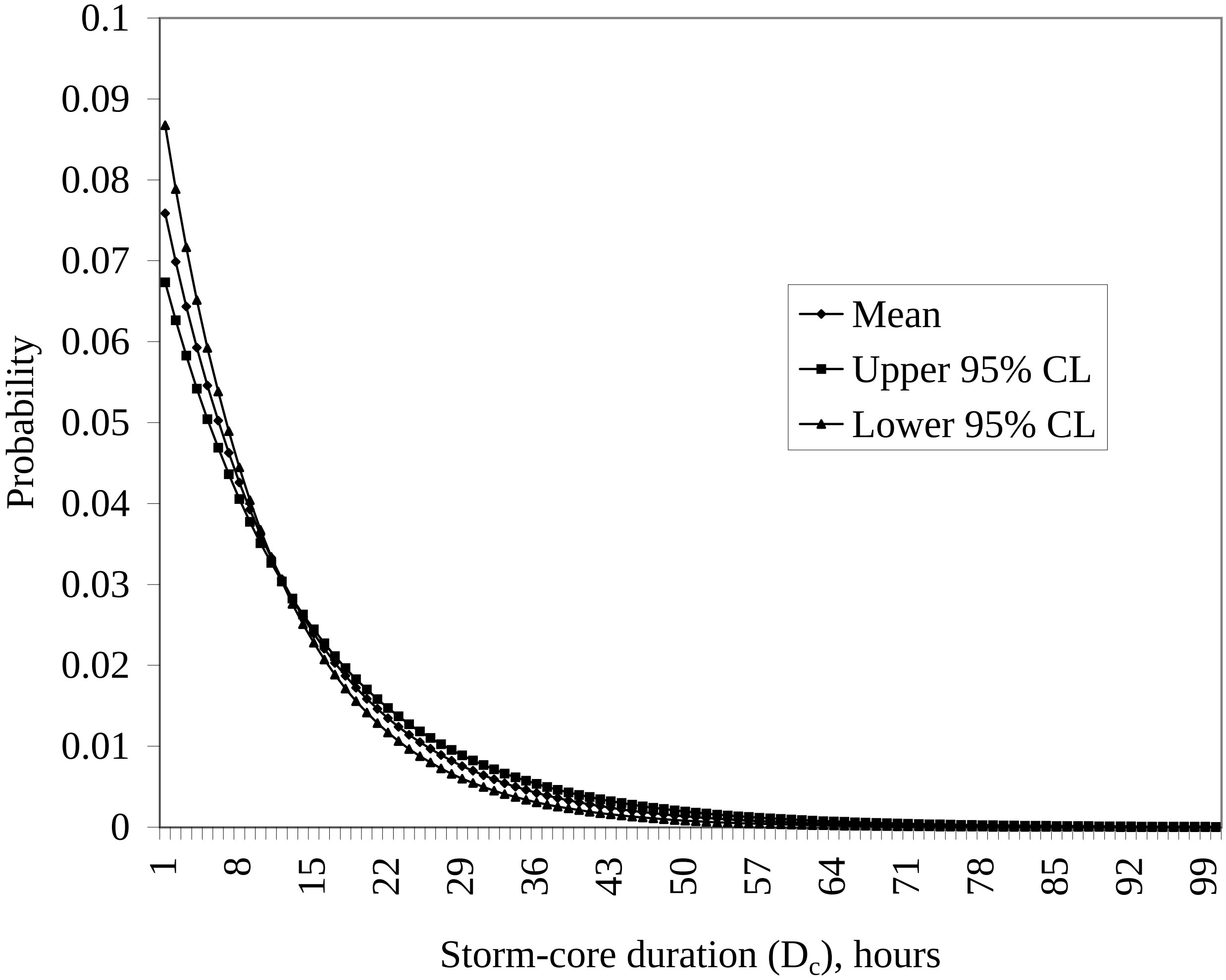


Figure 5.4 Regional distribution of storm-core duration ($D_c$) in Study Zone 4

## 5.2 Storm-Core Rainfall Intensity

In practice, the conditional distribution of rainfall intensity is expressed in the form of intensity-frequency-duration (IFD) curves, where rainfall intensity is plotted as a function of rainfall duration and frequency. In the Joint Probability Approach adopted here, the IFD curves for storm-core rainfall intensity have been developed in a number of steps, as described below. A comparison of these curves with storm burst IFD curves (i.e. ARR IFD curves) is also presented.

### 5.2.1 Development of Storm-Core IFD Curves

The rainfall intensity data from 15 pluviograph stations in Victoria (Table 5.2) were analysed to derive IFD curves. These stations are well distributed over Victoria with at least two stations from each of the four study zones. The stations have record lengths ($N$) in the range from 19 to 123 years (for 13 stations $N$ >34 years). The average number of selected storm-core events at a station is 218 (on average 5 events per year). These events were selected using the procedures and parameter values described in Section 4.

The initial examination of the storm-core data from these stations showed a strong relationship between storm-core rainfall intensity ($I_c$) and duration ($D_c$), as shown in Figure 5.5 for the example of Melbourne. The average coefficient of determination ($R^2$) for such relationships over the 15 stations is 0.83 (range: 0.77-0.90).

Table 5.2 Pluviograph station list for IFD analysis

| Station ID | Name | Study zone | Record length | No. of events | Av no. of events per year |
|---|---|---|---|---|---|
| 85034 | Glenmaggie Weir | 1 | 35 | 167 | 4.77 |
| 85072 | East Sale AMO | 1 | 40 | 197 | 4.93 |
| 86071 | Melbourne | 1 | 123 | 698 | 5.67 |
| 86314 | Koo Wee Rup | 1 | 34 | 236 | 6.94 |
| 82121 | Wangaratta | 2 | 36 | 208 | 5.78 |
| 83033 | Woods Point | 2 | 36 | 118 | 3.28 |
| 88023 | Lake Eildon | 2 | 36 | 241 | 6.69 |
| 76031 | Mildura MO | 3 | 40 | 151 | 3.78 |
| 80067 | Charlton | 3 | 42 | 167 | 3.98 |
| 79052 | Rockland Reserve | 4 | 38 | 189 | 4.97 |
| 86038 | Essendon Airport | 4 | 36 | 191 | 5.31 |
| 89002 | Ballarat comp. | 4 | 39 | 208 | 5.33 |
| 89016 | Lake Bolac | 4 | 25 | 115 | 4.60 |
| 90083 | Weeaproinah | 4 | 19 | 203 | 10.68 |
| 90153 | Camperdown RWC | 4 | 35 | 180 | 5.14 |
| | **Average** | | **41** | **218** | **5** |

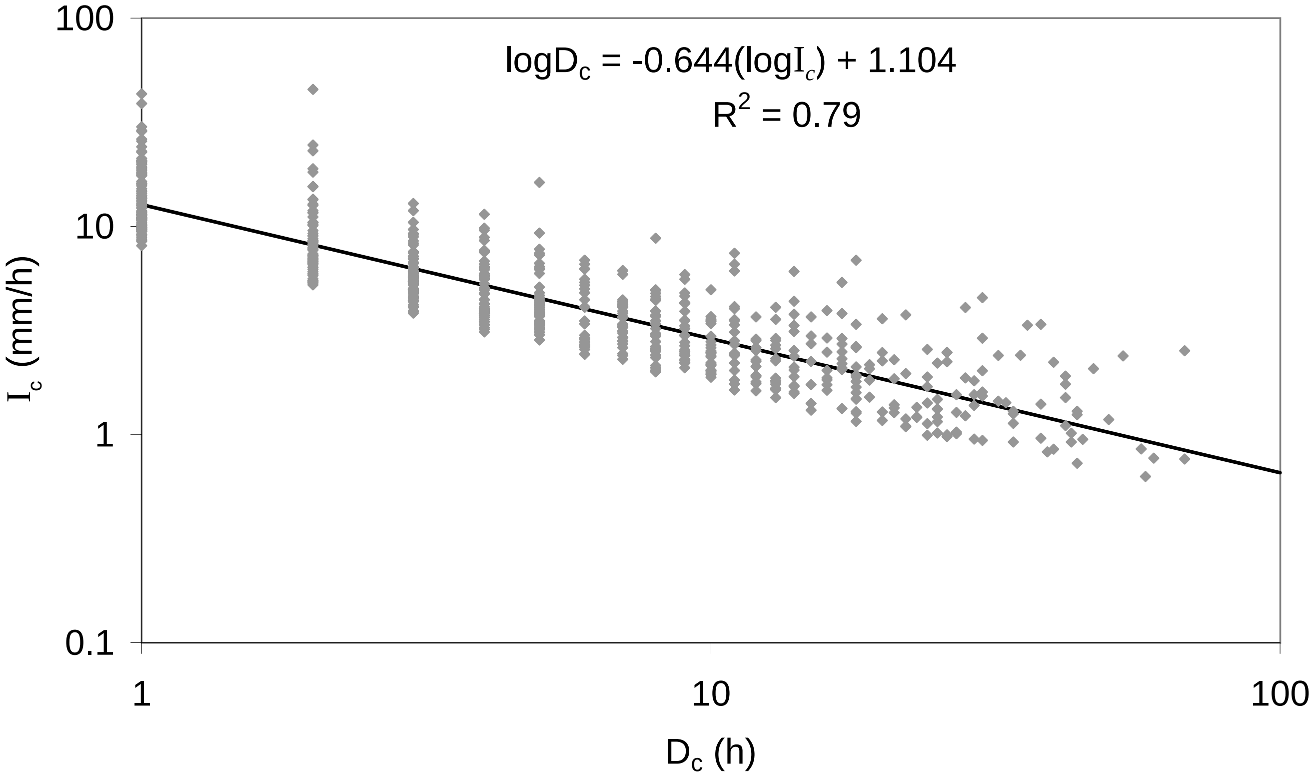


Figure 5.5 Relationship between storm-core duration $D_c$ (h) and storm-core rainfall intensity $I_c$ (mm/h) at Melbourne (Station 86071)

The strong relationship between $D_c$ and $I_c$ means that the distribution of $I_c$ needs to be conditioned on $D_c$. The procedure adopted to develop storm-core IFD curves is outlined below.

(i) The range of storm-core durations $D_c$ is divided into a number of class intervals (with a representative or mid point for each class). An example is given in Table 5.3.

(ii) For the data in each class interval (except the 1h class), a linear regression line is fitted between log($D_c$) and log($I_c$). The slope of the fitted regression line is used to adjust the intensities for all durations within the interval to the representative point. The procedure is illustrated in Figure 5.6, where the class interval is 4 to 12 hours (0.60 to 1.08 in log scale), the representative point is 6 hours (0.78 in log scale). Intensities for other than 6 hours are adjusted to the 6-hour equivalent. For example, for the 8-hour intensities:

$$I_{adjusted} = 10\text{^}(\log(I_a) + 0.6298*(\log D_a - \log D_b))$$

where the indices $a$ and $b$ correspond to the 8 and 6-hour durations, respectively.

Table 5.3 An example of class intervals and representative points for storm-core duration ($D_c$) for developing IFD curves

| Class interval (hours) | Representative point (hours) |
|---|---|
| 1 | 1 |
| 2 - 3 | 2 |
| 4 - 12 | 6 |
| 13 - 36 | 24 |
| 37 - 96 | 48 |

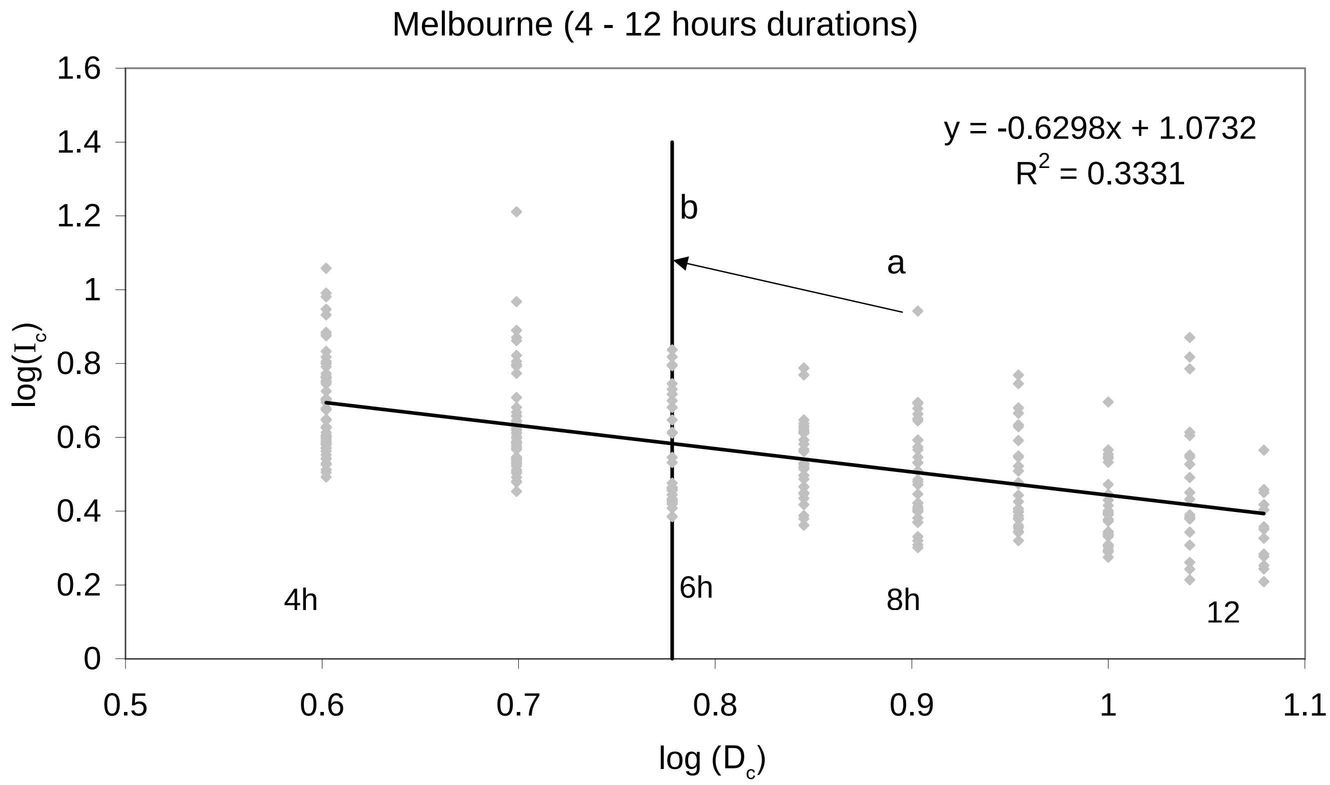


Figure 5.6 Adjustment of $I_c$ values of varying durations to a common duration (i.e. representative point of a class interval)

(iii) The adjusted intensity values in a duration class interval form a partial series. An exponential distribution is fitted to the to the partial series $I_i$ ($i$ = 1, …, $M$), where $M$ is the number of data points in a class. Quantiles are obtained from the following equation:

$$I(\mathrm{T}) = I_0 + \beta \ln(\lambda T) \qquad (5.2)$$

where $I_0$ is the smallest value in the series; $\beta = \Sigma I_i/M - I_0$; $\lambda = M/N$; $N$ is the number of years of data; and $T$ is the average recurrence interval (ARI) in years. (In addition to the exponential distribution, a Log Pearson Type 3 [$LP$3] distribution was also fitted to the partial series data, and it was found that the exponential distribution, in general, provides a better fit.)

Adopting the fitted distribution, design rainfall intensity values $I_c(T)$ for the given duration interval are computed for ARIs of 2, 5, 10, 20, 50 and 100 years.

(iv) For a selected ARI, the computed $I_c(T)$ values for each duration range are used to fit a second degree polynomial between $\log(D_c)$ and $\log(I_c)$ (Figure 5.7):

$$\log(I_c) = a(\log(D_c))^2 + b(\log(D_c)) + c \qquad (5.3)$$

where $a$, $b$ and $c$ are constants. As an example, for pluviograph station Melbourne (86071), for an ARI of 5 years, $a$ = 0.1039, $b$ = - 0.7998, $c$ = 1.3351 and $R^2$ = 99.7%.

For the 15 pluviograph stations and for all the selected ARIs, the observed $R^2$ values were greater than 98%, which implies that confidence can be placed on the fitted polynomials. These polynomials can be used to obtain for each selected ARI a value of rainfall intensity $I_c$ for any duration $D_c$. The observed $D_c$ values are normally less than 72 hours; however, there are some values near 100 hours for some stations. The limits for $D_c$ have thus been set as 1 to 100 hours to cover the practical range of interest in generated storm-core durations for the Monte Carlo simulation. The set of storm-core IFD curves obtained for Melbourne is presented in Figure 5.8; the separately fitted curves for different ARIs show a high degree of consistency.

The application of this procedure to the 15 pluviograph stations produced a generally consistent set of IFD curves. However, the limited record length available at some stations means that the 100 years ARI rainfall estimates are associated with considerable uncertainty.

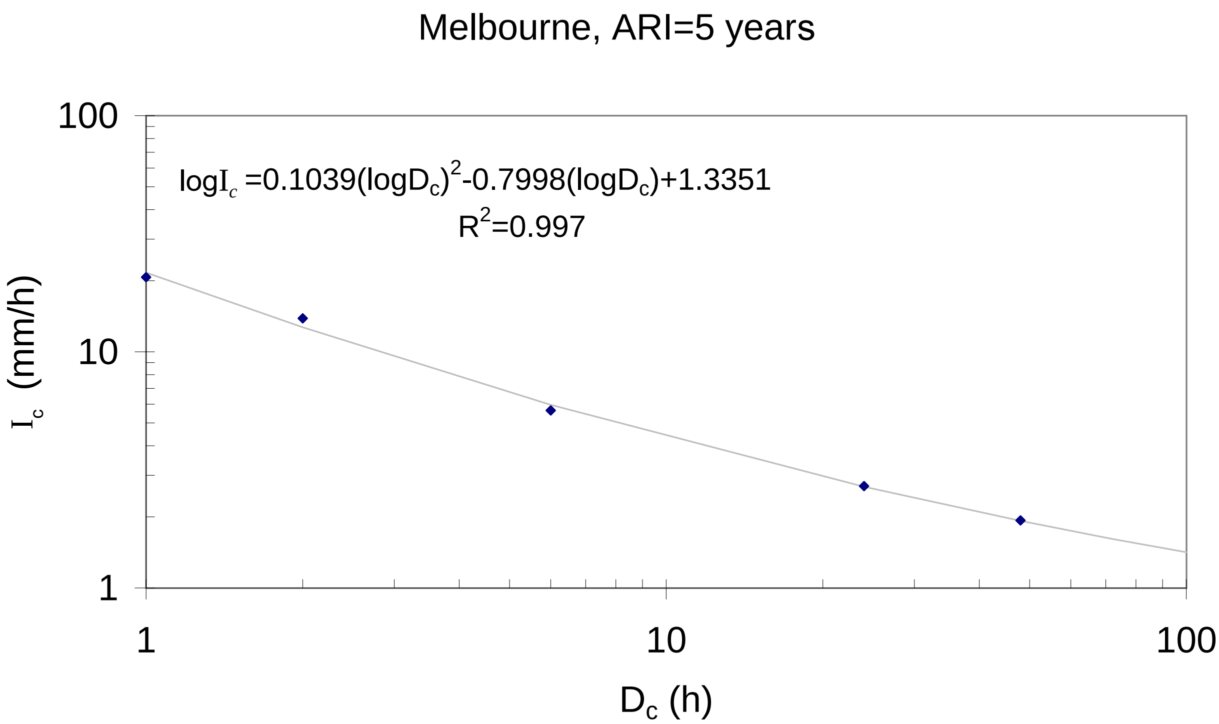


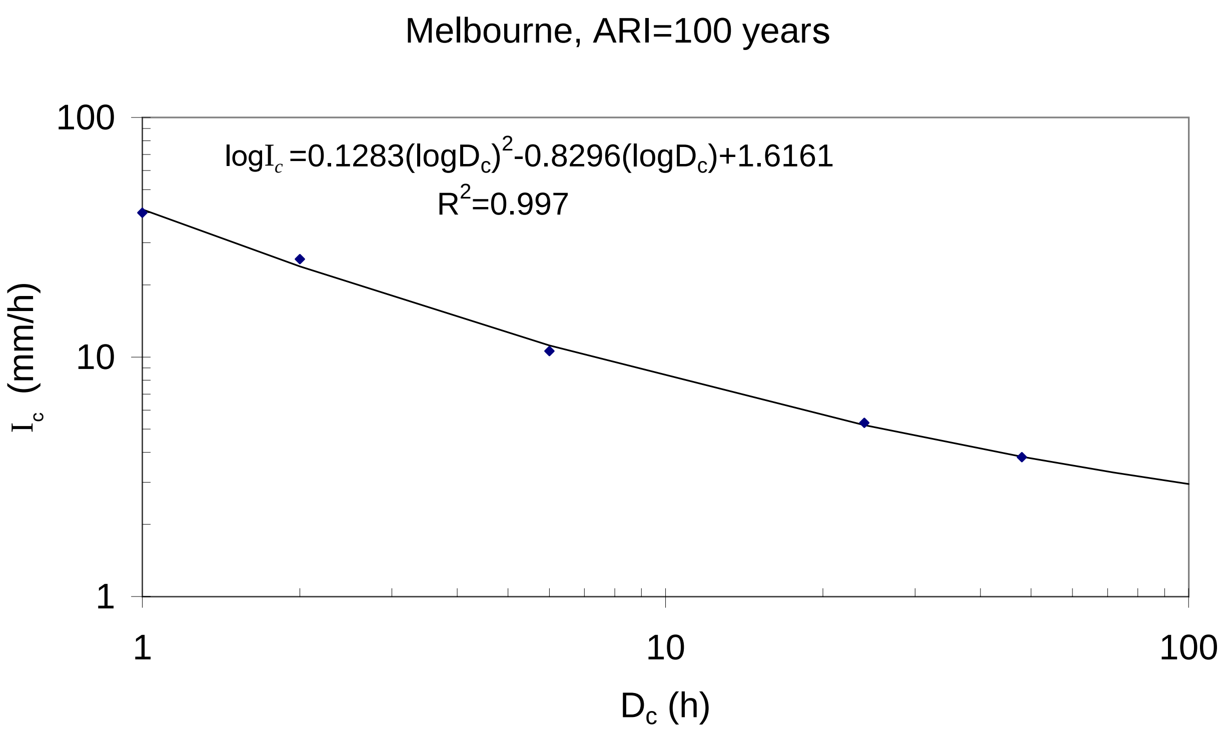


Figure 5.7 Fitting a second degree polynomial between $D_c$ and computed $I_c$ (Station: Melbourne, ARI of 5 and 100 years)

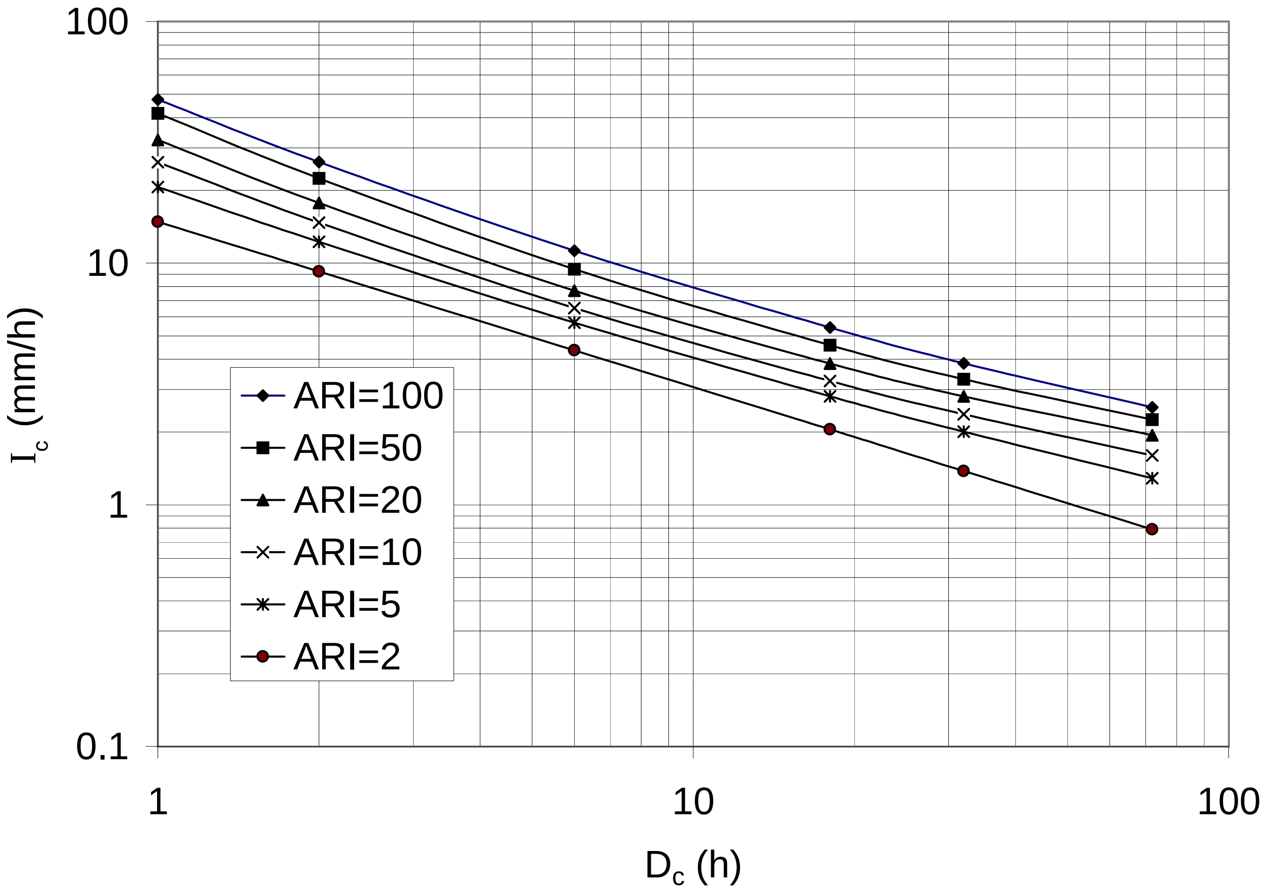


Figure 5.8 Storm-core IFD curves for Melbourne

**5.2.2 Preparation of IFD Table**

The adopted Monte Carlo simulation scheme will start with the generation of a $D_c$ value from its marginal distribution. Given this $D_c$ and a randomly generated ARI value, the rainfall intensity value $I_c$ will then be drawn from the conditional distribution of $I_c$, expressed in the form of IFD curves. This requires the definition of a continuous distribution function, ideally in the form of a functional relationship between $D_c$, $I_c$ and *ARI*. However, as it is difficult to derive a functional relationship that suits different conditions, an IFD table will be used with an interpolation procedure to generate $I_c$ values, for any given combination of $D_c$ and ARI.

Equations 5.2 and 5.3 are the basis of the IFD table; computed $I_c$ values for selected $D_c$ and ARIs are tabulated. An example of an IFD table, used for data generation in the adopted Monte Carlo simulation scheme, is shown in Table 5.4. Here, $I_c$ values are tabulated for $D_c$ values of 1, 2, 6, 24, 48, 72 and 100 hours, and ARIs of 0.1, 1, 1.11, 1.25, 2, 5, 10, 20, 50, 100, 500, 1,000 and 1,000,000 years. A selection of the corresponding IFD curves is plotted in Figure 5.9. A linear interpolation in the log domain is used between the tabulated values of $D_c$ and ARI.

It should be noted here that $I_c$ values for ARIs less than 1 year and greater than 100 years are of less direct interest in the development of derived flood frequency curves for design flood estimation up to the limit of the 100-year flood. However, these extrapolated values are required to cover the range that might arise in the Monte Carlo simulation. The part of the developed IFD curves for ARIs of 100 to 1,000,000 years is subject to very large estimation errors from pluviograph data of limited lengths (normally less than 50 years). Where the interest is on rare to extreme floods (ARI greater than 100 years), this part of the curves needs to be adjusted using design rainfall data from some appropriate regionalisation approach (e.g. the CRC-FORGE method [Nandakumar et al., 1997; Weinmann et al., 1999]). The effect on the derived flood frequency curve of adjustments to the upper tail of the rainfall frequency curve is discussed in Section 9.3.2.

Table 5.4 An example of IFD table used in data generation (Pluviograph station 83031, Catchment: Boggy Creek). Intensities are in mm/h.

| **Dc (hours)** | **ARI (years)** | | | | | | | | | | | | |
|---|---|---|---|---|---|---|---|---|---|---|---|---|---|
| | **0.1** | **1** | **1.11** | **1.25** | **2** | **5** | **10** | **20** | **50** | **100** | **500** | **1000** | **1000000** |
| 1 | 10.100 | 13.593 | 14.409 | 15.321 | 18.964 | 26.076 | 31.460 | 36.848 | 43.972 | 49.364 | 61.885 | 67.278 | 121.042 |
| 2 | 6.663 | 8.529 | 8.964 | 9.411 | 11.266 | 14.877 | 17.604 | 20.329 | 23.939 | 26.652 | 32.971 | 35.692 | 62.797 |
| 6 | 3.356 | 4.183 | 4.368 | 4.574 | 5.396 | 6.993 | 8.199 | 9.404 | 10.996 | 12.199 | 14.992 | 16.194 | 28.171 |
| 24 | 1.347 | 1.782 | 1.891 | 2.012 | 2.491 | 3.415 | 4.109 | 4.802 | 5.715 | 6.405 | 8.006 | 8.694 | 15.550 |
| 48 | 0.837 | 1.186 | 1.280 | 1.385 | 1.807 | 2.633 | 3.262 | 3.891 | 4.724 | 5.355 | 6.822 | 7.454 | 13.757 |
| 72 | 0.630 | 0.940 | 1.028 | 1.126 | 1.528 | 2.332 | 2.952 | 3.577 | 4.409 | 5.041 | 6.514 | 7.151 | 13.516 |
| 100 | 0.498 | 0.781 | 0.864 | 0.958 | 1.348 | 2.149 | 2.775 | 3.412 | 4.265 | 4.916 | 6.439 | 7.098 | 13.718 |

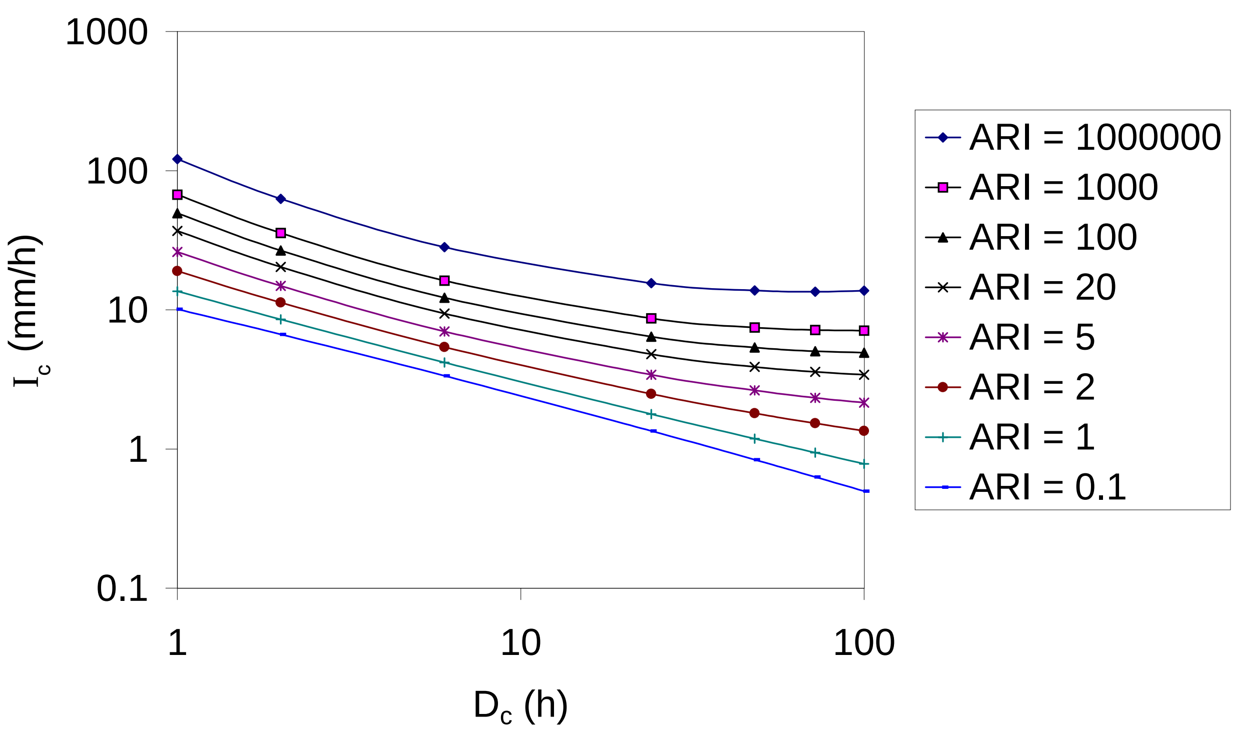


Figure 5.9 Storm-core IFD curves at Station 83031 (used in Chapter 9 to obtain the derived flood frequency curve for Boggy Creek). ARI in years.

### 5.2.3 Comparison of Storm-Core and ARR 87 IFD Curves

A key issue for the practical application of the new approach is whether the IFD curves for storm-cores, $IFD_{storm\text{-}core}$, are similar to the currently used design rainfall IFD curves for the storm bursts. The derived IFD curves for a station can be compared with two other IFD curves: (a) regional design values for fixed duration storm bursts from *ARR 87* (Chapter 2 and Vol 2), referred to as $IFD_{ARR}$, and (b) values from an at-site analysis of storm bursts using procedures consistent with ARR87 ($IFD_{burst}$). The type (b) curves are more directly comparable with the at-site IFD curves developed here, as they are directly based on the data available at the site, without the use of data from other stations or any form of regional smoothing. The $IFD_{burst}$ curves were obtained using a routine in the HYDSYS package (HYDSYS, 1994).

The storm bursts used in ARR87 and the storm-cores used here have different sampling properties: an observed intense rainfall spell is included only once in the storm-core database, but parts of it may have been included several times in the burst rainfall database, as a shorter duration burst may form part of a longer duration burst. Thus the burst series will consist of higher values relative to storm-cores, and hence the $IFD_{storm\text{-}core}$ curve will be consistently located below the $IFD_{burst}$ curve. However, the difference will reduce with increasing duration; at higher durations both the samples will share many common events. The empirical results for the 15 stations analysed here are generally consistent with the above sampling properties of bursts and storm-cores (see example in Figure 5.10).

Examination of the results of the IFD analysis for different stations shows a fairly regular relationship between the $IFD_{storm\text{-}core}$ and $IFD_{burst}$ curves. The ratio of these two IFD curves, the IFD adjustment factor, depends on $D_c$ and ARI, as shown in Figure 5.10. The IFD adjustment factor could be used to estimate storm-core *IFD* values from ARR87 *IFD* values for a given duration $D_c$ and ARI, to allow ready application to ungauged sites. However further work is required to generalise the relationship of the adjustment factors with duration and ARI.

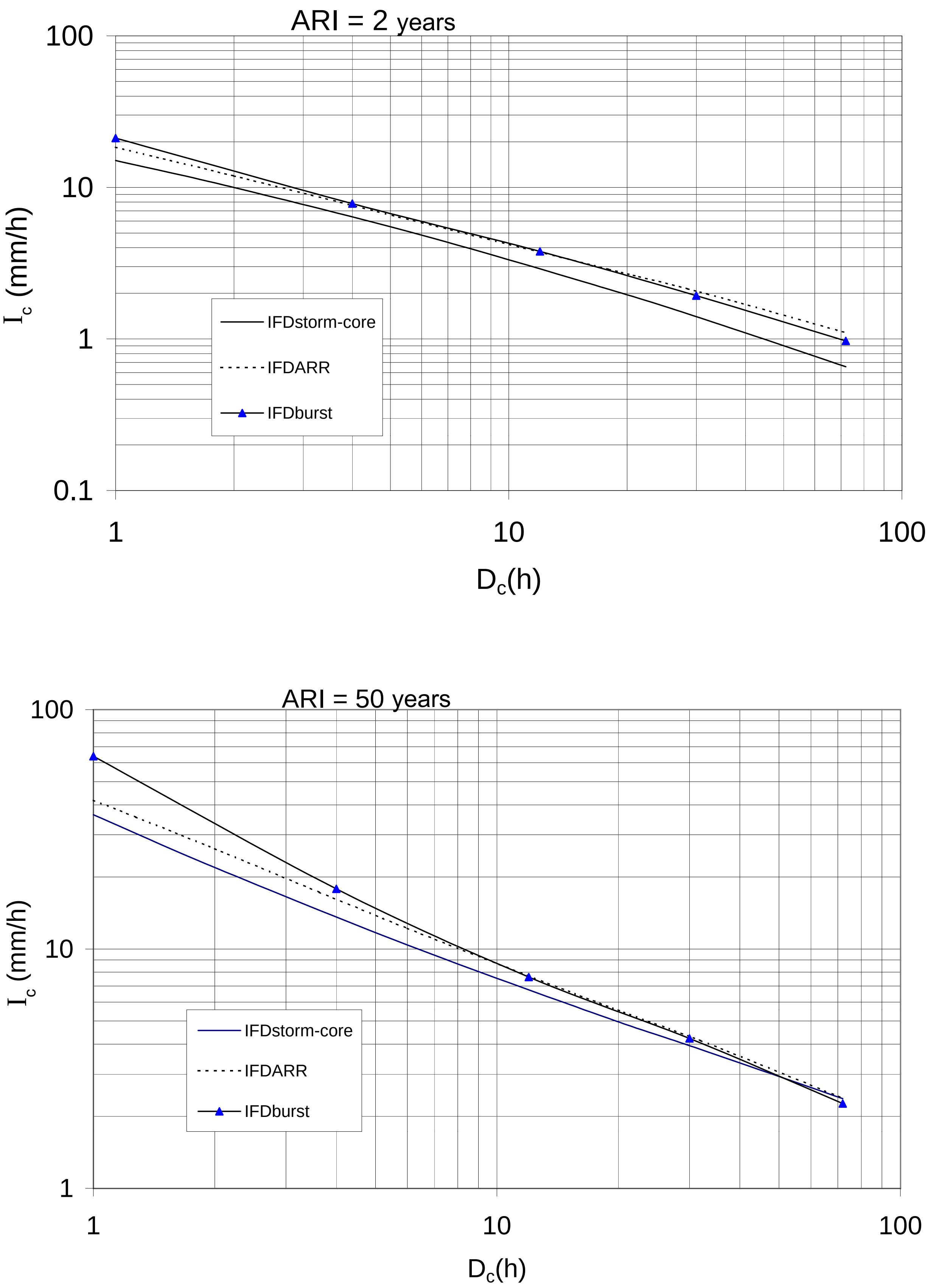


Figure 5.10 Comparison of storm-core IFD curves with storm burst IFD curves based on regional analysis [$IFD_{ARR}$] and at-site analysis [$IFD_{burst}$] (for Melbourne, Station 86071)

### 5.3 Storm-Core Temporal Pattern

A rainfall temporal pattern is a dimensionless representation of the variation of rainfall intensity over the duration of the rainfall event. In this project, the time distribution of rainfall during a storm has been characterised by a dimensionless mass curve, i.e. a graph of dimensionless cumulative rainfall depth versus dimensionless storm time with 10 equal time increments.

Following the procedure of Hoang (2001), the storm-core temporal patterns for 19 pluviograph stations of Study Zone 1 (south-east quadrant of Victoria) have been analysed. The results of the analysis indicated that the temporal patterns of rainfall depth for storm-cores ($TP_c$) are not dependent on season and total storm depth. This means that dimensionless temporal patterns from different seasons and for different rainfall depths could be pooled. However, the patterns were found to be dependent on storm duration, yielding two groups: (1) up to 12 hours duration, and (2) greater than 12 hours duration.

Design temporal patterns for storm-cores ($TP_c$) could be generated by the 'temporal pattern generation model' applied by Hoang (2001). However, in the present Monte Carlo technique, historic temporal patterns are used instead of generated temporal patterns. Here, the one-hourly temporal patterns of observed storms are first transformed into dimensionless mass curves defined by the ordinates at 10 equal time increments, as shown in Figure 5.11.

Storms with less than 4 hour durations are assumed to have the same temporal patterns as the observed 4 to 12-hour storms. For shorter storm durations, pluviograph data at hourly increments is insufficient to express the temporal patterns in dimensionless form in ten time increments. The available information on temporal patterns in ARR 87 does not indicate any marked difference between temporal patterns for less than 4 hours and 4 to 12 hours duration. Furthermore, for the size of catchments considered in this study, storms greater than 4-hour play a more important role. The effect on temporal patterns of representing short duration storms by a larger number of time increments is illustrated in Figure 5.11, where a 6-hour storm is resolved into 10 equal time increments (deciles).

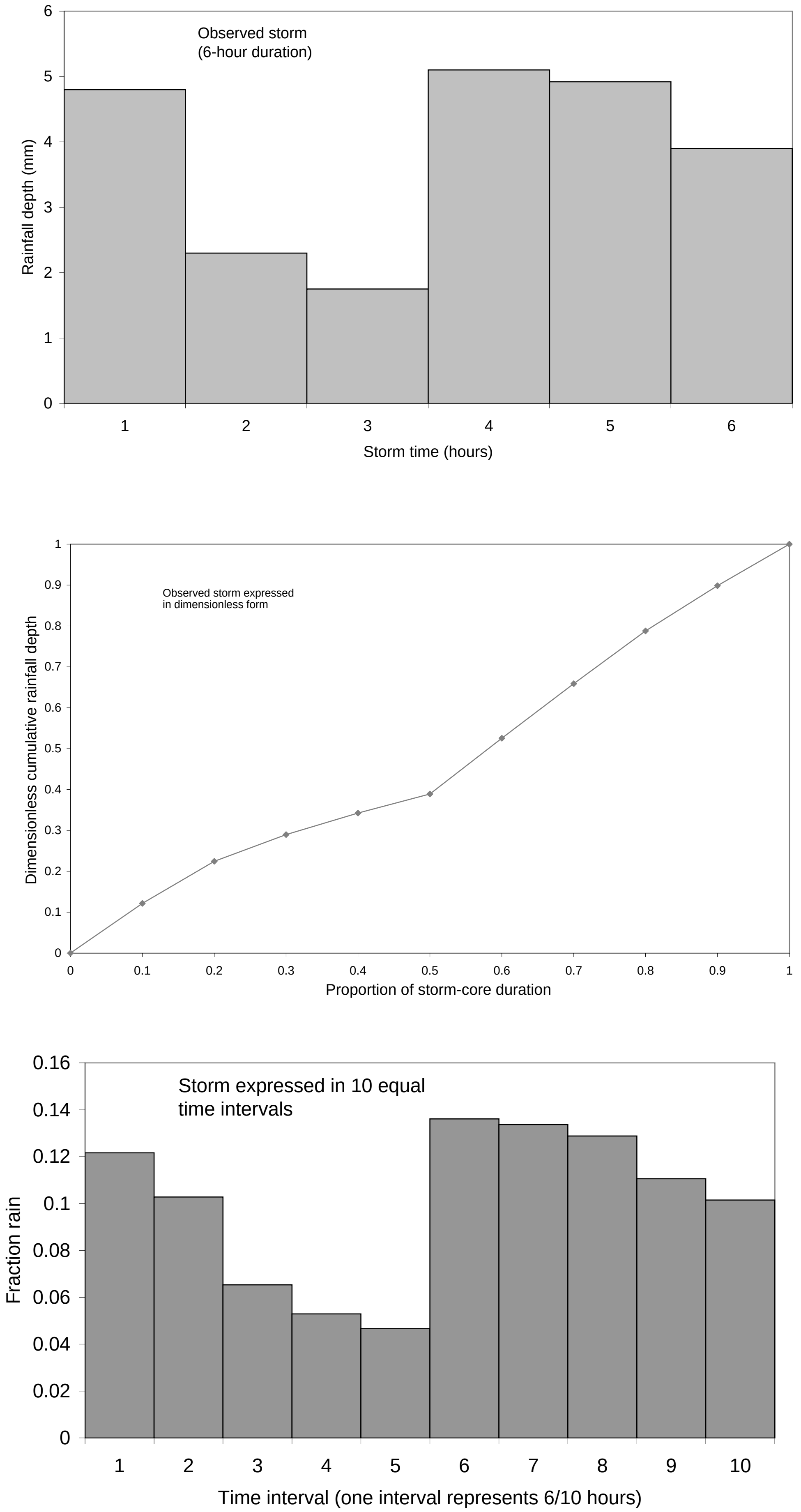


Figure 5.11 Representation of a short duration storm (6-hour) by the ordinates at ten equal time increments (deciles)

Fifteen randomly selected observed temporal patterns in the duration range from 4 to 12 hours (Station 83031) are presented in Figure 5.12. This figure demonstrates the large degree of variability of temporal patterns which is typical for all the storm core events analysed. The ARR87 temporal patterns can also be expressed in a similar way (i.e. in 10 equal time increments), as shown in Figure 5.13 for durations of 4, 6 and 12 hours. Comparison of these two figures indicates the advantage of random selection from the observed temporal patterns (as done in the adopted Monte Carlo simulation technique). Use of fixed ARR87 temporal patterns (as in the Design Event Approach) does not account for the inherent variability in temporal patterns, and may introduce significant bias in the derived flood frequency curve. The sensitivity of derived flood frequency curves to the temporal pattern representation is further discussed in Section 9.3.3.

The analysis and stochastic modelling of temporal patterns is treated in more detail in Hoang (2001).

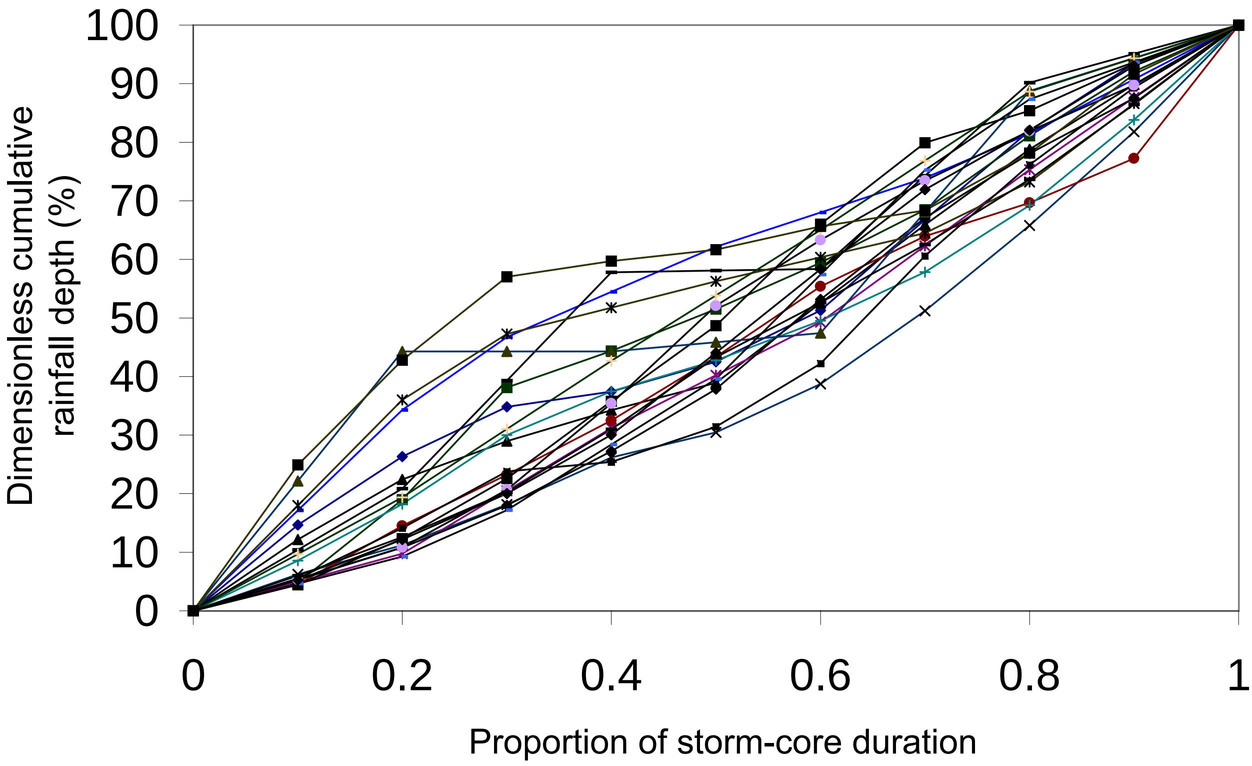


Figure 5.12 Variability in dimensionless temporal patterns of observed storms (Station 83031, storm durations: 4 to12 hours)

## 5.4 Storm-Core Initial Loss

The initial loss ($IL_s$) for a complete storm is estimated to be the rainfall that occurs prior to the commencement of surface runoff (following the approach adopted by Hill et al., 1996), as shown in Figure 5.14. The storm-core initial loss ($IL_c$) is the portion of $IL_s$ that occurs within the storm-core. The value of $IL_c$ can range from zero (when surface runoff commences before the start of the storm-core) to $IL_s$ (when the start of the storm-core coincides with the start of the storm event). In computing loss, a surface runoff threshold value equal to 0.01 mm/h has been used, similar to Hill et al. (1996); it is considered that surface runoff commences when the surface runoff threshold has been exceeded. Catchment average rainfall is used in the computation of losses in the cases where more than one pluviograph station is available within the catchment.

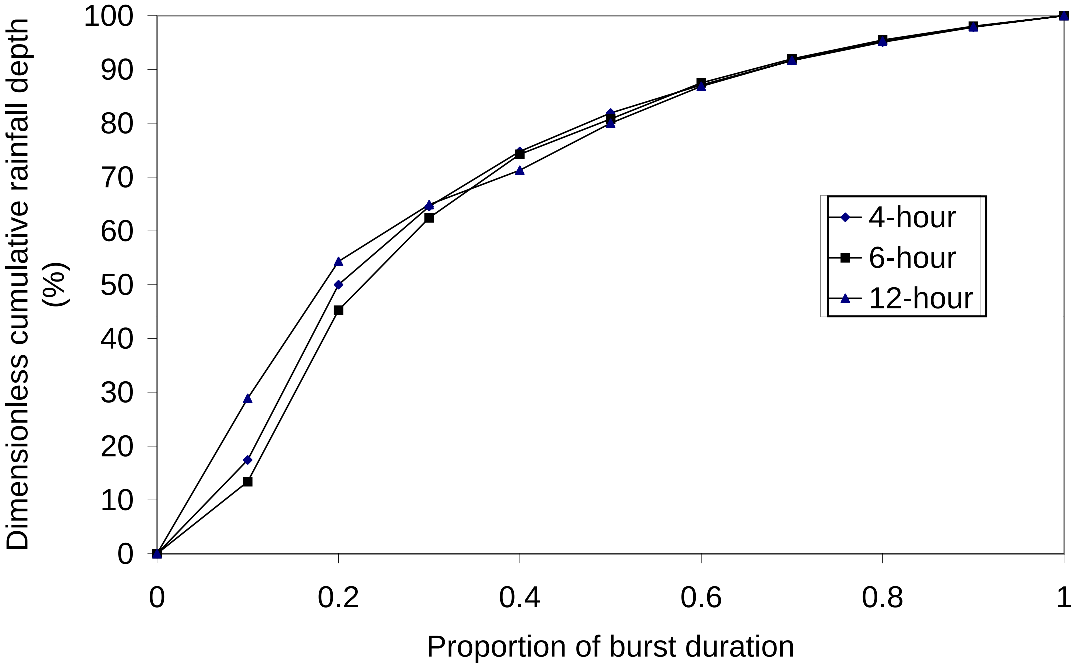


Figure 5.13 Fixed temporal patterns (ARR 87 Vol 2, Zone 2, ARI > 30 years)

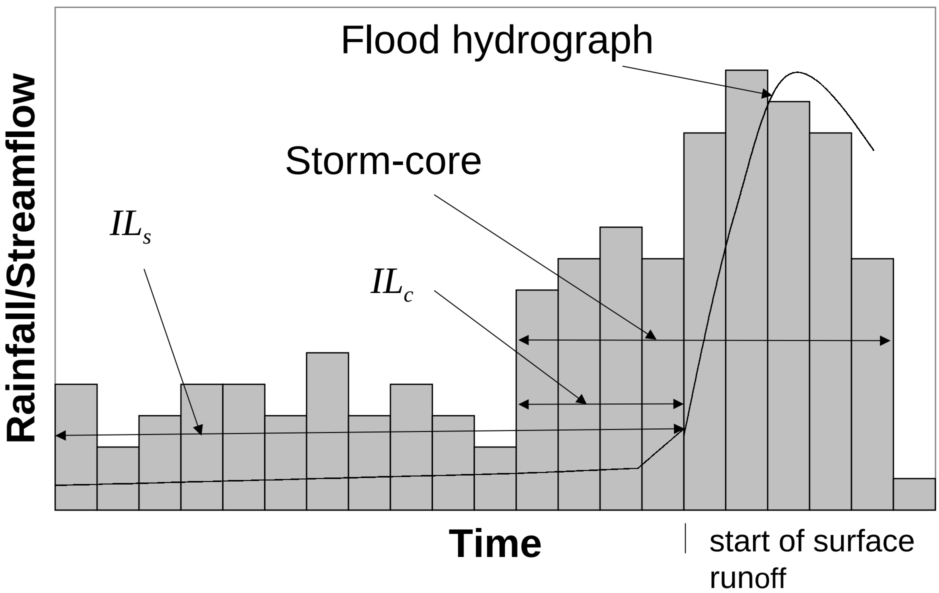


Figure 5.14 Initial loss for complete storm ($IL_s$) and initial loss for storm-core ($IL_c$)

Initial losses for eleven Victorian catchments have been analysed. The important statistics of the loss distributions are summarised in Table 5.5. The mean $IL_s$ and $IL_c$ values for the eleven catchments are 25.0 mm and 21.6 mm respectively i.e., the mean $IL_c$ is 14% lower than the mean $IL_s$. The median $IL_s$ and $IL_c$ values are 23.0 mm and 19.6 mm respectively. The mean, median and standard deviation of the obtained $IL_s$ values resemble the storm loss values derived by Hill et al. (1996) using the same methodology but a different storm definition. The average skewness values are 0.97 and 0.94 for $IL_s$ and $IL_c$ respectively, indicating that loss distributions have a positive skewness. This can be explained by the fact that the lower limit of $IL_s$ and $IL_c$ is zero, but they have no theoretical upper bound. Figure 5.15 shows typical distributions of $IL_s$ and $IL_c$ for the Tarwin River catchment.

Table 5.5 Summary of loss statistics for eleven Victorian catchments

| **Station ID** | **Name** | **Events No. analysed** | **Complete storm loss ($IL_s$) in mm** | | | | **Storm-core loss ($IL_c$) in mm** | | | |
|---|---|---|---|---|---|---|---|---|---|---|
| | | | **Mean** | **Median** | **SD** | **Skew** | **Mean** | **Median** | **SD** | **Skew** |
| 224209 | Cobbannah Creek near Bairnsdale | 19 | 41.33 | 38.11 | 24.94 | 0.48 | 36.14 | 31.45 | 25.56 | 0.68 |
| 226205 | La Trobe River at Noojee | 157 | 27.28 | 22.20 | 17.39 | 2.70 | 24.52 | 20.07 | 17.18 | 2.84 |
| 227226 | Tarwin River East Branch at Dumbalk | 49 | 24.23 | 22.20 | 11.63 | 0.47 | 19.08 | 18.71 | 10.76 | 0.80 |
| 231213 | Lerderderg River at Sardine Creek | 49 | 24.89 | 24.34 | 8.66 | -0.04 | 23.17 | 21.35 | 8.39 | -0.10 |
| 235219 | Aire River at Wyelangta | 130 | 18.74 | 17.86 | 8.90 | 0.75 | 13.00 | 13.79 | 9.55 | 0.45 |
| 236204 | Fiery Creek at Streatham | 162 | 23.50 | 21.55 | 10.09 | 1.26 | 20.87 | 17.69 | 10.21 | 1.28 |
| 403226 | Boggy Creek at Angleside | 163 | 23.32 | 22.80 | 18.88 | 0.84 | 19.10 | 18.83 | 17.14 | 1.04 |
| 404208 | Moonie Creek at Lima | 163 | 19.64 | 18.44 | 10.08 | 1.05 | 16.94 | 16.84 | 9.32 | 0.37 |
| 405261 | Spring Creek at Fawcett | 61 | 22.13 | 20.56 | 11.13 | 0.54 | 19.18 | 17.83 | 10.52 | 0.48 |
| 408202 | Avoca River at Amphitheatre | 101 | 22.29 | 19.92 | 11.38 | 1.27 | 20.34 | 17.86 | 10.84 | 1.17 |
| 415224 | Avon River at at Beazley's Bridge | 68 | 27.57 | 24.63 | 11.53 | 1.30 | 24.90 | 21.46 | 11.24 | 1.30 |
| | **Average** | **102** | **24.99** | **22.96** | **13.15** | **0.97** | **21.57** | **19.63** | **12.79** | **0.94** |

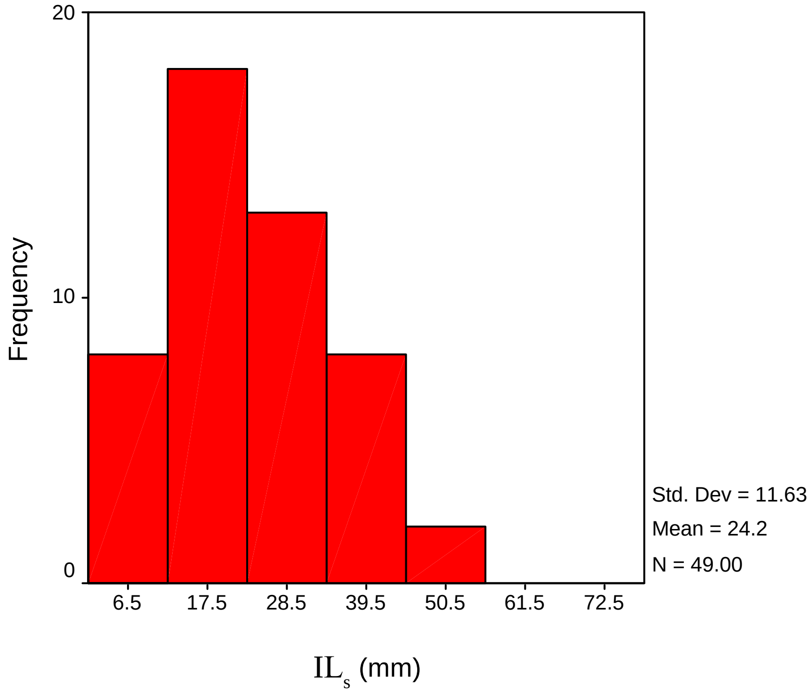


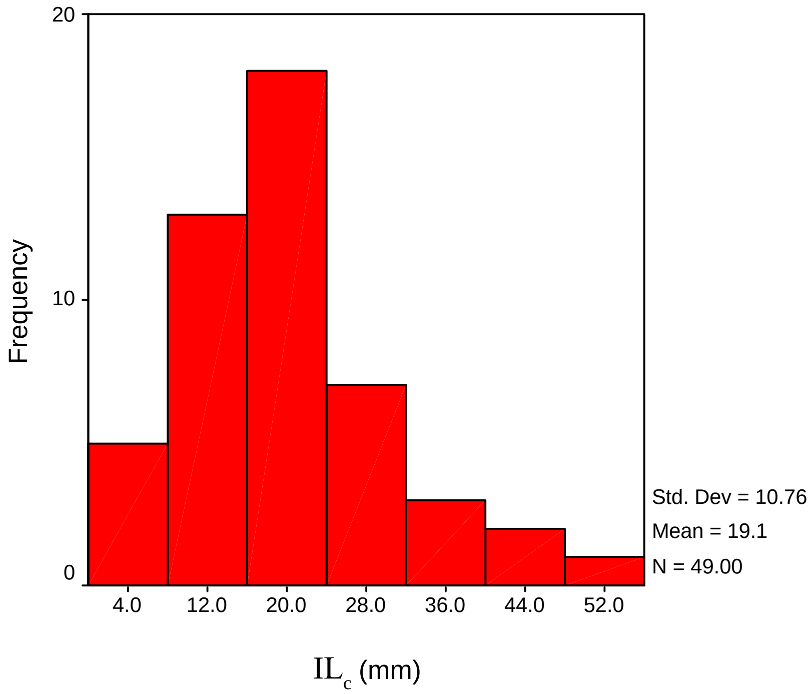


Figure 5.15 Distributions of initial losses ($IL_s$ and $IL_c$) for Tarwin River

***Fitting a theoretical distribution to initial loss data:***

It appears from Table 5.5 and Figure 5.15 that the observed distributions of losses are positively skewed. A four-parameter Beta distribution was found to be appropriate to approximate $IL_s$ and $IL_c$ distributions. The generated $IL_s$ data from the fitted Beta distribution for the Boggy Creek is compared with the observed $IL_s$ data in Figure 5.16. The fit is judged to be satisfactory. A similar degree of agreement was observed between the generated and observed $IL_s$ and $IL_c$ data for the other study catchments.

***Variation with rainfall intensity:***

Both $IL_s$ and $IL_c$ showed no relationship with rainfall intensity, as shown in Figure 5.17 for the case of $IL_s$.

***Variation with rainfall duration:***

The plot of $IL_s$ vs. $D_s$ (Figure 5.18) showed no relationship. This finding is similar to Hill et al. (1996) who found that storm losses are independent of storm duration. From these findings, it is reasonable to assume that $IL_s$ is independent of $D_s$.

The plot of $IL_c$ vs. $D_c$ (Figure 5.19) indicates a relationship such that $IL_c$, in general, increases with $D_c$; however, this relationship is not strong. In the case of storm bursts, Hill et al. (1996) found a dependence between burst losses and burst duration. By definition, $IL_c \leq IL_s$ ; the ratio $IL_c/IL_s$ varies between 0 to 1.0 (Figure 5.20). The plot of $IL_c/IL_s$ vs. $D_c$ (Figure 5.21) indicates that, as $D_c$ increases, $IL_c/IL_s$ approaches unity; with the exception of a few values of zero burst loss. From the above results and the finding of Hill et al. (1996b), it is reasonable to assume that at $D_c$ = 100 hour, $IL_c = IL_s$ .

A simplified relationship based on Hill et al. (1996b) has been adopted, as expressed by the following equation and illustrated in Figure 5.21:

$$IL_c = IL_s\,[0.5 + 0.25\log_{10}(D_c)] \qquad (5.4)$$

This relationship gives $IL_c = IL_s$ at $D_c$ = 100 hour, and $IL_c$ = 0.50 x ILs at $D_c$ = 1 hour. In the case of Boggy Creek, the adopted relationship, in general,

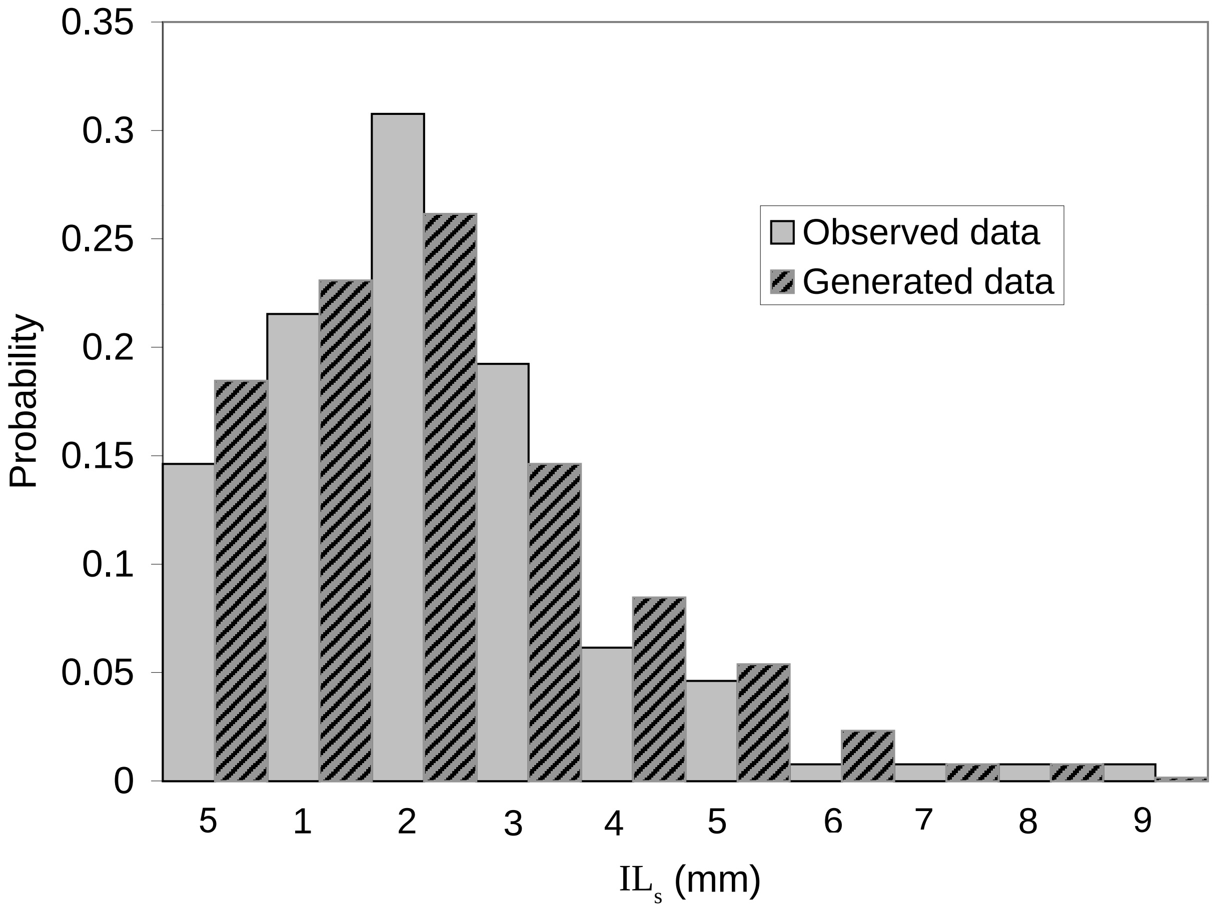


Figure 5.16 Generated $IL_s$ data from the fitted Beta distribution are compared with the observed $IL_s$ data (Boggy Creek)

underestimates $IL_c$ (Figure 5.21). The effect on the derived flood frequency curve of using the adopted relationship (Equation 5.4), or using the distribution of $IL_c$ directly, has been investigated in a sensitivity analysis (Section 9.3).

It might be noted here that the use of $IL_s$ distribution (with an adjustment factor), as proposed in Equation 5.4, is preferable to the use of $IL_c$ directly: $IL_s$ is more readily determined from data and can probably be derived using existing design loss data (eg Hill et al., 1996b).

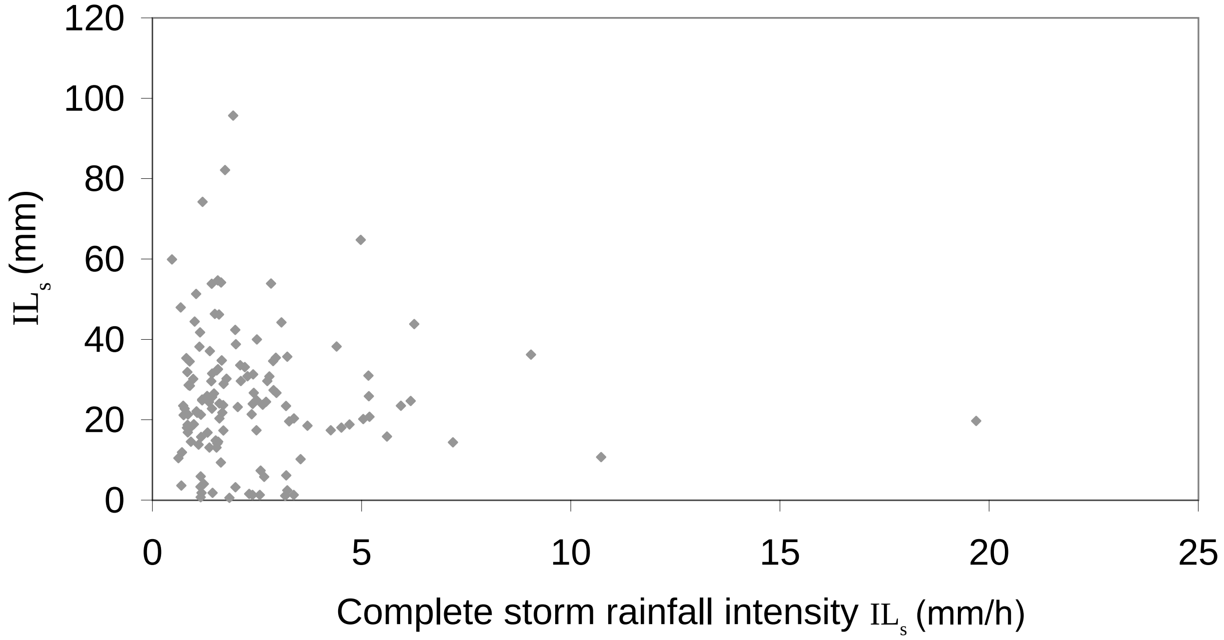


Figure 5.17 Plot of complete storm initial loss ($IL_s$) vs. rainfall intensity for Boggy Creek

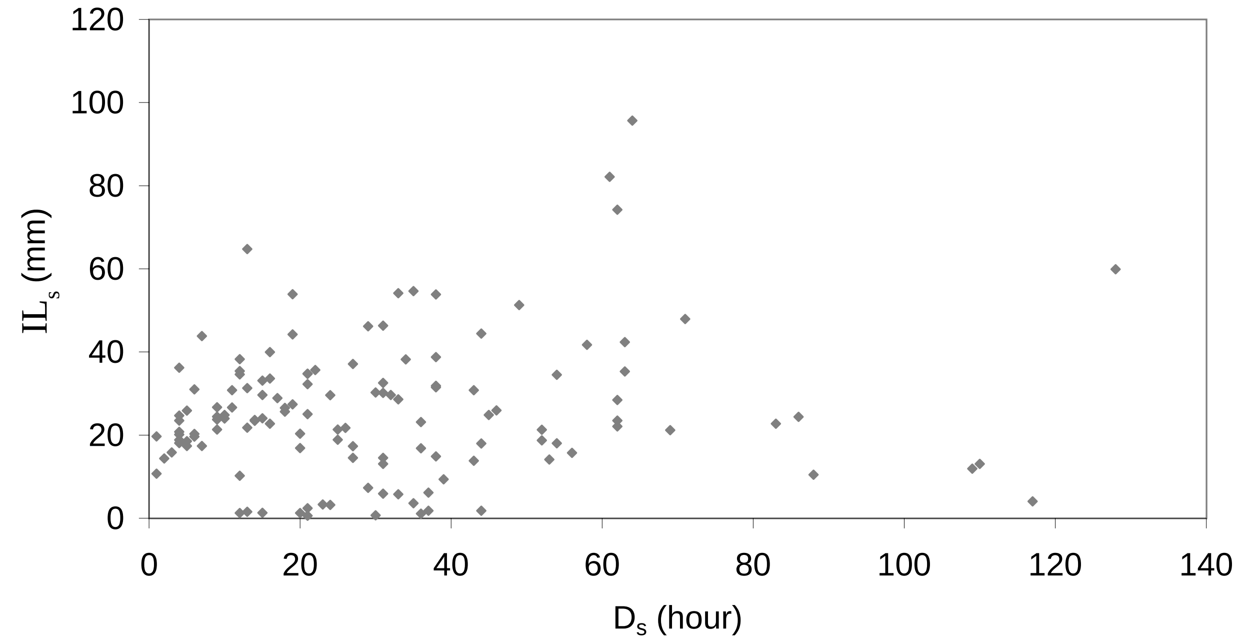


Figure 5.18 Plot of complete storm initial loss ($IL_s$) vs. duration of complete storm for Boggy Creek

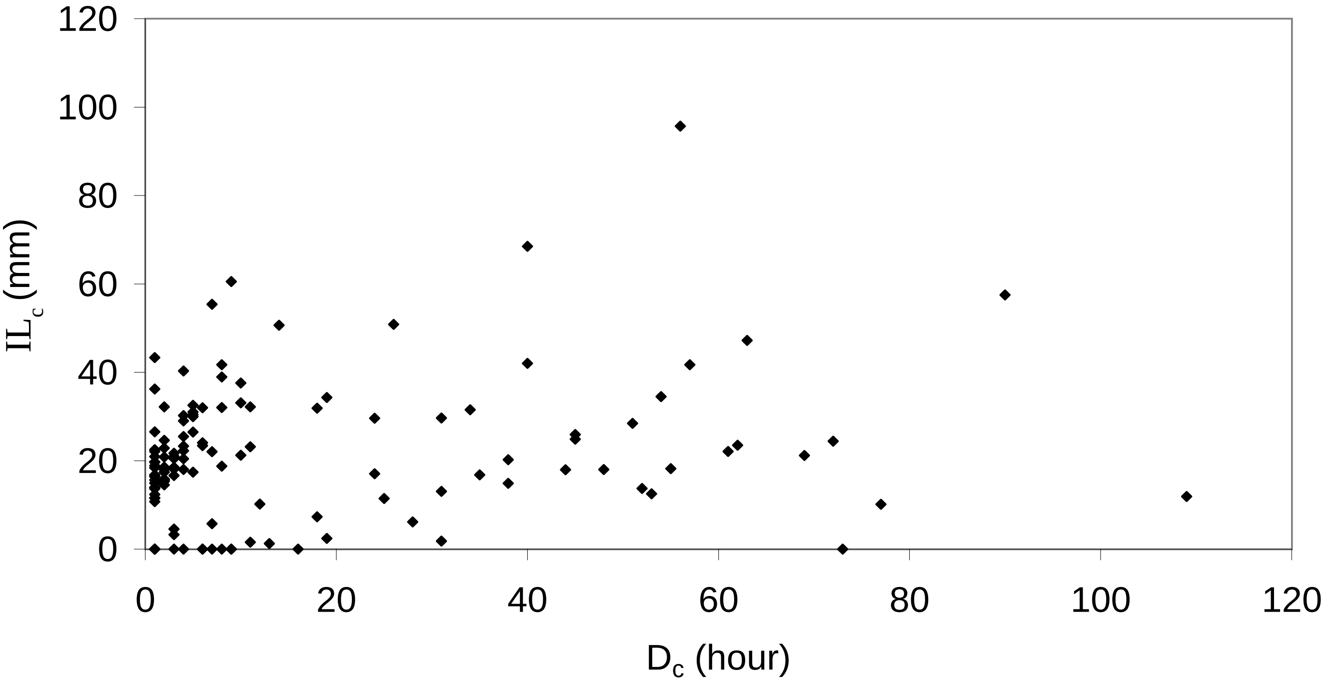


Figure 5.19 Plot of storm-core initial loss ($IL_c$) vs. storm-core duration ($D_c$) for Boggy Creek

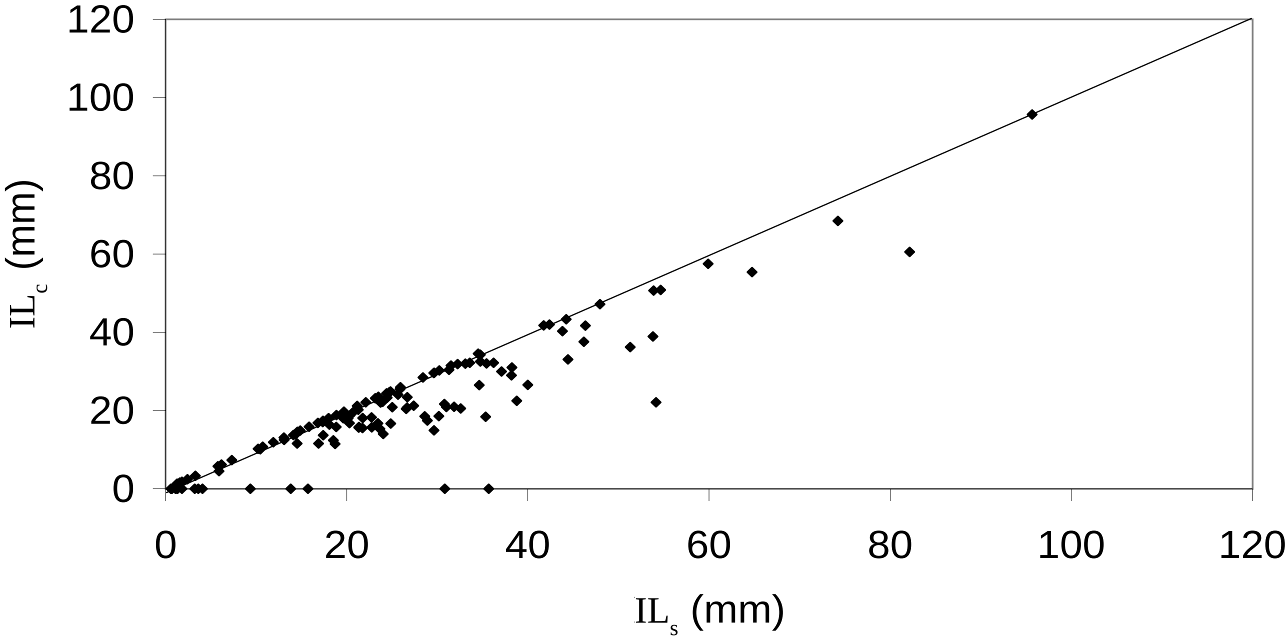


Figure 5.20 Plot of storm-core initial loss ($IL_c$) vs. complete storm initial loss ($IL_s$) for Boggy Creek

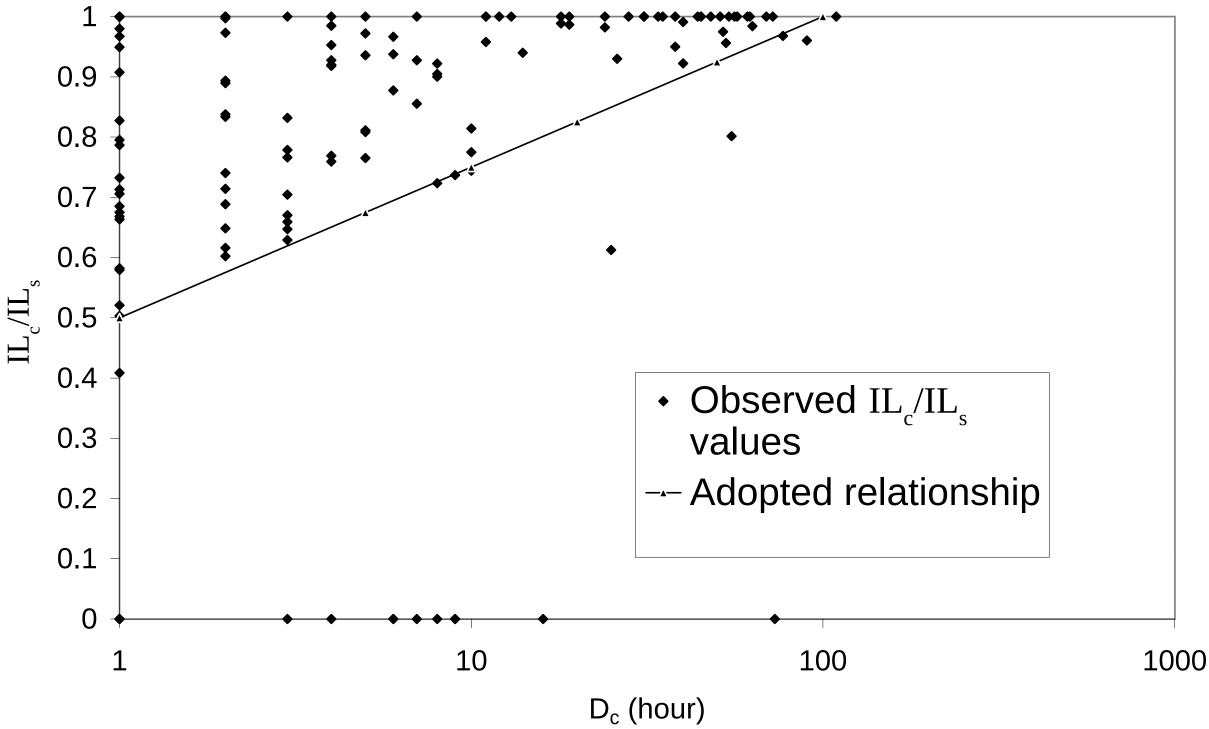


Figure 5.21 Plot of $IL_c/IL_s$ vs. $D_c$ for Boggy Creek

## 6. Calibration of Runoff Routing Model

To determine the derived flood frequency curve for a particular catchment, the adopted runoff routing model needs to be calibrated for the catchment. As mentioned in Section 2.1, the adopted runoff routing model, referred to as single non-linear storage model, uses a storage discharge relationship of the form $S = kQ^m$ with the exponent fixed at a value of 0.8. The objective of model calibration is to determine a value of $k$ that results in satisfactory fit for a range of recorded rainfall and runoff events at the catchment outlet. The calibration of the adopted model is similar to the techniques used for other runoff routing models (e.g. RORB). The following strategy has been found to be useful in calibration:

(i) Select a number of rainfall and runoff events from the observed data at the catchment outlet. Check the data for completeness, consistency and any gross errors.

(ii) For about two-thirds of the selected rainfall and runoff events, calibrate the model for an appropriate value of $k$. A good strategy is to first change initial and continuing loss values to match the rising limb of the computed and observed hydrographs and to obtain a volume balance (i.e. the computed runoff volume matches the observed streamflow volume). When these are achieved, provisionally fix the initial and continuing losses values but change the $k$ value to match the peak. An increase in $k$ reduces the peak and vice versa. Finally, the adopted initial loss, continuing loss and $k$ values should give a volume balance, and good matches in the rising limbs and peaks.

(iii) From the values of $k$ obtained above, select a global $k$ value for all events ( e.g. a median or a mean value) giving appropriate weight to the values from individual events depending on data quality, purpose of modelling, etc.

(iv) Finally, use the selected $k$ value with the remaining observed rainfall and runoff events to validate the calibrated model.

A FORTRAN program has been developed to calibrate the adopted runoff routing model interactively (Rahman, 1999).

Typical values of parameters for the Tarwin River catchment are presented in Table 6.1, and the quality of fit is illustrated in Figure 6.1. A value of $k$ = 33 was adopted in the simulation of streamflow hydrographs for Tarwin River (Section 8).

Table 6.1 Typical parameter values of the single non-linear storage model

| Catchment | Event | IL (mm) | CL (mm/h) | k | Difference in peak (%) | Difference in volume (%) |
|---|---|---|---|---|---|---|
| Tarwin River | 24/8/75 | 28 | 2.3 | 42 | -0.007 | -5.75 |
| | 7/8/76 | 17 | 1.25 | 30 | -2.03 | 1.32 |
| | 14/6/78 | 18 | 0.18 | 33 | 0.43 | -8.06 |

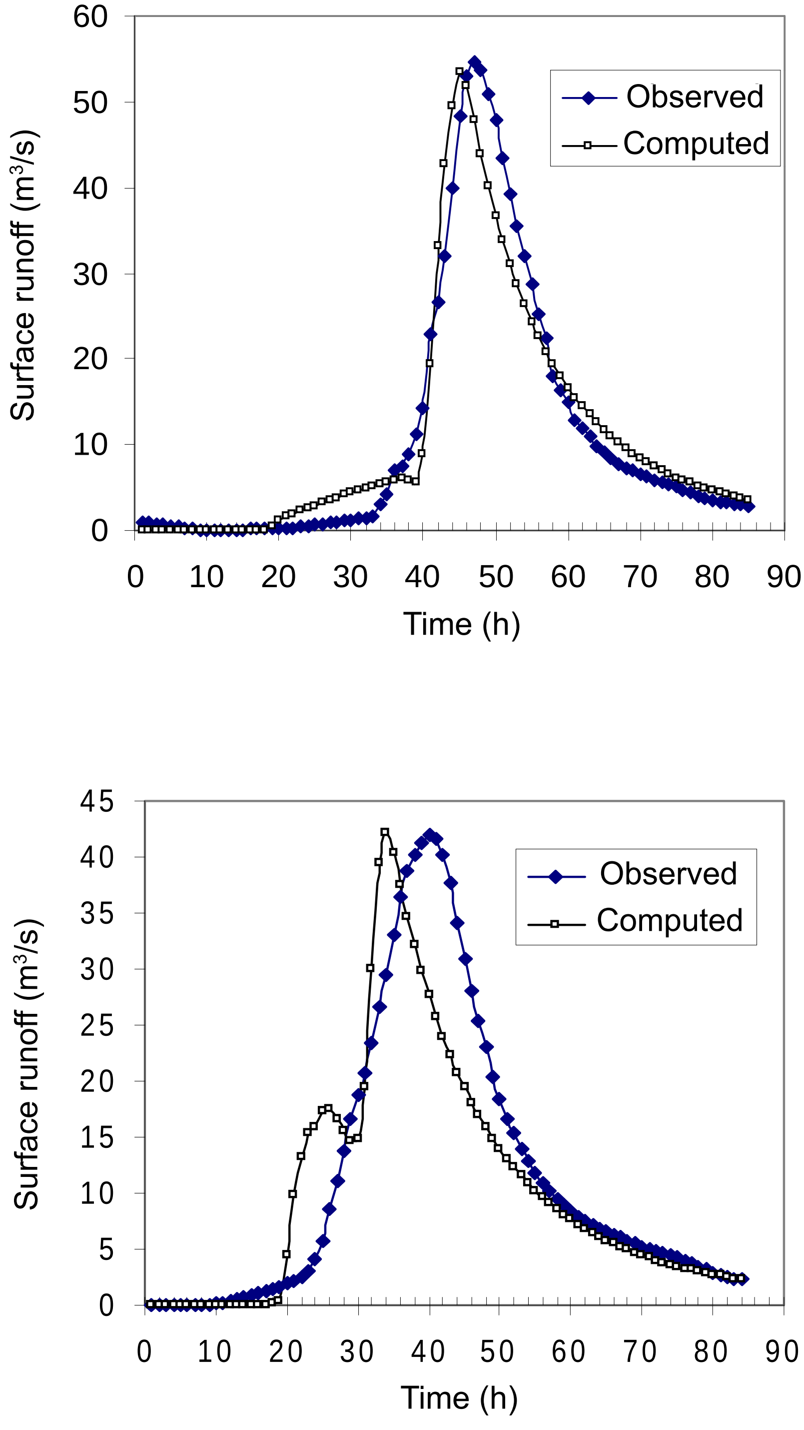


Figure 6.1 Fitting the single non-linear storage model for the Tarwin River catchment (events on 7/8/76 and 14/6/78, respectively)

# 7. Data Generation and Monte Carlo Simulation

## 7.1 Overview

A Monte Carlo approach is used to generate a sample of runoff/flood events. There are many possible ways of implementing the general approach; this chapter describes the specific method adopted here using storm-cores. For each event, a set of values of $D_c$, $I_c$, $TP_c$ and $IL_c$ is generated to define the rainfall excess hyetograph, which is then routed through the calibrated runoff routing model to produce a corresponding streamflow hydrograph. A large number of hydrographs (in the order of thousands) is generated; the resulting flood peaks can be extracted and subjected to a frequency analysis to obtain the derived flood frequency curve.

The distributions of component variables $D_c$, $I_c$, $TP_c$ and $IL_c$ have been identified in Chapter 5. Storm-core duration ($D_c$) has been found to be exponentially distributed (Section 5.1). The distribution of rainfall intensity has been expressed by IFD curves. An IFD table can be prepared for the catchment of interest following the procedure described in Section 5.2; this table is used to generate storm-core rainfall intensity ($I_c$) values for selected values of $D_c$ and $ARI$. The Monte Carlo technique described in this report uses historic temporal patterns at the site on interest (Section 5.3); this involves random selection of a historic storm-core temporal pattern ($TP_c$) depending on the generated $D_c$. The initial losses for complete storms and storm-cores ($IL_s$ and $IL_c$, respectively) have been found to have a beta distribution; the Monte Carlo simulation technique generates an $IL_s$ value from the fitted beta distribution and then converts it to a corresponding $IL_c$ value depending on the generated $D_c$ using Equation 5.4. The generated $D_c$, $I_c$, $TP_c$ and $IL_c$ data are stored in separate data files.

Details of the adopted procedures for the generation of data from each of the four component distributions and for the simulation of streamflow hydrographs are described below.

## 7.2 Generation of Data from Component Distributions

### 7.2.1 Number of Data Points to be Generated

The number of data points to be generated depends on the range of ARIs of interest and the degree of accuracy required. To determine the derived flood frequency curve for the ARI range from 1 to 100 years, it appears that generation of 2000 years of data would be adequate. The proposed modelling framework generates a partial series, and thus the average number of rainfall events per year to be generated for the catchment of interest needs to be selected. The number of data points to be generated ($NG$) is obtained from the following equation:

$$NG = \lambda * NY \quad (7.1)$$

where $\lambda$ is the average number of storm-core events per year, and $NY$ is the number of years of data to be generated. As an example, for $\lambda$ equal to 5, a total of 10,000 data points has to be generated to simulate 2000 years of data. The selected value of $\lambda$ should be similar to the average number of observed storm-cores per year obtained with the adopted storm-core definition (Section 4).

### 7.2.2 Generation of Rainfall Duration Data

The distribution of storm-core duration ($D_c$) has been found to be exponential, as mentioned in Section 5.1. In the Monte Carlo simulation, a total of $NG$ values of $D_c$ is to be generated from the fitted exponential distribution. The exponential distribution has one parameter $\beta$ (Equation 5.1), estimated as the observed mean $D_c$ value for the catchment of interest. [The regional mean $D_c$ should be used for an ungauged catchment or when the at-site pluviograph record length is too small (e.g. less than 20 years).] A FORTRAN program has been developed to generate and store $NG$ values of storm-core duration from the exponential distribution (Rahman, 1999).

### 7.2.3 Generation of Rainfall Intensity Data

The IFD table described in Section 5.2 is the basis of generating storm-core rainfall intensity ($I_c$) data. For a given $D_c$, an *ARI* value is randomly selected using the following relationship with *AEP* (after Stedinger et al., 1993, equation 18.6.3b):

$$ARI = \frac{-1}{1n(1 - AEP)} \tag{7.2}$$

where *AEP* is the annual exceedance probability, obtained from a uniform distribution *U* (0, 1). In the Monte Carlo technique described here, the primary aim is to develop derived flood frequency curves in the range of annual excedance probabilities of say 1 in 100 to 1 in 2; thus the limit *U* (0, 1) is too wide. However, to cover a sufficiently wide range of rainfall intensities that might be of interest in the simulation, *U* was limited to the range $10^{-6} \leq U \leq 1 - e^{-1}$. As an example, for an average number of storm-core events $\lambda$ equal to 5, this results in $10^{-6} \leq U \leq 0.993$; in terms of *ARI* (years) this is equivalent to $10^{-6} \leq U \leq 0.2$

Generation of $I_c$ data involves the following steps:

(i) Prepare an IFD table at the site of interest following the procedure described in Section 5.2.

(ii) Read a generated $D_c$ value.

(iii) Generate a $U$ ($10^{-6}$, $1 - e^{-\lambda}$) random number and compute an *ARI* using Equation 7.2.

(iv) Given the $D_c$ and *ARI*, read an $I_c$ value from the IFD table. This involves a log-log linear interpolation from the IFD table with respect to both duration and *ARI*.

(v) Store the generated value of $I_c$ in an array.

(vi) Repeat the procedure *NG* times.

A FORTRAN program has been developed to generate $I_c$ data following the above procedure (Rahman, 1999).

### 7.2.4 Sampling of Storm-Core Temporal Patterns

As described in Section 5.3, the storm-core temporal patterns ($TP_c$) are independent of storm-core rainfall intensity but dependent on storm-core duration ($D_c$). The adopted Monte Carlo simulation method randomly selects a historic temporal pattern recorded at the site of interest depending on the previously generated $D_c$ data. The procedure of making such a random selection is outlined below:

(i) Historic temporal patterns $TP_c$ are expressed in dimensionless form (i.e. mass curve with 10 equal time increments, as shown in Figure 5.12).

(ii) Depending on the observed duration of the storm-core rainfall event ($D_c$), the historic temporal patterns are put into two bins: Bin 1: $D_c \leq 12$ hours; and Bin 2: $D_c > 12$ hours. Temporal patterns in Bin 1 are labelled sequentially i.e. 1, 2, … $N_{bin\ 1}$. Similarly temporal patterns in Bin 2 are labelled as 1, 2, … $N_{bin\ 2}$.

(iii) Depending on the generated $D_c$ value, select either Bin 1 or Bin 2.

(iv) Generate a uniform random deviate *U* (0, 1) and convert it to an integer number *K* such that $1 \leq K \leq N_{bin\ 1}$ (when $D_c \leq 12$ hour) or $1 \leq K \leq N_{bin\ 2}$ (when $D_c > 12$ hour).

(v) Select the temporal pattern having label *K* from the appropriate bin and store it.

(vi) Repeat the steps (iii) to (v) *NG* times to sample *NG* temporal patterns.

A FORTRAN program has been developed to randomly sample storm-core temporal patterns following the above procedure (Rahman, 1999).

### 7.2.5 Generation of Storm-Core Initial Loss Data

Storm-core initial loss ($IL_c$) depends on storm-core duration $D_c$, as discussed in Section 5.4. Generation of $IL_c$ data involves the following steps:

(i) Fit a Beta distribution to the $IL_s$ data from observed events. The Beta distribution requires four parameters: lower and upper limits of $IL_s$, mean and standard deviation of $IL_s$ values. These are obtained from at-site loss analysis (regional loss values could be used, but this has not been tested yet).

(ii) Generate a complete storm initial loss ($IL_s$) value from this distribution.

(iii) Read a generated $D_c$ value.

(iv) Given the $IL_s$ and $D_c$ values, use Equation 5.4 to compute $IL_c$ and store this value.

(v) Repeat the procedure *NG* times to generate *NG* values of $IL_c$.

A FORTRAN program has been developed to generate $IL_c$ data following the above procedure (Rahman, 1999).

### 7.3 Simulation of Streamflow Hydrographs

The generated data of $D_c$, $I_c$, $T_c$ and $IL_c$ are stored in separate files. Each set of these data defines a rainfall excess hyetograph, as explained in Section 2.3 and illustrated in Figure 7.1. The net rainfall hyetograph is then routed through the catchment using the adopted runoff routing model. The model requires the following inputs:

(i) Catchment area in km$^2$.

(ii) An estimate of baseflow in m$^3$/s. The average baseflow at the time of commencement of surface runoff is used here as this is readily available from another study (Mein et al., 1995). Ideally, the baseflow at the time of hydrograph peak should be used; however, as baseflow is generally only a small fraction of total streamflow at the time of a flood, it appears reasonable to use average baseflow at the time of commencement of surface runoff as a representative value.

(iii) An estimate of continuing loss (*CL*) in mm/h. The average value of *CL* obtained by Hill et al. (1996) is used here.

(iv) The generated $D_c$ value.

(v) The generated $I_c$ value.

(vi) The randomly sampled temporal pattern ($TP_c$) values.

(vii) The generated $IL_c$ value.

With the above fixed and stochastic inputs to the calibrated runoff routing model, *NG* different streamflow hydrographs are simulated. The peak of each of the simulated hydrographs is stored for later analysis to determine a derived flood frequency curve. A FORTRAN program has been developed to carry out the above steps (Rahman, 1999).

Given the parameters of the distributions of $D_c$, $I_c$, $T_c$ and $IL_c$, the generation of data files from these distributions takes about 30 minutes (for 20,000 events), and the simulation of the corresponding streamflow hydrographs takes about 5 minutes on a Pentium 500 computer.

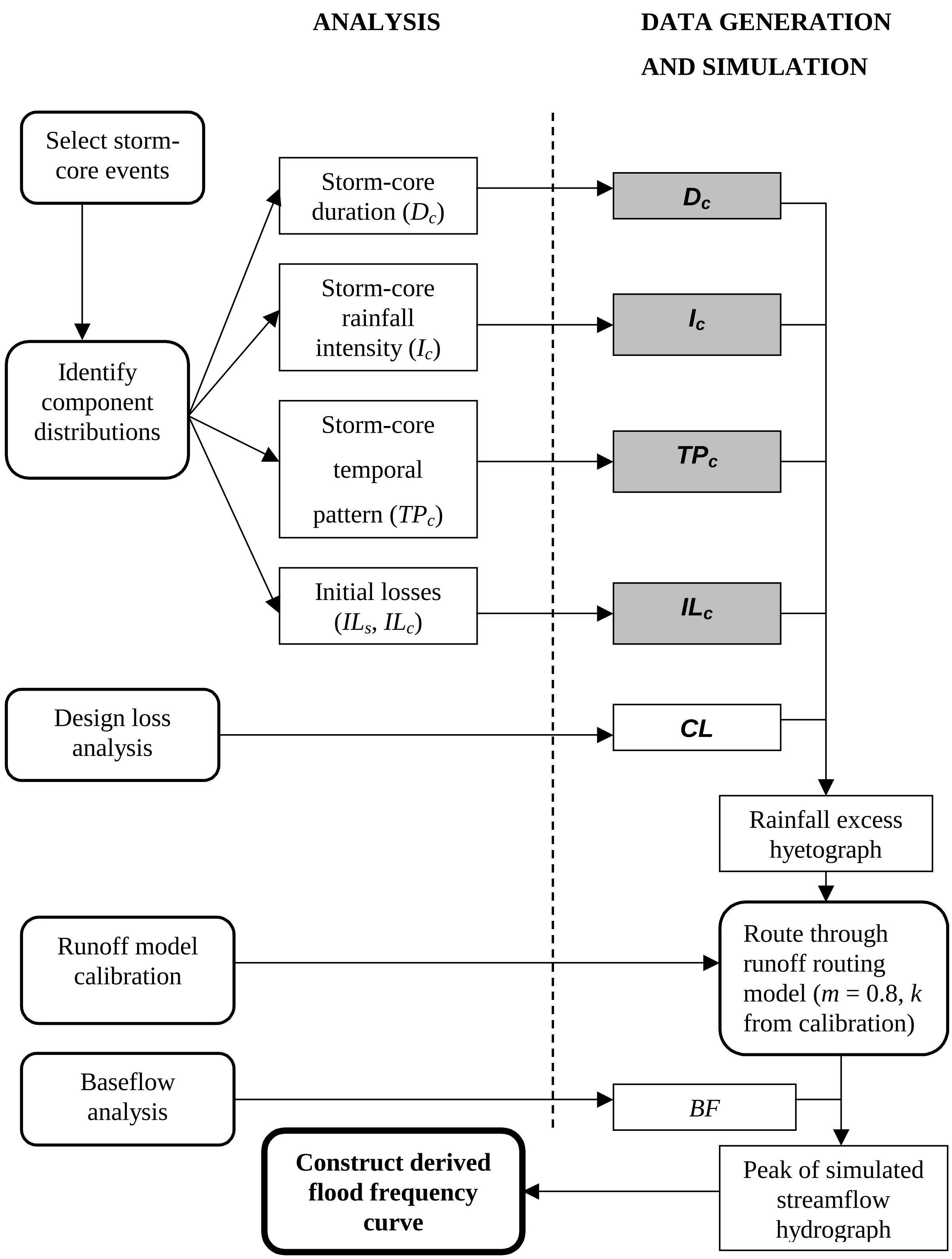


Fig 7.1 Schematic diagram of the overall methodology (probability distributed components shaded)

## 8. Flood Frequency Analysis

The set of *NG* simulated flood peaks, obtained in Section 7.3, is used to construct a derived flood frequency curve. As these flood peaks are obtained from a partial series of storm-core rainfall events, they also form a partial series. Construction of the derived flood frequency curve from the generated partial series of flood peaks involves the following steps:

(i) Arrange the *NG* simulated peaks in decreasing order of magnitude.

(ii) Assign rank ($m$) 1 to the highest value, 2 to the next and so on.

(iii) For each of the ranked floods, compute an *ARI* from the following equation:

$$ARI = \frac{NG+0.2}{m-0.4} \times \frac{1}{\lambda} \cong \frac{NY+0.2}{m-0.4} \qquad (8.1)$$

where *NG* is the number of simulated peaks, $m$ is the rank, $\lambda$ is the average number of storm-core events per year for the catchment of interest (with the value of $\lambda$ taken the same as for the computation of *NG* in Equation 7.1), and *NY* is the number of years of simulated flood data.

(iv) Prepare a plot of flood peaks versus *ARI*, i.e. a plot of the empirical flood frequency curve defined by the simulated flood peaks.

(v) Compute flood quantiles for selected values of *ARI* by interpolation between neighbouring points.

The derived flood frequency curve for the Boggy Creek is shown in Figure 8.1 (some data points have been omitted from this plot). The horizontal segment of this curve represents simulated events with zero surface runoff, i.e. where the simulated flood peak equals the design value of baseflow.

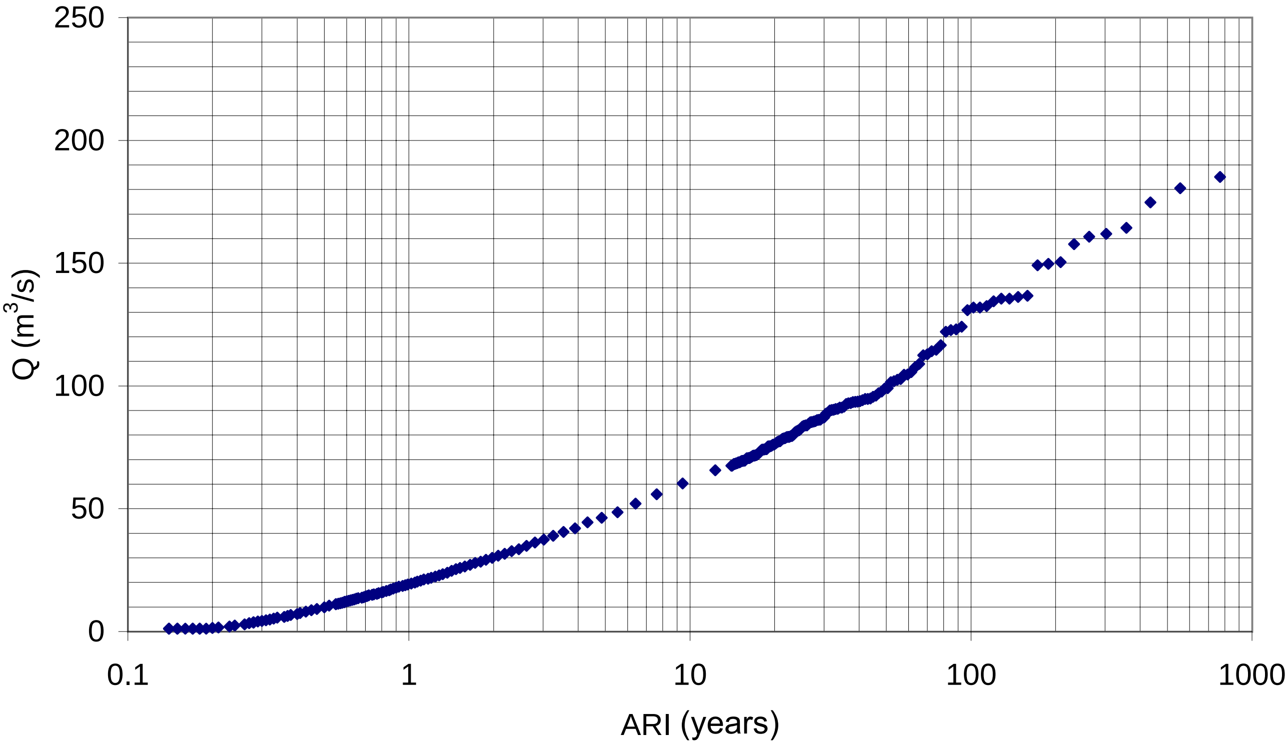


Figure 8.1 Derived flood frequency curve (partial series) for Boggy Creek. *Q* is flood peak.

# 9. Validation of Results and Sensitivity Analyses

## 9.1 Comparison of Derived Flood Frequency Curves With Results of Flood Frequency Analyses

The Monte Carlo simulation technique for storm-core events presented in this report has been applied to three catchments in Victoria. These catchments are listed in Table 9.1. In a somewhat modified form, using complete storms, it has also been applied to the La Trobe River catchment at Noojee (Hoang, 2001). The simulated flood series are based directly on the design inputs and model parameters derived in Chapters 5 and 6, with minor calibration of the continuing loss parameter against the flood frequency results.

The resulting derived flood frequency curves (partial series) for Boggy Creek, Tarwin River and Avoca River catchments are compared in Figures 9.1, 9.2 and 9.3 respectively with the results of frequency analyses of the partial flood series available at the sites (following the empirical distribution approach using Cunnane's plotting position formula). The results show that the derived flood frequency curves compare quite well with the results of flood frequency analyses of the flood series available at the sites (after a relatively small degree of adjustment of the continuing loss parameter). The results also show that the Monte Carlo simulation technique allows reproduction of observed frequency curves over a large range of ARIs, and can cope well with the non-linearity of the rainfall and runoff process.

The derived flood frequency curve for Boggy Creek has also been compared with the most recent flood frequency analysis for the data available at the site (Appendix 2). The result shows that the inclusion of the1993 flood (not directly measured but estimated as 180 $m^3/s$) affects significantly the at-site flood frequency curves. It also indicates the extent to which the sampling variability in the observed flood series data affects the fitted flood frequency curve, and thus the outcome of the comparison of derived flood frequency curve with the results of the at-site flood frequency analysis.

Table 9.1 Catchments used for model validation

| Catchment | Area ($km^2$) | Period of record of streamflow data (Years) | Pluvio station no. | Location of pluvio station | Period of record of pluvio data (Years) |
|---|---|---|---|---|---|
| Boggy Creek at Angleside (403226) | 108 | 1974 - 1998 (25) | 83031 | Within catchment | 1974 -1993 (20) |
| Tarwin River East Branch at Dumbalk (227226) | 127 | 1970 - 1997 (27) | 85106 | Near u/s boundary | 1957 - 1979 (22) |
| Avoca River at Amphitheatre (408202) | 78 | 1966 - 1997 (32) | 81038 | Outside catchment | 1974 - 1993 (20) |

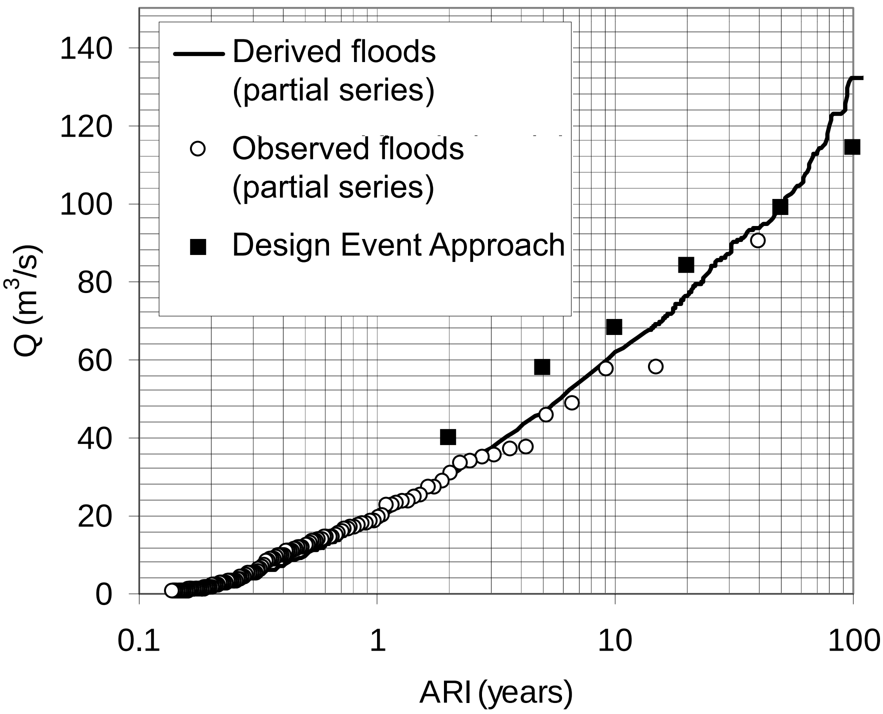


Figure 9.1 Comparison of derived flood frequency curve (partial series) with results of at-site flood frequency analyses and Design Event Approach for Boggy Creek

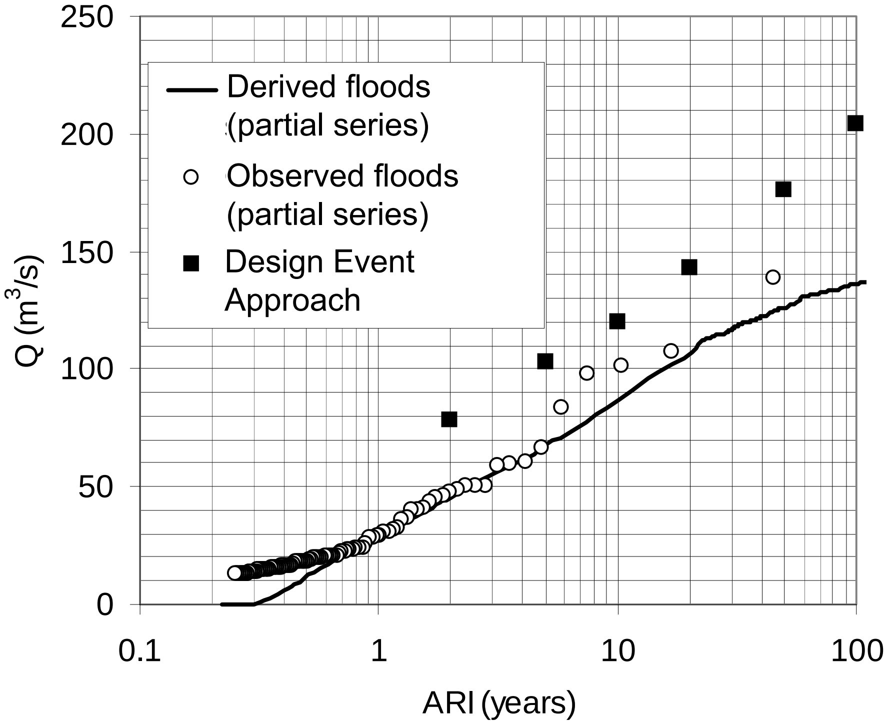


Figure 9.2 Comparison of derived flood frequency curve (partial series) with results of at-site flood frequency analyses and Design Event Approach for Tarwin River

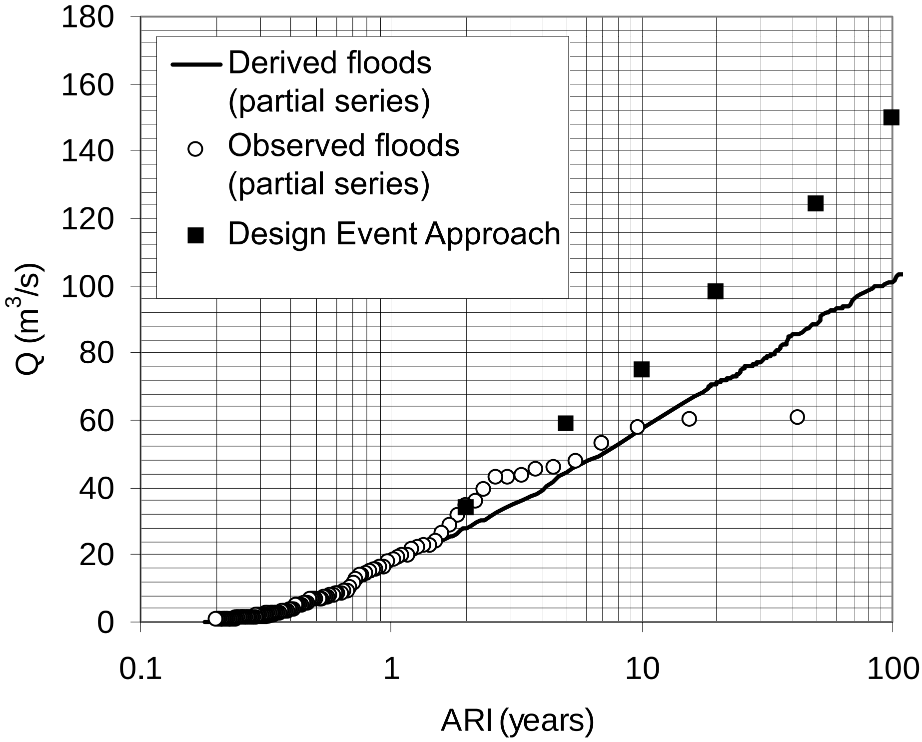


Figure 9.3 Comparison of derived flood frequency curve (partial series) with results of at-site flood frequency analyses and Design Event Approach for Avoca River

## 9.2 Comparison of Derived Flood Frequency Curves with Results of Design Event Approach

The currently used design event approach, as recommended in ARR and other design flood estimation guidelines, involves the definition of a "design event" i.e. a single combination of design rainfall and loss parameters for a given rainfall duration and ARI. This approach was applied to the three study catchments to obtain another basis for comparison.

The design rainfall intensities and temporal patterns from ARR Volume 2 were adopted. The storm burst initial losses were obtained based on the Hill et al. (1996b) recommendations (Equation 11.2). The same average baseflows and continuing loss values close to the ones used to determine the derived flood frequency curves for the three study catchments (Figures 9.1-9.3) were adopted here. Also, the same non-linear storage model with identical values of *m* and *k* was used for runoff routing.

In Figures 9.1 to 9.3, the design flood estimates obtained by the Design Event Approach are compared with the results from the other methods. It shows that the Design Event Approach significantly overestimates the observed flood series, particularly for Tarwin River (Figure 9.2) and Avoca River (Figure 9.3), and it could not well reproduce the slope of the observed flood frequency curve over a large range of ARIs. The analyses indicate that while the Design Event Approach can easily be tweaked to provide design flood estimates for a specific range of ARIs, the further one moves away from the range of events used in calibration, the less the results would have validity. By contrast, the proposed approach implicitly incorporates the non-linearities involved and is able to faithfully reproduce the skewed nature of the frequency curve. In addition, the Design Event Approach requires difficult decisions on the selection of critical rainfall duration, and smoothing of final design flood frequency curve that involve a degree of subjectivity. In contrast, the Monte Carlo Simulation technique considers rainfall duration as a random variable, and smoothing of the final flood frequency curve is not generally necessary.

## 9.3 Sensitivity Analyses

Sensitivity analyses were carried out to examine the effect of a change in any one of the component distributions on the final derived flood frequency curve. The following investigations were made:

### 9.3.1 Change in the Distribution of Storm-Core Duration

As mentioned in Section 5.1, the distribution of $D_c$ is exponential; its parameter $\beta$ (see Equation 5.1) has been taken as the mean of the observed $D_c$ values at a site. In the sensitivity analysis, the mean $D_c$ was changed from the observed at-site value to a value corresponding to the upper 95% confidence limit of the regional distribution. A change in the distribution of $D_c$ also results in a change in the generated data for other component variables ($I_c$, $TP_c$ and $IL_c$), as these distributions are conditional on $D_c$.

For Boggy Creek, the at-site mean $D_c$ is 14.3 hours, and the upper 95% confidence limit of the regional distribution is 17.8 hours. The derived flood frequency curves using these two different $D_c$ values are shown in Figure 9.4. The difference appears to be insignificant for the ARIs up to 500 years. For Tarwin River, the at-site mean is 12.5 hours, and the upper 95% confidence limit of the regional distribution is 13.9 hours. The derived flood frequency curves using these two different $D_c$ values showed little difference (similar to Boggy Creek). These results indicate that a change in the parameter of the distribution of $D_c$ of about 10 - 15% would not have any significant effect on the derived flood frequency curve. It can thus be concluded that the derived frequency curve is not sensitive to small uncertainties in the adopted distribution of storm-core duration.

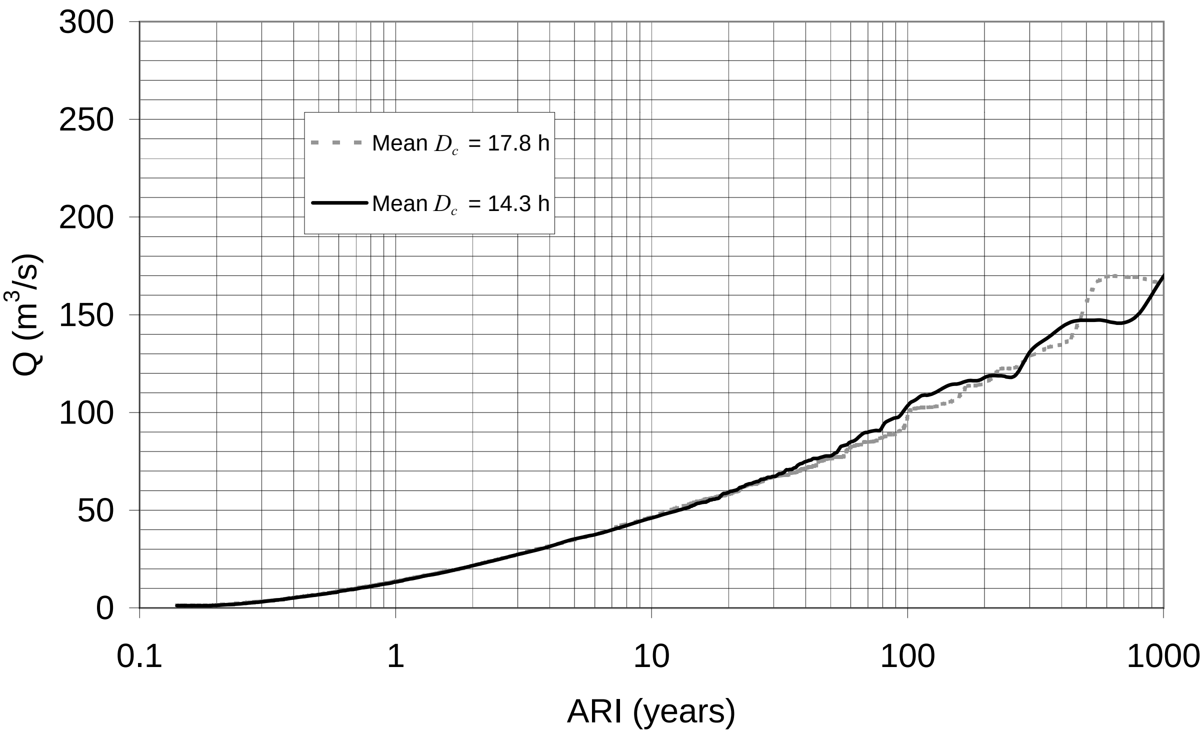


Figure 9.4 Effect of changing the parameter of the distribution of $D_c$ on the derived flood frequency curve for Boggy Creek

### 9.3.2 Change in the Distribution of Storm-Core Rainfall Intensity

As discussed in Section 5.2, the adopted method to develop storm-core IFD curves is unsuitable to provide estimates of storm-core rainfall intensity ($I_c$) for ARIs greater than 100 years. In an attempt to examine the effect on the final derived flood frequency curve of adjusting the at-site IFD curve to give more reliable values for longer durations and match the regional estimates for higher ARIs, the design rainfall estimates derived by the CRC-FORGE method (Nandakumar et al., 1998; Weinmann et al., 1999) were used to adjust parts of the IFD curves derived in Section 5.2. For Boggy Creek, the adjusted IFD table is shown in Table 9.2, and the difference between the two IFD tables is illustrated in Figure 9.5 for durations of 2 and 24 hours. The derived flood frequency curves based on these two IFD tables (keeping all other component distributions unchanged) are presented in Figure 9.6. The two derived flood frequency curves are similar up to an ARI of 100 years, but for larger ARIs, the derived flood frequency curve obtained from the CRC-FORGE-based rainfall estimates reflects the much higher design rainfall inputs. For example, at an ARI of 1,000,000 years (the last column of the IFD tables) and duration of 2 hours, the CRC-FORGE-based design rainfall estimates are twice as high; and for 6 hours duration, this ratio is 2.65. These results show that the input distribution of rainfall intensity has a dominant effect on the final derived flood frequency curve, as is in the case for the Design Event Approach.

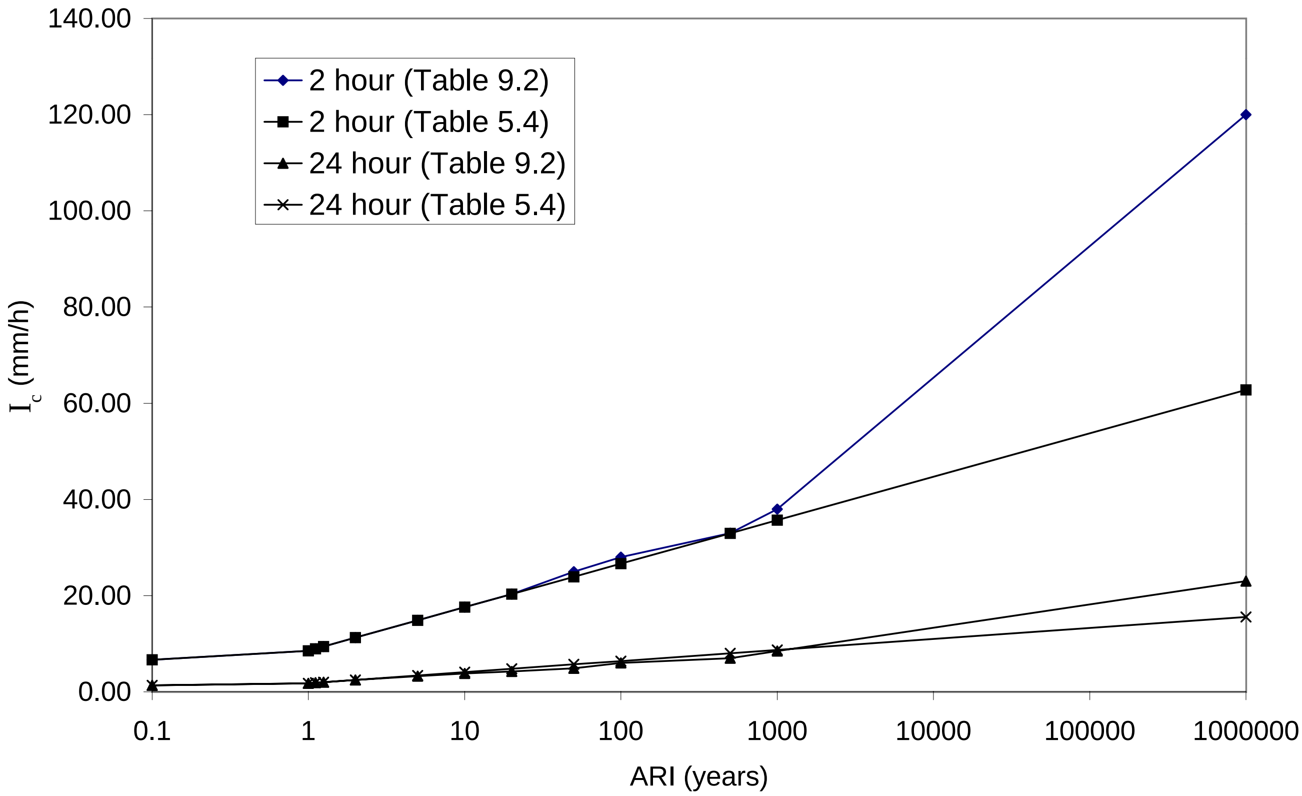


Figure 9.5 Comparison of IFD curves for Boggy Creek: original *IFD* values from Table 5.4 have been adjusted to match regional estimates obtained from the CRC-FORGE method

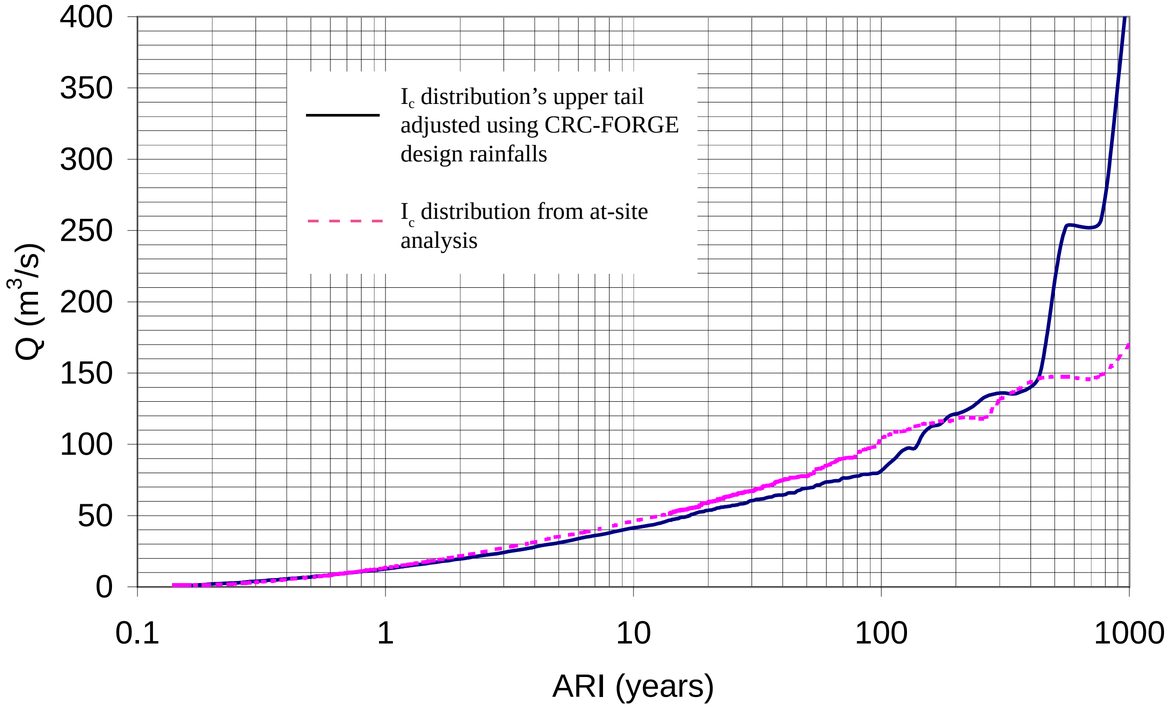


Figure 9.6 Effect on the derived flood frequency curve for Boggy Creek of changing the upper tail of the distribution of $I_c$

Table 9.2 IFD table for Boggy Creek (upper tail adjusted according to CRC-FORGE estimates), intensities in mm/h

| $D_c$ (hour) | ARI (years) | | | | | | | | | | | |
|---|---|---|---|---|---|---|---|---|---|---|---|---|
| | 0.1 | 1 | 1.11 | 1.25 | 2 | 5 | 10 | 20 | 50 | 100 | 500 | 1000 | 1000000 |
| 1 | 10.10 | 13.59 | 14.41 | 15.32 | 18.96 | 26.07 | 31.46 | 36.84 | 42.00 | 45.00 | 54.00 | 60.00 | 180.00 |
| 2 | 6.66 | 8.53 | 8.95 | 9.41 | 11.27 | 14.87 | 17.60 | 20.32 | 25.00 | 28.00 | 33.00 | 38.0 | 120.00 |
| 6 | 3.36 | 4.18 | 4.37 | 4.57 | 5.40 | 6.99 | 8.19 | 9.40 | 11.20 | 13.00 | 16.00 | 19.00 | 56.00 |
| 24 | 1.35 | 1.78 | 1.89 | 2.01 | 2.49 | 3.25 | 3.80 | 4.25 | 4.90 | 6.00 | 7.00 | 8.50 | 23.00 |
| 48 | 0.84 | 1.19 | 1.28 | 1.39 | 1.81 | 2.25 | 2.60 | 3.00 | 3.50 | 4.00 | 4.90 | 5.80 | 14.00 |
| 72 | 0.63 | 0.94 | 1.03 | 1.13 | 1.53 | 1.85 | 2.10 | 2.40 | 2.70 | 3.20 | 3.90 | 4.60 | 11.00 |
| 100 | 0.50 | 0.78 | 0.86 | 0.96 | 1.35 | 1.60 | 1.80 | 2.00 | 2.25 | 2.60 | 3.25 | 3.80 | 9.00 |

### 9.3.3 Change in the Distribution of Storm-Core Temporal Pattern

As outlined in Section 5.3, storm-core temporal patterns ($TP_c$) are dependent on $D_c$, that is, temporal patterns up to 12 hours duration are different from those with $D_c$ > 12 hours. In the sensitivity analysis, the effect of dependence of temporal patterns on $D_c$ was examined. Initially, a dependence between $TP_c$ and $D_c$ was considered, and a derived flood frequency curve was obtained, as described in Chapter 7. Then the dependence between $TP_c$ and $D_c$ was neglected, i.e. the temporal patterns for all durations were pooled for random sampling. The distributions of other components were not changed.

The two derived flood frequency curves for the Boggy Creek, obtained as above, are compared in Figure 9.7. The results show that, in this case, neglecting the dependence of the temporal patterns on $D_c$ results in slight under-estimation of the derived flood frequency curve. A similar result was obtained for the Tarwin River. It can be concluded that the derived flood frequency curve is moderately sensitive to the correct representation of temporal pattern variability.

In order to examine the effect on the derived flood frequency curve of using fixed temporal patterns (e.g. ARR design temporal patterns), the appropriate temporal patterns were selected depending on the generated duration ($D_c$) and ARI, and used in the Monte Carlo simulation. The Boggy Creek is located in ARR Temporal Pattern Zone 2. Here the ARR temporal patterns for both Zones 1 and 2 were used to gain an indication of the sensitivity of design flood estimates to regional differences in patterns. The derived flood frequency curves for Boggy Creek obtained in this way are compared in Figure 9.8 with the curve obtained from the randomly selected at-site temporal patterns. The results confirm that the derived flood frequency curve is sensitive to the selection of temporal patterns. The use of fixed ARR temporal patterns for Zones 1 and 2 overestimates the flood frequency curves obtained using the at-site temporal patterns indicating that the unfiltered design temporal patterns tend to be too severe. The differences between the IFD curves obtained from ARR Zone 2 temporal patterns and at-site temporal patterns are relatively consistent, thus indicating some potential for using ARR temporal patterns with the new Monte Carlo simulation technique. The results also indicate that the random combination of a set of fixed temporal patterns (e.g. ARR temporal patterns) with other probability distributed inputs (particularly initial losses) may offer some improvement over the current Design Event Approach, by avoiding the problems of selecting a critical rainfall duration and smoothing of the design flood frequency curve.

It should be noted that the results of this sensitivity analysis are specific to the characteristics of the Boggy Creek catchment; they cannot be readily extrapolated to other catchment conditions (e.g. rapidly responding catchments may be more sensitive to the selected representation of temporal patterns).

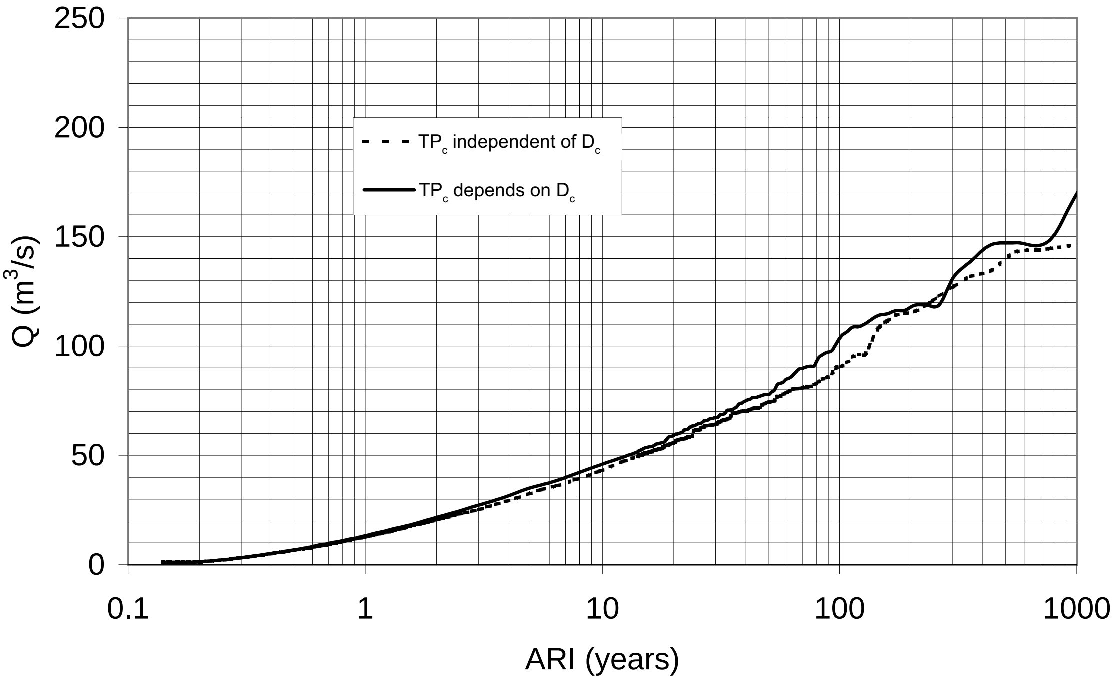


Figure 9.7 Effect on the derived flood frequency curve for Boggy Creek of variation of $TP_c$ with $D_c$

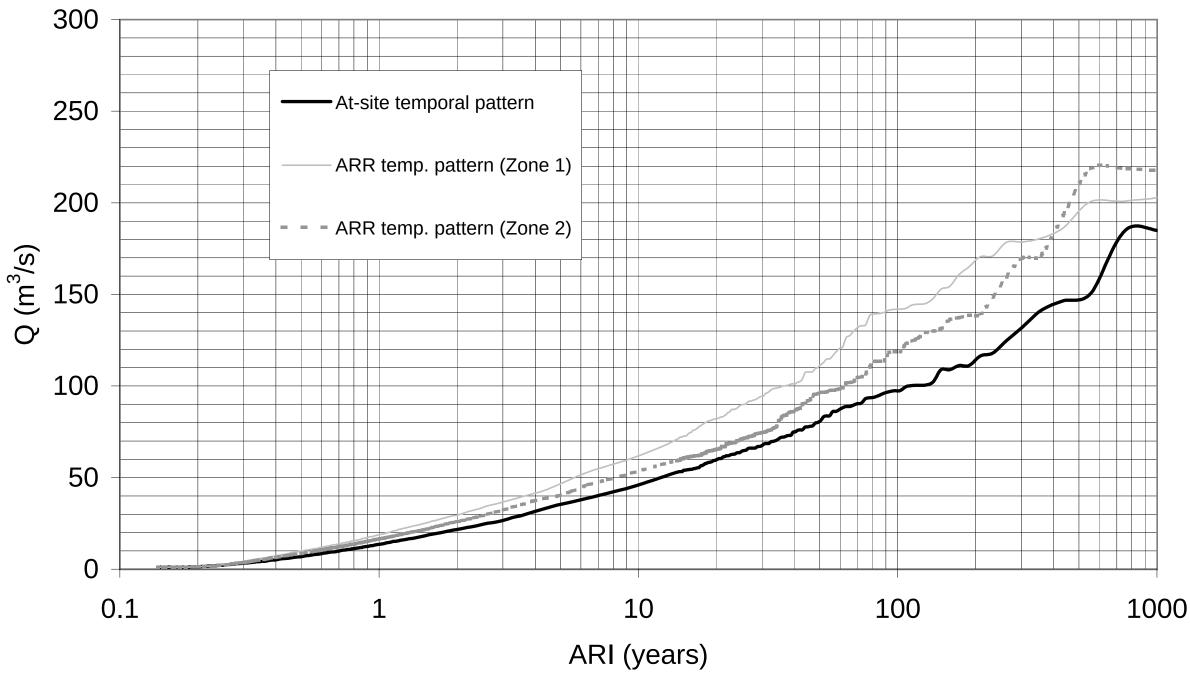


Figure 9.8 Effect on the derived flood frequency curve for Boggy Creek of using ARR design temporal patterns

### 9.3.4 Change in the Distribution of Initial Loss

The effect on the derived flood frequency curve of using a single value rather than a distribution of initial loss in the Monte Carlo simulation was examined (keeping all other distributions unchanged). This single value was taken to be the observed at-site mean value. The result for Boggy Creek is presented in Figure 9.9. At smaller ARIs, the use of a fixed mean value results in significant reduction of flood magnitude relative to that obtained from the probability-distributed initial losses; e.g. 35% to 20% reduction for ARI ≤ 1 year, and 20% to 10% reduction for ARI in between 1 to 10 years. The difference becomes insignificant near 100 year ARI. For greater ARIs, flood magnitudes increase by about 5%. The results indicate the significance of a adopting probability-distributed initial loss in the Monte Carlo simulation.

The effect of changing the parameters of the initial loss distribution (beta distribution) was also examined; the mean $IL_s$ value was changed from 23.0 mm to 15.0 mm for generating the $IL_c$ values. The results show that, at smaller ARIs, use of a smaller mean value of initial loss increases the magnitude of the generated floods significantly. However, at higher ARIs, the difference becomes insignificant (Figure 9.10).

The effect of generating $IL_c$ data directly from the distribution of $IL_c$, instead of generating $IL_c$ from the distribution of $IL_s$ (using Equation 5.4), is examined in Figure 9.11. The results show that the derived flood frequency curves are very similar in both cases, indicating that the use of Equation 5.4, in data generation provides reasonable values of $IL_c$.

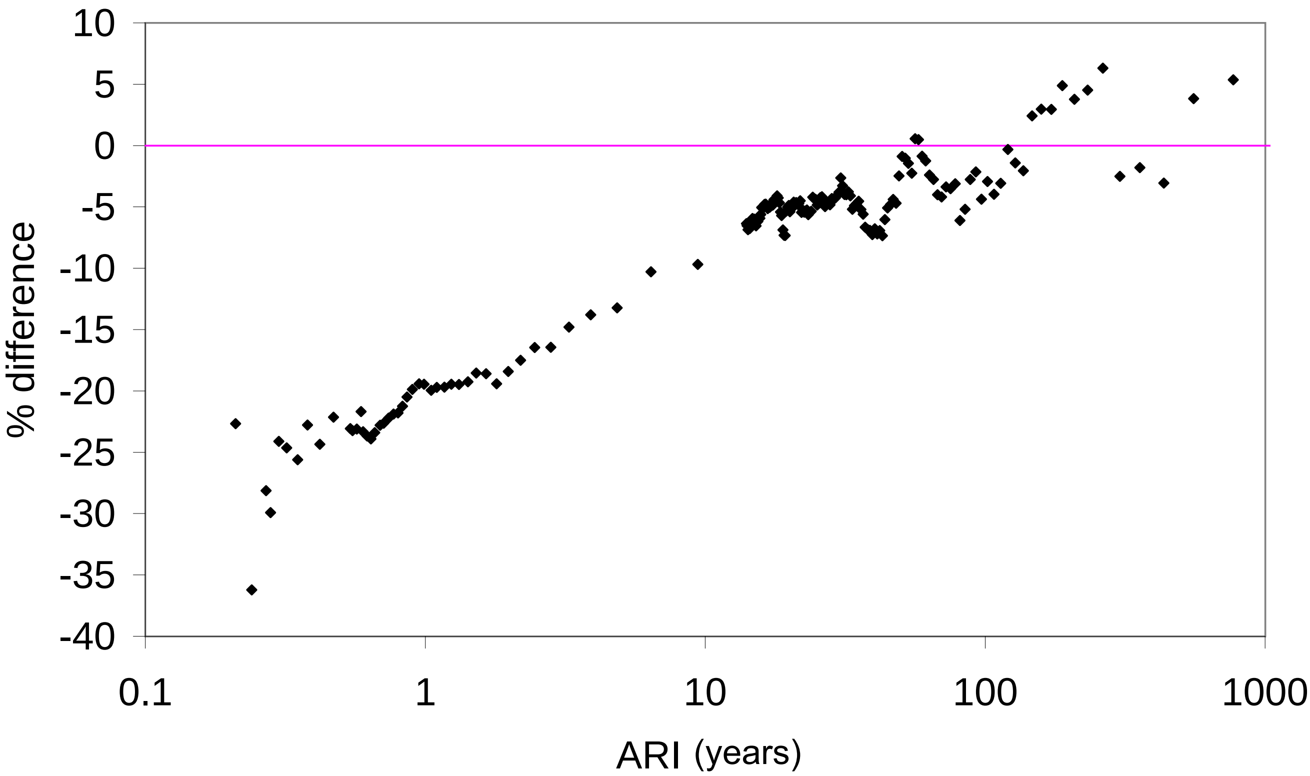


Figure 9.9 Effect on derived flood frequency curve for Boggy Creek of using single-valued initial loss instead of a distribution

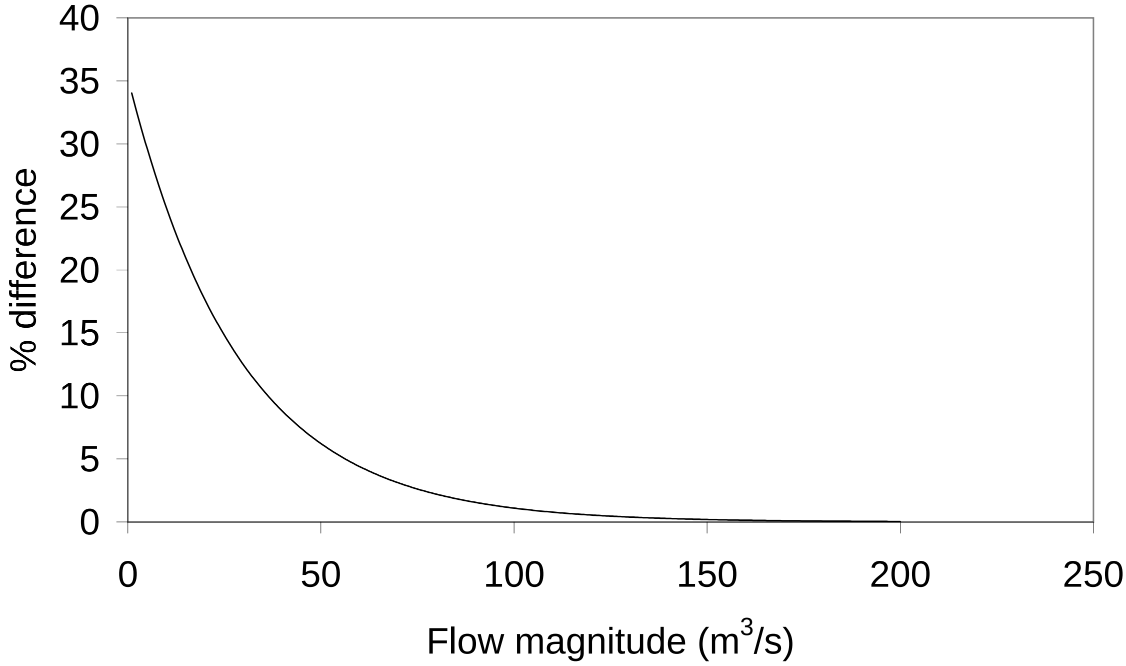


Figure 9.10 Effect on the magnitude of derived floods of using smaller mean initial loss value in data generation (mean value changed from 23 mm to 15 mm)

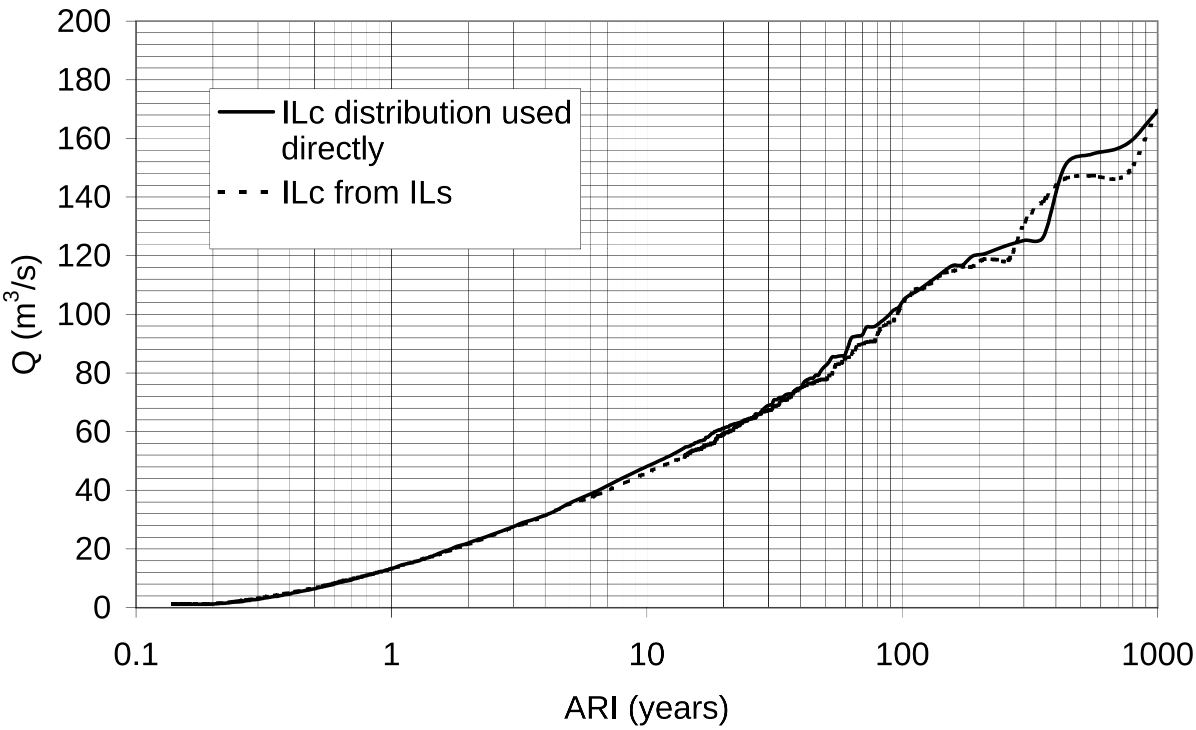


Figure 9.11 Effect on the derived flood frequency curve for Boggy Creek of using $IL_c$ distribution directly

### 9.3.5 Effect of Seed in Simulation

The generated distribution values for $D_c$, $I_c$, $TP_c$ and $IL_c$ used in the initial series of simulation runs were stored in a data file to allow selective changes of individual inputs without changes in others. However, if a new set of random deviates is used for a subsequent set of simulation runs, a different set of distribution values for $D_c$, $I_c$, $TP_c$ and $IL_c$ will be generated, even if the parameters of the distributions remain unchanged. Thus each new series of simulation runs will result in a different derived flood frequency curve. To examine the degree of variation in the derived flood frequency curve from one series of simulation runs to another, five series of runs of 15,000 events were implemented without changing the parameters of the component distributions. The results are compared in Figure 9.12. They show that the derived flood frequency curves are essentially the same, to an ARI of say 100 years.

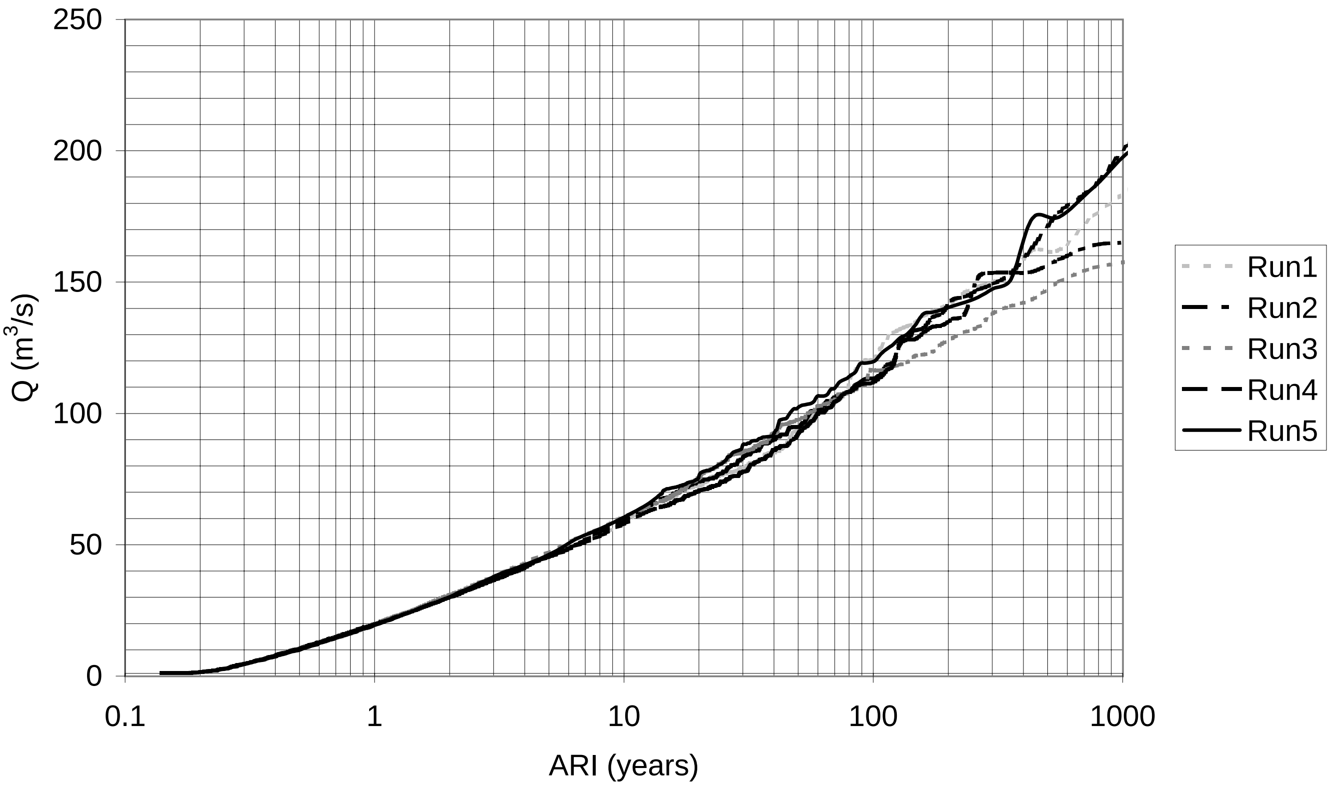


Figure 9.12 Derived flood frequency curves for five series of simulation runs (Boggy Creek)

### 9.4 Evaluation

The derived flood frequency curves for the three study catchments compare quite well with the results of flood frequency analyses of the flood series available at the sites. A relatively small degree of calibration, e.g. by adjustment of the continuing loss parameter, would produce a closer match of the derived distributions and the observed ones.

The particular strength of the described Monte Carlo simulation technique is that it allows reproduction of frequency curves over a large range of ARIs, while the Design Event Approach generally focuses on reproducing frequency curves over a narrower ARI range. It can thus be concluded that the new technique deals better with non-linearity effects than the Design Event Approach.

The results of the sensitivity analyses indicate that some of the existing design data could be used with the new approach, although further investigation is needed to draw a firm conclusion. The results also indicate that regionalisation of the parameters of the component variables would be possible, thus, the technique can be extended easily to ungauged catchments.

Given appropriate data for the catchment of interest and a calibrated runoff routing model, the new approach takes less than an hour to produce a derived flood frequency curve. Overall, the approach shows a strong potential to become a practical design tool. Section 10.3 outlines the work needed before this can happen.

# 10. Conclusion

## 10.1 Summary

In this report, a Monte Carlo simulation technique is presented to determine derived flood frequency curves. The method uses probability distributed and correlated design rainfall and loss data to determine a probability distributed flood output. The new method has been applied to a number of catchments in Victoria.

The following elements of the adopted methodology represent a further development beyond the recent work on the Joint Probability Approach (e.g. Muzik, 1993; Sivapalan et al., 1996; Blöschl and Sivapalan, 1997):

- Deterministic elements: The adopted modelling approach uses a commonly applied loss model (as a runoff production function) and runoff routing model (as a transfer function). In this initial application, a simple conceptual runoff routing model (with a single non-linear storage concentrated at the catchment outlet) was adopted. However, the ultimate goal is to adopt a semi-distributed runoff routing model (e.g. RORB or URBS). These models are most commonly applied in current Australian design practice.
- Design data: The approach establishes links with currently available design data (e.g. rainfall intensity, temporal patterns, losses) and offers the promise of application to ungauged catchments.
- Dependencies between design inputs: The approach explicitly treats the dependencies between different design inputs.
- Estimation of frequent floods: Use of partial series of design rainfalls and generated floods allows better estimation of frequent floods.

In the adopted Monte Carlo simulation technique, four input (component) variables are treated as random variables: rainfall duration, rainfall intensity, rainfall temporal pattern and initial loss. The proposed modelling framework is illustrated in Figure 2.1. The technique can be used with two different definitions of stochastic rainfall events: complete storms and storm-cores. This report uses storm-cores as these have more similarity with the currently used storm bursts. A storm-core is defined in Section 4.

The distributions of the four component variables have been identified in Section 5. The storm-core duration ($D_c$) has been found to be exponentially distributed in the study area. The storm-core IFD curves for a particular site have been developed based on the partial series of storm-core rainfall events. The new IFD curves show a fairly consistent relationship with ARR IFD curves for storm bursts (I. E. Aust., 1987), raising some hope that this relationship may be able to be generalised at a later stage, thus allowing regional estimation of storm-core IFD curves. Interpolation/extrapolation of these curves yields an IFD table for selected ARIs and durations (e.g. Table 5.4) which is the basis of data generation from the distribution of storm-core rainfall intensity ($I_c$). The observed rainfall temporal patterns have been used here to randomly draw a historic temporal pattern from the sample, depending on the generated $D_c$ value. Initial loss was found to have a Beta distribution with parameters closely related to the results of recent loss studies (Hill et al., 1996b).

The procedure for calibration of the adopted runoff routing model is similar to the calibration of the RORB model, as described in Section 6.

Generation of data from the four component distributions and simulation of streamflow hydrographs are described in Section 7, and illustrated in Figure 7.1. Typically, several thousand simulations are run to produce a partial series of flood peaks and define the desired flood frequency curve.

The new technique has been applied to three catchments in Victoria with different hydrologic characteristics: Tarwin River, Boggy Creek and Avoca River (Section 9.1). The derived flood frequency curves for these catchments have been compared with the results of frequency analyses of the flood series available at the sites, and it has been found that the new method provides relatively accurate design flood estimates compared to the existing Design Event Method.

A sensitivity analysis was conducted to examine the effect on the derived flood frequency curve of a change in any of the component distributions (Section 9.3). The results show that, not surprisingly, the derived flood frequency curve is very sensitive to a change in the distribution of rainfall intensity. They also indicate moderate sensitivity to changes in the representation of rainfall temporal patterns and initial loss distribution.

Use of fixed ARR design temporal patterns with the new Monte Carlo simulation technique was also investigated, indicating considerable sensitivity to the adopted patterns. These initial results show some potential for using the ARR design temporal patterns with the new approach. The derived frequency curves are not sensitive to small uncertainties in the adopted distribution of storm-core duration. For the ARI range of interest, no appreciable difference was noticed in the final derived flood frequency curves from one series of simulation runs to another (provided that the parameters of the component distribution are not changed).

### 10.2 Conclusions

The following conclusions can be drawn from this study:

- The new Monte Carlo simulation technique based on the joint probability approach offers a theoretically superior method of design flood estimation as it allows explicitly for the effects of inherent variability in the flood producing factors and correlations between them. It is readily applicable to gauged catchments with good pluviograph data and limited streamflow data.
- At this stage, determination of the distributions of the input variables requires good at-site data for rainfall and streamflow, but initial results indicte that many of the existing design data (rainfall intensity, rainfall temporal patterns, losses, baseflow) could be adapted for use with the new Monte Carlo simulation technique.
- Derived flood frequency curves for a site can be produced in less than an hour, once the parameters of the distributions of the input variables have been determined.
- The new technique avoids difficult decisions on the selection of a critical rainfall duration (which is required in the Design Event Approach), and smoothing of the final design flood frequency curve that involves a degree of subjectivity.
- For the three study catchments, the new technique reproduces observed flood frequency curves with reasonable accuracy over a wide range of frequencies and it can cope well with the non-linearity of the rainfall and runoff process.
- The new technique shows strong potential to become a practical design tool, however, further work is needed before the technique can be handed over for routine application by practitioners.
- The new technique is appropriate for the derivation of flood frequency curves in the ARI range from 1 to 100 years. However, use of more reliable estimates of rare rainfall intensities (e.g. based on the CRC-FORGE method) and appropriate adjustment to other design parameters should allow reliable estimation of design floods beyond 100 years ARI.
- The Monte Carlo simulation technique presented here could be used to determine the derived frequency curve of other streamflow hydrograph characteristics, e.g. flood volume, time to peak. With the inclusion of a distribution of reservoir storage contents, the approach could easily be extended to derive the frequency curves of reservoir outflow characteristics.
- The technique also lends itself to estimating design floods on a seasonal basis, taking account of distinct seasonal variations of design inputs such as rainfall and loss characteristics, and the likelihood of the joint occurrence of critical values.

### 10.3 Future Work

It is desirable to undertake the following work to further develop the proposed Monte Carlo simulation technique:

- A semi-distributed runoff routing model (e.g. URBS) to be incorporated instead of the single storage runoff routing model in the present simulation technique.
- The approach to be tested on additional catchments representing a broader range of hydrologic conditions and compared with the Design Event Approach.
- A relationship to be developed between storm-core and ARR storm burst IFD curves so that the latter can be used directly with the Monte Carlo simulation technique in catchments with inadequate pluviograph data.

- The design rainfall estimates from the CRC-FORGE method to be used with the present procedure (and other appropriate design parameters) to extend the applicability of the method to design floods beyond 100 years ARI.
- The potential of the approach for application in ungauged catchments to be evaluated.
- The potential of using the current (fixed) design temporal patterns (ARR temporal patterns) with the new technique to be further investigated.
- The addition of the distribution of continuing loss to the present four stochastic input variables/ parameters to be investigated.
- The importance of seasonal effects in the design rainfall and loss inputs to be examined and, if found important, seasonal distributions of design inputs to be derived and applied in the simulation technique.

## References


Blöschl, G. and Sivapalan, M. (1997). Process Controls on Flood Frequency. 2. Runoff Generation, Storm Properties and Return Period. Centre for Water Research Environmental Dynamics Report, ED 1159 MS, Department of Civil Eng., The University of Western Australia.

Carroll, D. G. (1994). The BCC Catchment Management Runoff Routing Model Manual, Version 3.3, Brisbane City Council, Brisbane, Australia.

Eagleson, P. S. (1972). Dynamics of Flood Frequency. Water Resources Research, 8, 4, 878-898.

Hill, P. I. (1994). Catalogue of Hydrologic Data for Selected Victorian Catchments. CRC for Catchment Hydrology Working Document No 94/1. Department of Civil Engineering, Monash University, Australia.

Hill, P. I. and Mein, R. G. (1996). Incompatibilities between Storm Temporal Patterns and Losses for Design Flood Estimation. Hydrology and Water Resources Symposium 1996, Hobart, Tasmania, 2, pp. 445-451.

Hill, P. I., Mein, R. G., Weinmann, P. E. (1996a). Testing of Improved Inputs for Design Flood Estimation in South-Eastern Australia. CRC for Catchment Hydrology Report 96/6, Department of Civil Engineering, Monash University, Australia.

Hill, P. I., Maheepala, U. K., Mein, R. G. and Weinmann, P. E. (1996b). Empirical Analysis of Data to Derive Losses for Design Flood Estimation in South-Eastern Australia. CRC Report No 96/5, CRC for Catchment Hydrology, Department of Civil Engineering, Monash University, Australia.

Hoang, T. M. T (2001). Joint Probability Approach to Design Flood Estimation. PhD Thesis (under preparation), Department of Civil Engineering, Monash University, Australia.

Hoang, T., Rahman, A., Weinmann, P. E., Laurenson, E. M., Nathan, R. J. (1999). Joint Probability Descriptions of Design Rainfalls. Intl. Hydrology and Water Resour. Symp of the I.E. Aust. and 2nd Int. Conference on Water Resour. and Env. Research, Brisbane, Australia, 6-8 July, 1999.

HYDSYS (1994). HYDSYS User Manual. Release 5.0, HYDSYS Pty Ltd, ACT, Australia.

I. E. Aust. (1987). Australian Rainfall and Runoff - A Guide to Flood Estimation. Institution of Engineers, Australia.

Lacey, G. (1996). Relating Baseflow to Catchment Properties: A Scaling Approach. CRC Report No 96/8, CRC for Catchment Hydrology, Department of Civil Engineering, Monash University, Australia.

Laurenson, E. M. (1974). Modelling of Stochastic-Deterministic Hydrologic Systems. Water Resources Research, 10, 5, 955-961.

Laurenson, E. M. and Mein, R. G. (1997). RORB Version 4 Runoff Routing Program User Manual, Dep. of Civil Eng., Monash University. pp. 186.

Mein, R.G., Nandakumar, N, Siriwardena, L (1995). Estimation of Initial Loss from Soil Moisture Indices (Pilot Study). CRC Working Document 95/1. CRC for catchment Hydrology, 59 pp.

Muzik, I. (1993). Derived, Physically Based Distribution of Flood Probabilities. Extreme Hydrological Events: Precipitation, Floods and Droughts. Proceedings of the Yokohama Symp., July 1993, IAHS Publ. No. 213. pp. 183-188.

Nandakumar, N., Weinmann, P. E., Mein, R. G. and Nathan, R. J. (1997). Estimation of Extreme Rainfalls for Victoria using the CRC-FORGE Method (for rainfall durations 24 to 72 hours). Report No. 97/4 CRC for Catchment Hydrology, 118 pp.

Rahman, A. (1996). Flood Estimation for Ungauged Catchments: A Regional Approach Using Flood and Catchment Characteristics. Unpublished PhD thesis, Dept. of Civil Eng., Monash University (292 pp).

Rahman, A. (1999). Determination of Derived Flood Frequency Curve by Monte Carlo Simulation: Programs. Unpublished CRC Working Document (27 pp).

Rahman, A., Hoang, T., Weinmann, P. E., Laurenson, E. M. (1998). Joint Probability Approaches to Design Flood Estimation: A Review. Research Report 98/8, Cooperative Research Centre for Catchment Hydrology, Department of Civil Engineering, Monash University, Australia. 70 pp.

Siriwardena, L. and Weinmann, P. E. (1996). Derivation of Areal Reduction Factors for Design Rainfalls in Victoria. CRC for Catchment Hydrology Report 96/4, Dept. of Civil Eng., Monash University, pp. 60.

Sivapalan, M., Blöschl, G. and Gutknecht, D. (1996). Process Controls on Flood Frequency. 1. Derived Flood Frequency. Centre for Water Research Environmental Dynamics Report, ED 1158 MS, Department of Civil Eng., The University of Western Australia.

Stedinger, J. R., Vogel, R. M., Foufoula-Georgiou, E. (1993). Frequency Analysis of Extreme Events. In Handbook of Applied Hydrology. Edited by Maidment, D. R., McGRAW-HILL, INC.

Weinmann, P. E., Rahman, A., Hoang, T., Laurenson, E. M., Nathan, R. J. (1998). A New Modelling Framework for Design Flood Estimation. International Conference on Hydraulics in Civil Engineering, Adelaide, Australia, 1998: 393-398.

Weinmann, P.E., Nandakumar, N., Siriwardena, L., Mein, R.G. and Nathan, R.J. (1999). Estimation of Rare Design Rainfalls for Victoria using the CRC-FORGE Methodology. Intl. Hydrology and Water Resour. Symp of the I.E. Aust. and 2nd Int. Conference on Water Resour. and Env. Research, Brisbane, Australia, 6-8 July, 1999, pp 284-289.

## Appendix 1: Selected Catchments for Joint Probability Study[1]

| Catchment ID | Catchment name | Latitude (degree) | Longitude (degree) | Catchment area ($km^2$) | Mean annual rain (mm) | Mean annual evaporation (mm) |
|---|---|---|---|---|---|---|
| 221201 | Cann River (West Branch) @ Weeragua | 37.38 | 149.2 | 311 | 975 | 1314 |
| **226205** | **Latrobe River @ Noojee** | 37.83 | 145.96 | 290 | 1360 | 1100 |
| 226220 | Loch River @ Noojee | 37.81 | 145.99 | 106 | 1360 | 1000 |
| 226410 | Traralgon Creek @ Koornalla | 38.33 | 146.53 | 89 | 1000 | 1200 |
| 231213 | Lerderderg River @ Sardine Creek | 37.46 | 144.32 | 153 | 1020 | 1164 |
| 236204 | Fiery Creek @ Streetham | 37.5 | 143.15 | 956 | 557 | 1214 |
| 403205 | Ovens River @ Bright | 36.84 | 147.04 | 495 | 1423 | 1155 |
| **403226** | **Boggy Creek @ Angleside** | 36.72 | 146.33 | 108 | 1020 | 1400 |
| 407253 | Picanniny Creek @ Minto | 36.65 | 144.4 | 668 | 460 | 1560 |
| 415224 | Avon River @ Beazley's Bridge | 36.81 | 143.16 | 259 | 540 | 1800 |
| **408202** | **Avoca River @ Amphitheatre** | 37.18 | 143.41 | 78 | 745 | 1333 |
| **227226** | **Tarwin River, East branch @ Dumbalk** | 38.51 | 146.16 | 127 | 1020 | - |
| 404208 | Moonee Creek @ Lima | 36.75 | 145.98 | 91 | 860 | 1344 |
| 235219 | Aire River @ Wyelangta | 38.67 | 143.54 | 90 | 1940 | - |

Continued …

[1] ${}^{2}I_{24}$ (2 years ARI and 24 hours duration design rainfall intensity); BFI (baseflow index); GVI (Geo-vegetation index) obtained from Lacey, 1996; and "-" stands for missing data. The new technique was applied to the four catchments (bold).

| Catchment ID | Rainfall intensity ($^{2}I_{24}$) mm/h | Streamflow record (years) | Large flood: year, AEP | Quality of rating index (until 1987) | Forest area (Fraction) | Slope (m/km) | BFI | GVI |
|---|---|---|---|---|---|---|---|---|
| 221201 | 4.28 | 36 | 1971 1:100 | 0.164 | 0.98 | 10.9 | 0.45 | - |
| **226205** | 3.16 | 36 | 1963 1:50 | 1.00 | 0.93 | 6.7 | 0.77 | - |
| 226220 | 3.39 | 28 | 1971 1:100 | 0.448 | 0.87 | 9.7 | - | C |
| 226410 | 2.52 | 33 | 1993 1:100 | 0.520 | 0.75 | 13.3 | 0.34 | L |
| 231213 | 2.92 | 33 | 1974 1:100 | 0.566 | 0.94 | 9.4 | 0.36 | J |
| 236204 | 1.91 | 64 | 1934 1:100 | 0.972 | 0.06 | 2.7 | - | - |
| 403205 | 3.38 | 48 | 1974 1:100 | 0.736 | 0.94 | 12.6 | 0.56 | - |
| **403226** | 3.11 | 25 | 1993 1:100 | 0.421 | 0.6 | 13.8 | 0.49 | - |
| 407253 | 2.03 | 26 | 1974 1:100 | 0.402 | 0.35 | 1.3 | 0.21 | - |
| 415224 | 2.02 | 24 | - | 0.597 | - | - | - | - |
| **408202** | 2.29 | 24 | 1973 1:100 | 0.635 | 0.47 | 7.6 | 0.28 | J |
| **227226** | - | - | - | 0.205 | - | - | - | - |
| 404208 | - | - | - | 0.198 | 0.84 | 27.4 | 0.6 | - |
| 235219 | - | - | - | 0.117 | - | - | - | - |

## Appendix 2: Comparison of Derived Flood Frequency Curve with the Observed Data at Boggy Creek (with Latest Flood Data)